中央大学博士論文

Synthesis of Hemoglobin–Albumin Clusters as an Artificial O_2-Carrier

人工酸素運搬体としての

（ヘモグロビン–アルブミン）クラスターの合成

Ryosuke Funaki

船木　亮佑

博士（工学）

中央大学大学院
理工学研究科
応用化学専攻

令和元年度
２０２０年３月

Contents

Abstract

Blood shortages are serious problems worldwide, and demand for blood for transfusion therapy is only expected to increase. In Japan, the Red Cross Society estimates that approximately 850,000 people will face medical challenges due to blood shortages each year by 2027. The development of an artificial O_2-carrier as a red blood cell (RBC) substitute is widely considered an optimal solution. In the last few decades, several types of hemoglobin (Hb)-based O_2-carriers (HBOCs) have been developed, but none have been approved for transfusion therapy because the side effects, including vasoconstriction and increased blood pressure, cannot be avoided.

Recently, we synthesized core-shell protein clusters comprising a bovine (HbBv) or human adult hemoglobin (HbA) in the center and human serum albumins (HSAs) at the periphery. This Hb–HSA_3 cluster, named "HemoAct," is a promising RBC substitute and O_2 therapeutic reagent. The Hb–HSA_3 cluster has a large molecular weight (264 kDa) and a strong negative net surface charge (pI: 5.0), which may prove effective in preventing hypertensive action with extravasation and prolonging blood-circulation persistence. To evaluate the safety and efficacy of the Hb–HSA_3 cluster in preclinical and clinical tests, enlargement of the preparation scale and simplification of the procedure are required.

In this thesis, the author presents an improved preparation procedure for HbBv–HSA_3 clusters with O_2-binding ability comparable to those of clusters synthesized by conventional procedures. Second, the author establishes an expression system of recombinant HbA (rHbA) using *Pichia pastoris* by genetic engineering, and prepared rHbA–$rHSA_3$ clusters as an entirely synthetic O_2-carrier. Furthermore, an rHbA(X)–$rHSA_3$ cluster variant with an O_2 affinity similar to that of human RBCs is prepared by site-direct mutagenesis in the heme pocket of the core rHbA.

Chapter 1

General Introduction

1.1 Structure and Function of Hemoglobin

Hemoglobin (Hb) is a tetrameric O_2-transporting hemoprotein composed of two α- and β-globins ($\alpha_2\beta_2$). Each globin has iron(II)-protoporphyrin IX (Mw: 616.49, Figure 1-1) as a prosthetic heme group.[1–3] In the case of human adult Hb (HbA), the molecular weight is approximately 64,500 Da (including 4 hemes) and the number of amino acid residues is 141 for α-globin (15,126 Da) and 146 for β-globin (15,867 Da), respectively. These globins have 7 (α-globin) or 8 (β-globin) α-helices designated A to H from the N-terminus, but α-globin lacks the D helix (Figure 1-1).[4] The heme is located in the cavity between the F helix (proximal side) and the E helix (distal side) known as the "heme pocket." The heme iron has 6 coordination bonds. Four are occupied by pyrrole nitrogens of heme, the fifth site is bound to a proximal histidine (F8 His: α58, β63) in the globin, and the sixth makes a complex with gaseous molecules such as dioxygen (O_2), carbon monoxide (CO), and nitric monoxide (NO).

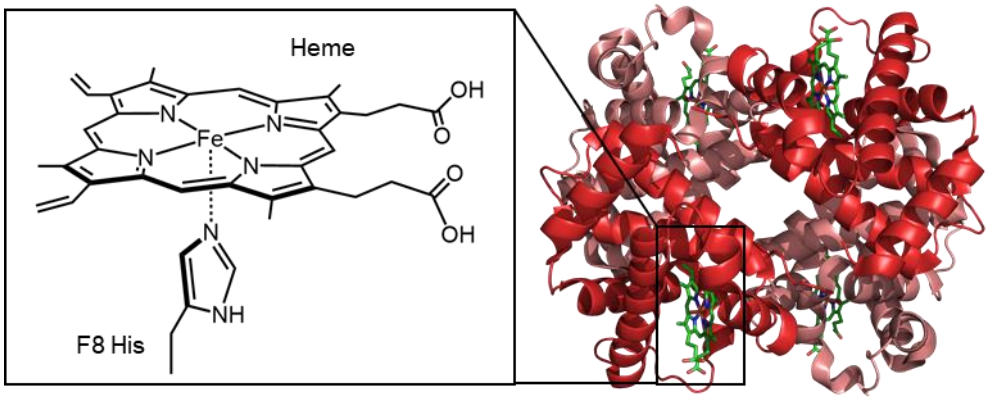

Figure 1-1. Structure of heme and oxy HbA (Protein Data Bank ID: 2DN1): α-globin (red) and β-globin (pink).

Since the X-ray crystal structure horse Hb was reported by Perutz *et al*. in 1960,[5,6] the relationship between three-dimensional (3-D) structure and O_2-binding ability has been clarified. The tertiary structures of each globin of Hb and myoglobin (Mb) are almost

identical, although the O_2-equilibrium curves differ. Mb produces a rectangular hyperbolic curve, but Hb displays a characteristic sigmoidal curve (Figure 1-2A). The quaternary structural transition of Hb between the relaxed (R) state (high O_2 affinity) and the tense (T) state (low O_2 affinity) (Figure 1-2B) can be attributed to cooperativity, which is induced by ligand binding and enhanced by an allosteric effector such as 2,3-bisphosphoglycerate (2,3-BPG) and inositol hexaphosphate (IHP). Arnone first reported the 2,3-BPG binding site on HbA.[7] Richard *et al*. and Xia *et al*. reported a detailed location, which is surrounded by His-β2, Lys-β82, (Asn-β139), and His-β143.[8,9]

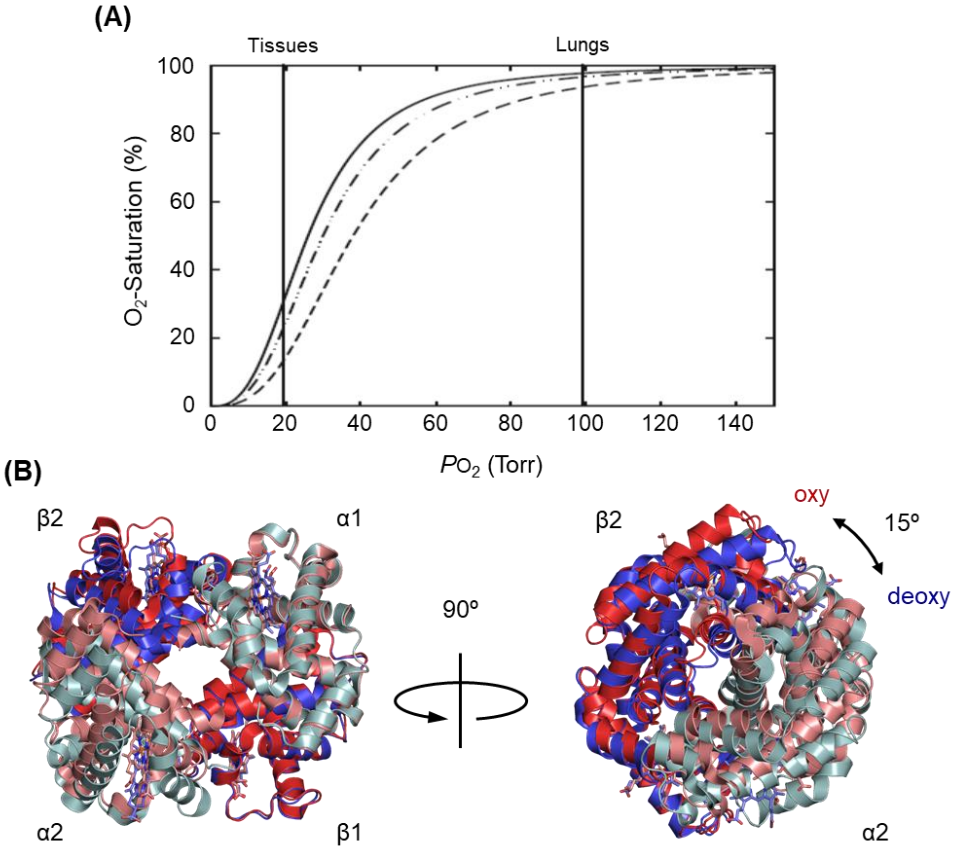

Figure 1-2. (A) O_2-dissociation curves of HbA at several CO_2 pressures (solid line: P_{CO2} = 0 Torr pH 7.4; dot-dot line: 0 Torr pH 7.2; and dashed line: 40 Torr pH 7.2) at 37 °C.[2] (B) Superimposed structure of the oxy HbA (R-state) (α-globin: red, β-globin: pink; Protein Data Bank [PDB] ID: 2DN1) and deoxy HbA (T-state) (α-globin: blue, β-globin: pale green; PDB ID: 2DN2).

Two monumental descriptions of the cooperativity of Hb have been proposed; stepwise dioxygenation and a two-state allosteric model.[10,11] The stepwise model proposed by Adair in 1925 presumed that O_2-binding to Hb is a 4-step sequential reaction that does not distinguish between the reactivity of α- and β-globins. In comparison, the 2-state Monod–Wyman–Changeux (MWC) model proposed by Monod *et al*., assumed a 2-state equilibrium between the T and R states with different O_2 affinities. We can obtain the O_2-binding parameters of Hb by analyzing the O_2-dissociation curve. The O_2 affinity of Hb is commonly expressed as a P_{50} value, which means the O_2 partial pressure at which 50% of Hb is dioxygenated. Cooperativity is expressed by an n value, the Hill coefficient, which can be calculated from the Hill equation:

$$\mathrm{Y} = \frac{(P_{\mathrm{O}_2}/P_{50})^n}{1 + (P_{\mathrm{O}_2}/P_{50})^n}$$

$$\log\frac{Y}{1-Y} = n\log\left(\frac{P_{\mathrm{O}_2}}{P_{50}}\right) = n\log P_{\mathrm{O}_2} - n\log P_{50},$$

where Y is the O_2 saturation of Hb, P_{O2} is O_2 partial pressure, and n is the Hill coefficient. In fact, O_2-dissociation curve fitting can be performed as a function of Adair's theory or MWC models.[12,13]

Adair's model can be expressed by:

$$\mathrm{Y} = \frac{a_1 P_{\mathrm{O}_2} + 2a_2 {P_{\mathrm{O}_2}}^2 + 3a_3 {P_{\mathrm{O}_2}}^3 + 4a_4 {P_{\mathrm{O}_2}}^4}{4(1 + a_1 P_{\mathrm{O}_2} + a_2 {P_{\mathrm{O}_2}}^2 + a_3 {P_{\mathrm{O}_2}}^3 + a_4 {P_{\mathrm{O}_2}}^4)}$$

where Y is O_2 saturation of Hb, P_{O2} is O_2 partial pressure, and a_i (i = 1–4) is a constant composed of the intrinsic Adair association constants: $a_1 = 4\ k_1$, $a_2 = 6\ k_1\ k_2$, $a_1 = 4\ k_1\ k_2\ k_3$, and $a_1 = k_1\ k_2\ k_3\ k_4$.

The MWC model can be expressed as:

$$\mathrm{Y} = \frac{Lc\alpha(1 + c\alpha)^3 + \alpha(1 + \alpha)^3}{L(1 + c\alpha)^4 + (1 + \alpha)^4}$$

where L is an allosteric constant, c is the ratio of intrinsic association constant (= K_T/K_R), and

α is the O_2 activity, including the K_R (= K_R P_{O2}). The O_2-binging properties (P_{50}, n) of human Hb (HbA) and bovine Hb (HbBv) are summarized in Table 1-1.[14–20]

Table 1-1. O_2-binding properties of HbA and HbBv in several conditions

Buffer condition	HbA		HbBv	
	P_{50} (Torr)	n (–)	P_{50} (Torr)	n (–)
10 mM HEPES (pH 7.2), [Cl] = 0 at 37 °C[a]	4.4	2.2	12.8	2.7
50 mM bis-Tris (pH 7.2), [Cl] = 0.1 M at 37 °C[a]	11.5	2.8	26.4	2.7
100 mM PB (pH 7.4) at 37 °C[c]	15	2.5	29	2.1
PBS (pH 7.4) at 37 °C	14.4[d]/12[e]	2.8[d]/2.4[e]	23[f]	2.6[f]
Hemox buffer (pH 7.4) at 37 °C	12[e]/13.5[g]	2.4[e]/2.6[g]	–	–
50 mM bis-Tris (pH 7.2), [Cl] = 0.1 M at 25 °C[a]	5.4	2.7	14.5	3.0
50 mM bis-Tris (pH 7.4), [Cl] = 0.1 M at 25 °C[b]	5.3	3.02	16.7	2.98

[a] Ref. 14, [b] ref. 15, [c] ref. 16 (only HbBv added 0.1 M NaCl), [d] ref. 17, [e] ref. 18, [f] ref. 19, [g] ref. 20.

1.2 Development of a Red Blood Cell Substitute as an Artificial O_2-Carrier

The development of an artificial O_2-carrier as an RBC substitute is attracting attention because of serious concern regarding blood shortages associated with declining birth rates and aging populations. The ideal artificial O_2-carrier has a long preservation period and no blood type, so it could be transfused to anyone at any time without cross-matching.[21–23] RBC products cannot be treated (heat sterilization or filtration) for virus inactivation, while an artificial O_2-carrier poses no risk of infection by, for example, hepatitis or human immunodeficiency virus.[24]

Artificial O_2-carriers can be divided into two categories: (i) perfluorocarbon (PFC)-based O_2-carriers, and (ii) Hb-based O_2-carriers (HBOCs) (Table 1-2). Liquid PFC is colorless and insoluble in water, and must be emulsified before transfused. The PFC emulsion formulation Fluosol (Green Cross Corp., Japan) was the first and only product to be approved in the US (in 1989) and European countries as an O_2 therapeutic reagent, but it was withdrawn in

1994.[23,25–27] HBOCs can be further subdivided into cellular types: also called liposome-encapsulated Hb, which is a liposome composed of a phospholipid filled with Hb,[28–30] and acellular types: chemically modified Hb with intramolecular[31–34] or intermolecular cross-linking,[35–38] or biocompatible polymers conjugation, such as polyethylene-glycol (PEG),[17,39–41] oligosaccharides,[20,42–45] and proteins.[18,46–49] Currently, development of artificial O_2-carriers is dominated by HBOCs because of their high O_2-transporting efficacy and biocompatibility. Stroma-free (unmodified) Hb transfused in the bloodstream dissociates to an αβ dimer and is rapidly eliminated through the spleen, kidney, and liver.[21] Intramolecularly cross-linked Hb, which is designed to avoid dimer dissociation, has been tested. However, it produced an unfavorable increase in blood pressure by vasoconstriction because nitric oxide (NO) was scavenged by Hb released from blood vessels. To avoid these problems, several groups have developed polymerized Hbs and PEGylated Hbs to increase molecular size and circulation lifetimes. Unfortunately, none has reached practical use.[50,51]

Table 1-2. List of representative artificial O_2-carriers

Category	Product name	Major component	Developer	Ref.
Perfluorocarbon (PFC)	Fluosol®	Perfluorodecalin, perfluoro tripropylamine	Green Cross Corp., Japan	25, 26
	Oxygent™	Perfluoro-octyl bromide	Alliance Pharm. Corp., US	25, 27
Hb-based O_2-carrier (HBOC)				
Cross-linked Hb	HemAssist™	HbA, DBBF	Baxter, US	22, 31
	Optro™ (rHb1.1)	Recombinant HbA(di-α)	Somatogen, Inc., US	22, 32
Polymerized Hb	Hemopure® (HBOC-201, Hb glutamer-250)	HbBv, glutaraldehyde	Biopure Corp., US	22, 38
	Oxyglobin® (HBOC-301)	HbA, glutaraldehyde	Biopure Corp., US	22
	PolyHeme™	HbA, glutaraldehyde	Northfield Lab., US	22

Table 1-2. List of representative artificial O_2-carriers

Category	Product name	Major component	Developer	Ref.
PEGylated Hb	Hemospan® (MP4)	HbA, iminothiolane, Mal-PEG_{5k}	Sangart, Inc., US	39
	PEG-Hb	HbA, iminothiolane, Mal-PEG_{5k}	Manjula and Acharya *et al*., US	17, 40
Conjugated Hb	Hemolink™ (*o*-Raffinose polyHb)	HbA, glutaraldehyde, raffinose	Hemosol Inc., Canada	20, 43
	PolyHb-SOD-CAT	HbBv, CAT (bovine), SOD (bovine), glutaraldehyde, pyridoxal-phosphate	D'Agnillo and Chang *et al*., US	46
	HemoAct™ (Hb–HSA_3)	Hb (bovine or human), HSA	Komatsu *et al*., Japan	18, 48
Liposome-encapsulated Hb	Neohemocyte	HbA, cholesterol, DPPC, DPPG	Burnette *et al*., US	28, 30
	HbV (Hb-vesicles)	HbA, cholesterol, DPPC, DPPG, PEG_{5k}-DPEA	Tsuchida and Sakai *et al*., Japan	29, 30

Abbreviation; DBBF: 3,5-dibromosalicyl-bis-fumalate, Mal: maleimide group, SOD: superoxide dismutase, CAT: catalase, DPPC: dipalmitoyl phosphatidylcholine, DPPG: dipalmitoyl phosphatidylglycerol, DPEA: dipalmitoyl L-glutamate-*N*-succinic acid.

1.2.1 Cross-Linked Hb

Diaspirin Cross-Linked Hb (DCLHb) "HemAssist"

The diaspirin cross-linked HbA (DCLHb), which is cross-linked between Lys-α99 in HbA by bis(3,5-dibromosalycil) fumarate (DBBF) in an N_2 atmosphere and the presence of 2,3-BPG, was reported by Walder *et al*. in 1986.[31] The DCLHb shows a high O_2 affinity (P_{50} = 27 Torr at 37 °C, pH 7.4) and Hill coefficient (n = 2.7).[34] The DCLHb produced by Baxter Corp. (USA) was named "HemAssist." Hb concentration of the formulation is 10 g/dL.[52] DCLHb is one of the first-generation HBOCs to be evaluated in preclinical and clinical tests. However, in phase III trials, DCLHb was associated with significantly higher mortality rates compared with control groups,[52] possibly due to hypertension by NO scavenging and organ injury by free-radical generation.[34]

1.2.2 Polymerized Hb

Polymerized HbBv "Hemopure"

Biopure Corp. (USA) developed glutaraldehyde polymerized HbBv, which consists of intermolecular cross-linked HbBv with glutaraldehyde with a relatively large molecular weight of 130–500 kDa.[51] The product name is "Hemopure"[34] The P_{50} value (38 Torr) was higher than that of human RBCs (25 Torr). The Hb concentration of the formulation in modified Ringer's lactate was 13 g/dL. The tetrameric and polymeric HbBv contents were determined by size-exclusion chromatography (SEC); tetrameric content was less than 1% and polymeric (> 500 kDa) content was approximately 10%.[53] Hemopure can be stored in a deoxy form at room temperature for at least 3 years.[38] The product was approved for human use in South Africa in 2001. Hemopure advanced phase III clinical trials in the US, but it has not been approved by the US Food and Drug Administration because of concerns regarding vasoconstriction.[38]

Polymerized HbA "PolyHeme"

Northfield Lab. (USA) developed pyridoxalated and polymerized HbA, which is cross-linked by glutaraldehyde and pyridoxal 5'-phosphate (PLP) with a molecular weight of 130–250 kDa.[24,51] The product, known as "PolyHeme,"[34] had a P_{50} value (28–30 Torr) slightly higher than that of human RBCs and a moderate Hill coefficient (n = 1.7). Hb concentration of the formulation in a physiological electrolyte solution was 10 g/dL. The monomeric HbA content was less than 1%. The product showed no serious adverse effects in phase I and II studies. However, trials of PolyHeme were suspended because there was no significant improvement in 30-days mortality, and more adverse events in the group.[54]

1.2.3 PEGylated Hb

PEGylated HbA (MP4) "Hemospan"

Maleimide-PEG (Mal-PEG)-conjugated HbA (MP4), which is prepared by Mal-PEG_{5k} and thiolated HbA by 2-iminothiolane, was reported by Winslow *et al*. in 2003.[39] The molecular weight of MP4 as determined by SEC was approximately 95 kDa, with a PEG-binding number of approximately 6. The O_2-binding parameters (P_{50}, n) are 6 Torr and 1.2 in PBS at 37 °C. MP4 was produced by Sangart Inc. (USA) with a formulation name of "Hemospan." The formulation has high O_2 affinity and colloid osmotic pressure (COP; 55 mmHg) and a low Hb concentration (4.3 g/dL).[24] Hemospan showed non-hypertensive action in clinical experiments. However, only transient elevations were observed in typical liver function markers such as aspartate aminotransferase, alanine aminotransferase, and lactate dehydrogenase.[55] Phase III clinical trials in orthopedic surgery patients were carried out in Europe, but revealed no significant improvement in adverse events compared with a control.[56]

Chapter 2

Synthesis of Hemoglobin–Albumin Clusters

2.1 Introduction

In 2013, our laboratory (Komatsu *et al*.) first reported a core-shell structured-protein cluster comprising HbBv wrapped covalently with HSAs — an HbBv–HSA$_3$ cluster.[48] Similar protein clusters using HbA were synthesized in 2015[18] in a formulation named "HemoAct." Hb–HSA$_3$ clusters feature a high molecular weight (264 kDa) and negative net surface charge (pI 5.0). The cluster achieved long blood-circulation lifetimes and produced no side effects such as increased blood pressure and cardiac toxicity in animal experiments.[57,58]

Evaluations of the safety and efficacy of HbBv–HSA$_3$ and HbA–HSA$_3$ cluster formulations in preclinical and clinical tests require enlarged preparation scales and establishment of a simple purification system. Earlier reported procedures suffered from two drawbacks: (i) water solubility of the cross-linker was low, and (ii) scale-up of purification method was difficult. The cross-linker, *N*-succinimidyl 4-(maleimidemethyl) cyclohexane-1-carboxylate (SMCC), would not dissolve in water above 1.6 mM because it had a hydrophobic cyclohexane spacer. We therefore used a more soluble cross-linker. The Hb concentration in the reaction can be increased and the synthesis efficiency improved. Meanwhile the purification method used gel-filtration chromatography (GFC), which limits the maximum separable volume at one time. Generally, a loading sample volume of less than 5 vol% of the gel volume is recommended,[59] which is an impediment to large-scale purification. As a result, we tried to isolate HbBv–HSA$_3$ clusters from the reaction mixture using anion exchange chromatography (AEC).

2.2 Structure and Function of Human Serum Albumin

HSA is a globular protein with a molecular weight of 66,438 Da, and no prosthetic group or glycosylation.[60] It consists of 585 amino acid residues, including 35 cysteine (Cys) residues, 34 residues of which form disulfide bonds (17 pairs), which contributes to the stabilization of

the tertiary structure of HSA. The remaining Cys (Cys-34) is unpaired and has a free sulfhydryl (-SH) group. HSA consists of three homologous domains: I (loops 1–3), II (loops 4–6), and III (loops 7–9) (Figure 2-1). Each domain is categorized by subdomain A and B from the N-terminus: loops 1–2, IA; loops 4–5, IIA (drug-binding site I); loops 7–8, IIIA (site II); loop 3, IB; loop 6, IIB; and loop 9, IIIB, respectively.

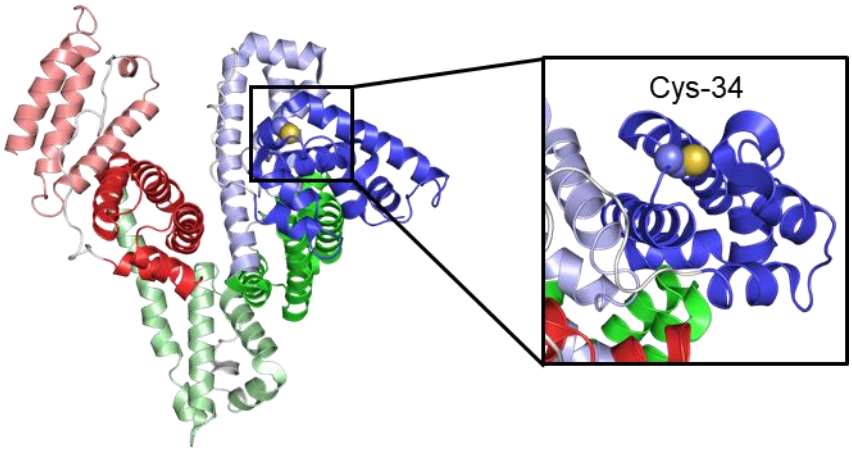

Figure 2-1. Structure of HSA (PDB ID: 1E78) and enlarged view around Cys-34. The color indicates each subdomain; blue: IA, light blue: IB, green: IIA, palegreen: IIB, red: IIIA, pink: IIIB, respectively.

An expression system for recombinant HSA (rHSA) has been established in various species such as *Escherichia coli*,[61,62] *Saccharomyces cerevisiae*,[63] and *Pichia pastoris*.[64] An rHSA formulation as the drug excipient "Recombumin" (Albumedix Ltd.) was approved by the US Food and Drug Administration and by agencies in other countries. Some rHSA formulated as blood expanders are in clinical trials. In addition, HSA exhibits superior retention in the bloodstream, because its strong negative net surface charge (pI: 4.9) inhibits glomerular filtration and blood vessel permeation. Chemical and genetic conjugation with HSA has therefore been commonly used to prolong the blood-circulation lifetime of drugs and therapeutic proteins.[65–69]

2.3 Synthesis of Hemoglobin–Albumin Clusters

2.3.1 Preparation of Highly Purified Hemoglobin from Bovine Blood

A method for preparing highly purified HbBv has been reported previously,[48] but we improved the procedure. Using tangential flow filtration (TFF) to remove RBC membranes allowed us to purify 2 liters of bovine blood, which is equivalent to a 100-fold increase in volume compared with the previous method. SDS-PAGE showed two bands and native-PAGE showed a single band (Figure 2-2). The HbBv concentration was measured using the extinction coefficient of cyano-met Hb assay (ε_{541} = 4.4 × 10^4 M^{-1} cm^{-1}).[70] The HbBv yield was 52% from washed RBC (wRBC).

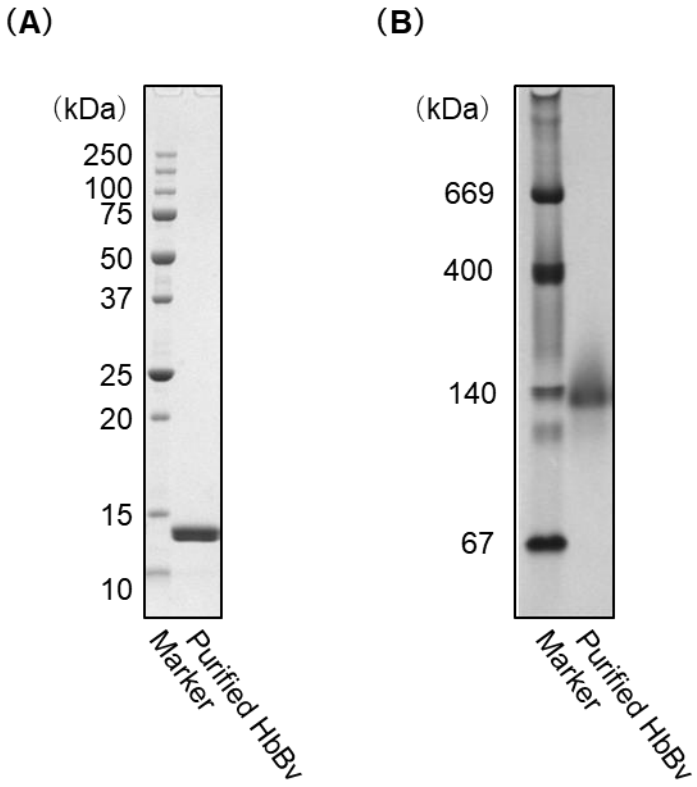

Figure 2-2. (A) SDS-PAGE and (B) native-PAGE patterns of HbBv.

2.3.2 Synthesis of Hemoglobin–Albumin Clusters

Komatsu *et al*. previously reported synthesizing core-shell structured-protein clusters

comprising an Hb in the center and HSA at the periphery in the form of Hb–HSA$_3$ clusters.[18,48] The conventional cross-linker *N*-succinimidyl 4-(maleimidomethyl) cyclohexane-1-carboxylate (SMCC) shows low solubility in water. We employed *N*-succinimidyl 3-maleimidopropionate (SMP, Figure 2-3A) with a high water solubility to achieve the reaction at a high HbBv concentration.[19]

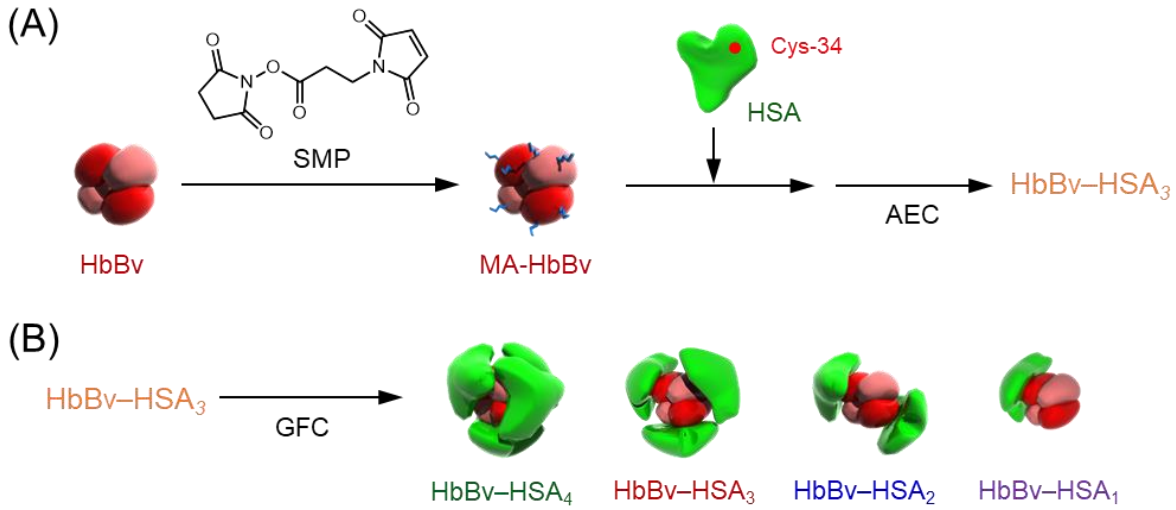

Figure 2-3. (A) A synthetic scheme of the HbBv–HSA$_3$ cluster using the SMP cross-linker and AEC purification. (B) Isolation of individual components of the HbBv–HSA$_3$ cluster by GFC.

SMP was reacted with carbonyl HbBv to yield maleimide-activated HbBv (MA-HbBv). To avoid autoxidation of the hemes in HbBv during the reaction process, carbonyl HbBv was used as a raw material. Subsequently, the maleimide terminals of MA-HbBv were coupled site-specifically with a free sulfhydryl group (Cys-34) of HSA. A cluster formation was confirmed using SEC. Multiple peaks based on the HbBv–HSA$_m$ cluster appeared in the chromatogram of the resulting reaction mixture (retention time 13–18 min, Figure 2-4). The unreacted free MA-HbBv was not detected (retention time 20.3 min), indicating complete reaction of MA-HbBv to the cluster.

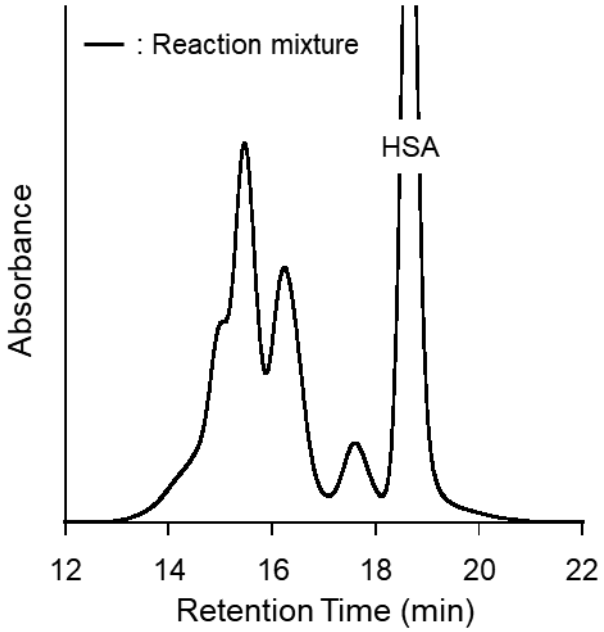

Figure 2-4. SEC profiles of the resulting reaction mixture (MA-HbBv + HSA).

The SMP was soluble in phosphate-buffered saline (PBS) solution containing 9% dimethyl sulfoxide (DMSO) at 13.6 mM, but SMCC did not dissolve at the same concentration. Consequently, the coupling reaction was conducted in 1 mM of HbBv, which is a concentration 10 time that used in the conventional method. The spacer length (5.9 Å) of SMP is short (SMCC: 8.3 Å), and we anticipated that reactivity of Hb would decline. Nevertheless, the cluster was obtained in a condition with 15-fold excess moles of SMP to HbBv, which is 75% of the previously reported amount using SMCC (20-fold moles).[48] Using a similar cross-linking agent, *N*-succinimidyl 4-maleimidobutanoate (SMB), under the same conditions as SMP also yielded a cluster. However, SMB is more expensive that SMP, which is one of the more affordable *α*-maleimide-*ω*-succinimide cross-linking agents.

2.3.3 Experimental Section

Preparation of Highly Purified Hemoglobin from Bovine Blood

Bovine blood was purchased from Tokyo Sibaura Zouki Co. Ltd. Sodium citrate was used as

an anticoagulant. First, the bovine blood in 750 mL bottles (total 2 L, [HbBv] = 12 g/dL) was centrifuged (1,000 *g* at 4 ºC) for 30 min. After removing the plasma component, an equivalent volume of saline solution (Otsuka Pharmaceutical Co., Ltd.) was added and the mixture was centrifuged. This cycle was performed 3 times to obtain wRBC ([HbBv] = 4.2 mM, 0.65 L). The same volume of deionized water (0.65 L) was then added to the wRBC and incubated for overnight at 4 ºC for hemolysis. The suspended solution in 750 mL bottles was centrifuged (4,415 *g* at 4 ºC) for 45 min to precipitate the insoluble RBC membrane components. The obtained red supernatant was filtered through 100 μm and 45 μm stainless-steel sieves. The solution was then filtered through two TFF modules (Pellicon 2 Mini Cassette; Durapore 2 0.22 μm, Biomax 2 300 kDa molecular weight cutoff [MWCO]) using a TFF system (flow rate: 150 mL/min) to remove RBC membrane debris, yielding 1.8 L of HbBv solution. Finally, sufficient carbon monoxide (CO) gas was flowed to prepare carbonyl HbBv. A portion of the solution (0.6 L) in a 1 L round-bottomed flask was heated at 70 ºC for 4 h on a dry aluminum block with stirrer (Tokyo Rikakikai Co., Ltd.), with gentle stirring in a CO atmosphere in the dark to exclude remaining plasma proteins. After centrifugation (4,415 *g* at 4 ºC) for 20 min, the obtained supernatant was dialyzed against deionized water using a membrane tube (6–8 kDa MWCO), followed by the addition of 5.3% (1/19) volume of 20× PBS, yielding 1.4 L of HbBv ([HbBv] = 1.1 mM).

Synthesis of Hemoglobin–Albumin (HbBv–HSA$_3$) Clusters

A freshly prepared DMSO solution of SMP (150 mM, 9.6 mL) was added dropwise to a PBS solution (10 mM phosphate, 137 mM NaCl, pH 7.4) of carbonyl HbBv (1 mM, 96 mL) in a 300 mL round-bottom flask. The mixture was stirred for 90 min in a CO atmosphere at 4 °C. After removing the unreacted excess SMP with a GFC column (Sephadex G-25 superfine; GE Healthcare UK Ltd.) using PBS as running buffer, the volume of the MA-HbBv was adjusted

to 288 mL ([HbBv]= 0.33 mM) by adding PBS. Then, 25% HSA (3.76 mM, 153.2 mL) was diluted by a unique phosphate buffer (PB; 38.8 mL, 58.3 mM sodium phosphate, 435.7 mM NaCl, 13.4 mM KCl, pH 7.2). The PBS solution of HSA (3 mM, 192 mL) was added gradually to the MA-HbBv. Subsequently, the reaction mixture (total 480 mL) was stirred for 72 h in a CO atmosphere in the dark at 4 °C. An HbBv–HSA_3 cluster formation was confirmed using SEC on a high-performance liquid chromatography (HPLC) system (Prominence LC-20AD/CTO-20A/SPD-20A; Shimadzu Corp.) with an SEC column (YMC-Pack Diol-300 S-5; YMC Co. Ltd.) using a 50 mM PB (pH 7.4) as the mobile phase.

The SMP was reacted with surface Lys residues on HbBv. The maleimide terminals of MA-HbBv coupled site-specifically with a free sulfhydryl group (Cys-34) of HSA, yielding the HbBv–HSA_3 cluster.

2.4 Purification of a Hemoglobin–Albumin Cluster using Anion Exchange Chromatography

2.4.1 Purification of the HbBv–HSA_3 Cluster using AEC

In the previously describe method, we separated the HbBv–HSA_3 clusters and unreacted HSA from reaction mixture using GFC (Superdex 200pg. column).[18,48] Although, GFC is a common separation procedure, it suffers from two shortcomings when scaled up. First, the separation efficiency depends strongly on the sample injection volume, and second, each fractionated sample needs to be analyzed to confirm the existence of the target molecules. To overcome these difficulties, we attempted to use AEC, which has been applied widely at industrial scales.[19]

Negatively charged proteins bind strongly to the positively charged AEC gel (Q Sepharose Fast Flow). They are eluted by decreasing the pH and/or increasing the ionic strength of the running buffer. Separating the HbBv–HSA_3 cluster and HSA with very close

isoelectric points (pI) using AEC appeared to be difficult, but an HbBv–HSA$_3$ cluster and HSA are separable only by changing the NaCl concentration of the running buffer. This improved effect is probably attributable to the large surface area of the cluster molecules, which provides multipoint interactions with the cationic gel surface and engenders stronger adsorption compared with HSA.

The HbBv–HSA$_3$ cluster is a mixture of four components with different binding numbers of HSA without unreacted HSA (SEC retention time = 18.7 min, Figure 2-5A). The average number of HSAs per Hb core was ascertained from [total protein]/[HbBv unit] assays to be 3.0 ± 0.2 (mean ± standard deviation [SD]), which is identical to the value of the HbBv–HSA$_3$ cluster prepared using SMCC.[48] The obtained cluster is denoted as HbBv–HSA$_3$ (with an italicized subscript 3). The circular dichroism (CD) spectrum of the HbBv–HSA$_3$ cluster coincided with the sum of the HbBv spectrum and a 3-fold enlarged HSA spectrum (Figure 2-5B). From the 480 mL reaction mixture, the obtained solution volume was 74 ± 6 mL (yield 60 ± 4%, mean ± SD, n = 5, Figure 2-6). The metHb content of the cluster was only 3 ± 1%.

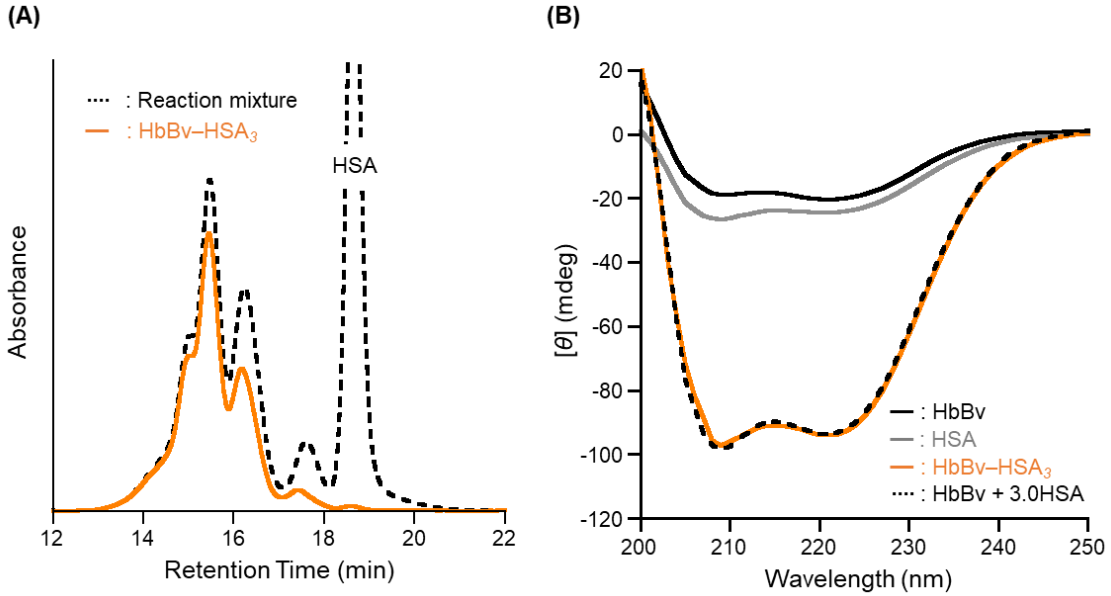

Figure 2-5. (A) SEC profiles of the reaction mixture and HbBv–HSA$_3$ cluster after AEC separation and (B) CD spectra of HbBv–HSA$_3$ cluster, HbBv ([HbBv unit] = 0.2 μM), and HSA (0.2 μM) at 25 ºC.

Figure 2-6. HbBv–HSA$_3$ cluster solution ([HbBv unit] = 5 g/dL in PBS) in 100 mL-bottle.

2.4.2 Isolation of Individual Components of HbBv–HSA$_3$ Clusters

Native-PAGE of the HbBv–HSA$_3$ cluster also revealed four bands with different migration distances (Figure 2-7A). Each component was isolated carefully by GFC using a Superdex 200 pg column (Figure 2-3B, Figure 2-7). The eluent fractions showing a single band in native-PAGE were collected (Figure 2-7A). Each component was checked again using SEC measurements (Figure 2-7B). On the basis of the protein and Hb assay, the HSA/Hb ratios of each component appearing at 15.0, 15.5, 16.2, and 17.5 min in the SEC curve were ascertained to be 4.0, 3.0, 2.0, and 1.0, respectively (Figure 2-7B). From [total protein]/[HbBv unit] assays, native-PAGE, and CD spectroscopy, we identified the individual components as the HbBv–HSA$_4$ heteropentamer, HbBv–HSA$_3$ heterotetramer, HbBv–HSA$_2$ heterotrimer, and HbBv–HSA$_1$ heterodimer (Figure 2-7).

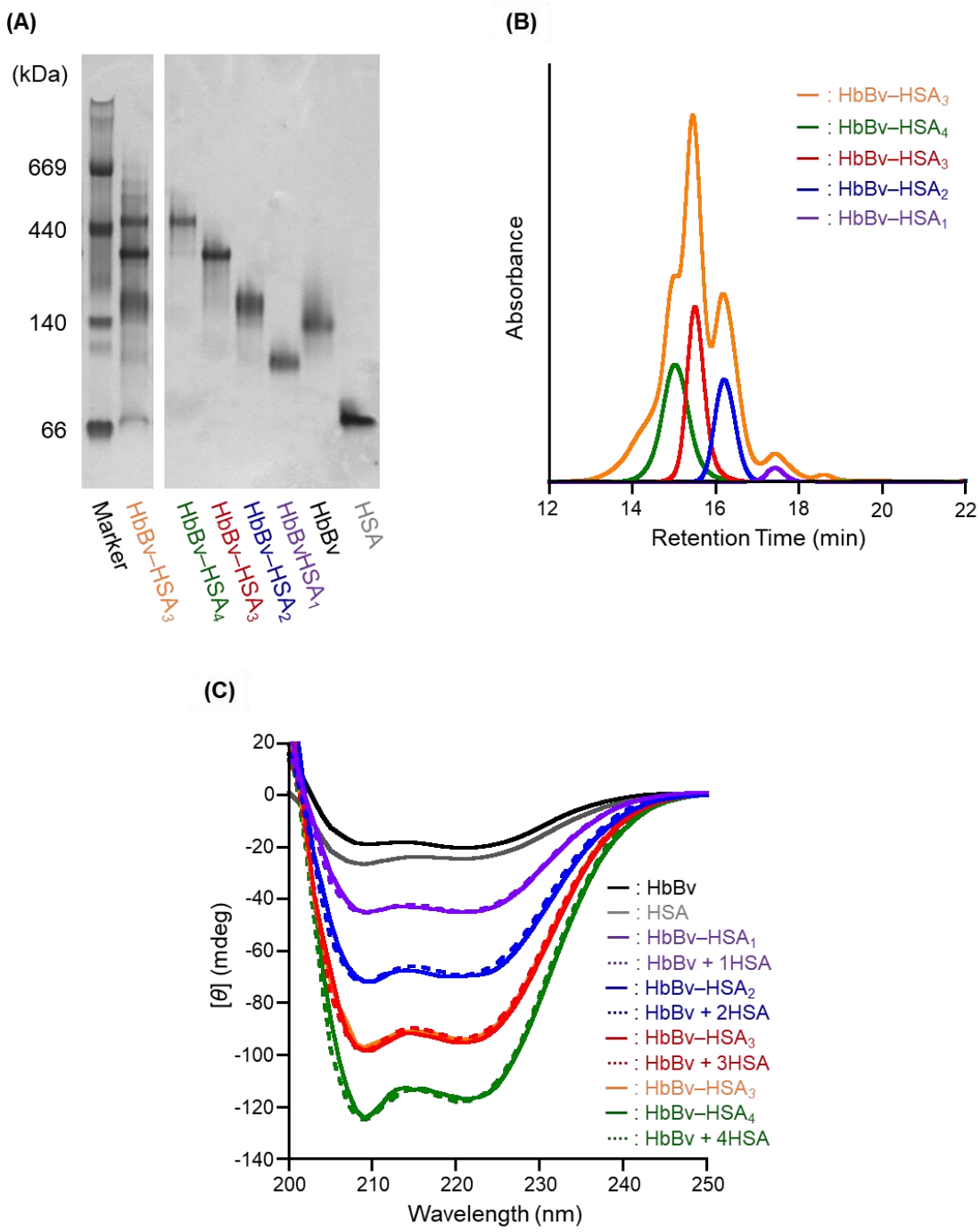

Figure 2-7. (A) Native-PAGE and (B) SEC profiles of HSA, HbBv, HbBv–HSA$_3$ cluster, and its component (50 mM PB, pH 7.4), and (C) their CD spectra ([HbBv unit] = 0.2 μM) at 25 ºC.

The isoelectric points of all the clusters (pI: 5.0) were markedly lower than that of naked HbBv (pI: 7.0), and nearly identical to the value of HSA (pI: 4.9), indicating that the surface charge is independent of HSA number (Figure 2-8). Binding of a single HSA to Hb is

sufficient to reduce the net surface charge to pI 5.0, because HSA is a strong acidic protein.

Dynamic light scattering (DLS) measurements demonstrated that the hydrodynamic diameters of the clusters increased markedly in proportion to the number of the HSA moiety (Table 2-1).

Table 2-1. Average binding numbers of HSA, isoelectric points, and diameters of the HbBv–HSA$_3$ and its components

Hemoprotein	HSA/HbBv ratio (mol/mol)	pI (–)	Diameter (nm)
HbBv	–	7.0	6.4
HSA	–	4.9	8.2
HbBv–HSA$_3$	3.0 (average)	5.0	14.4
HbBv–HSA$_1$	1.0	5.0	9.5
HbBv–HSA$_2$	2.0	5.0	11.4
HbBv–HSA$_3$	3.0	5.0	13.0
HbBv–HSA$_4$	4.0	5.0	14.8

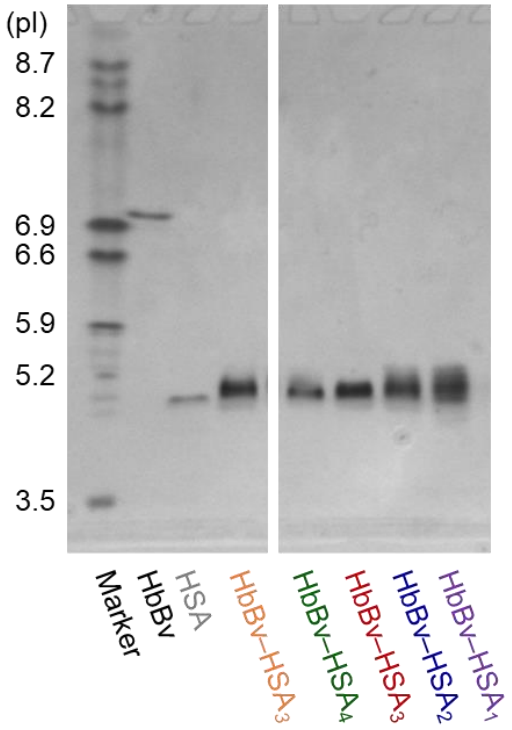

Figure 2-8. IEF patterns of the HbBv–HSA$_3$ and its components.

2.4.3 Experimental Section

Purification of HbBv–HSA$_3$ Clusters using AEC

The reactant (240 mL) of MA-HbBv and HSA was subjected to AEC with a Q Sepharose Fast Flow (500 mL; GE Healthcare UK Ltd.) in a glass chromatography column (5 cm internal diameter, 50 cm length) using PBS as running buffer. After flushing with a 10 mM PB (167 mM NaCl, pH 7.4, five-column volume) to wash out the excess HSA, HbBv–HSA$_3$ was eluted with a 10 mM PB (297 mM NaCl, pH 7.4). The eluent was then dialyzed against deionized water at 4 °C using a TFF system (Pellicon XL Ultrafiltration Module Biomax 30 kDa; Millipore Corp.), followed by the addition of 5.3% volume of 20× PBS. Finally, the HbBv–HSA$_3$ was concentrated ([HbBv unit] = 5 g/dL) using centrifugal ultrafilters (Amicon Ultra 15, 10 kDa MWCO; Merck Millipore Ltd.). The total protein concentration and HbBv concentration were measured using a protein assay kit (Pierce 660 nm; Thermo Fisher Scientific Inc.) and the extinction coefficient of cyano-metHb ($\varepsilon_{541} = 4.4 \times 10^4$ M^{-1} cm^{-1}).

Isolation of Individual Components of HbBv–HSA$_3$ Clusters

The resultant HbBv–HSA$_3$ cluster was subjected to GFC on a fast protein liquid chromatography (FPLC) system (Äkta Prime Plus; GE Healthcare UK Ltd.) with a Superdex 200 pg (HiLoad 26/60; GE Healthcare UK Ltd.) column using a 50 mM PB (pH 7.4) as running buffer. The eluent was monitored at 280 nm and each component was carefully isolated. Fractions showing a single band in native-PAGE were collected. Each component was checked again using SEC measurements.

Native-PAGE was performed using 5–15% poly(acrylamide) precast gel (SuperSep Ace 5–15%; Fujifilm Wako Pure Chemical Corp.). Isoelectric focusing (IEF) was conducted using a pH 3–10 IEF gel (Novex pH 3–10; Thermo Fisher Scientific Inc.). CD spectra were obtained at 25 ºC using a CD spectrometer (J-820; Jasco Corp.). DLS measurements were

conducted using a zeta potential and particle-size analyzer (ELSZ-2000ZS; Otsuka Electronics Co., Ltd.) in a PBS solution (pH 7.4) with a protein concentration of 10 μM at 25 ºC.

2.5 O_2-Binding Property of Hemoglobin–Albumin Cluster

2.5.1 O_2-Binding Property of Hemoglobin–Albumin Cluster

The visible absorption spectral patterns of HbBv–HSA_3 clusters and native HbBv in a PBS solution (pH 7.4) under N_2, O_2, and CO atmospheres (deoxy, oxy, carbonyl forms) were fundamentally equivalent to those of naked HbBv, suggesting that the coordination structures and electronic states of the hemes are identical (Figure 2-9, Table2-2).

Table 2-2. Visible absorption spectral data of HbBv and HbBv–HSA_3 clusters in PBS solution (pH 7.4) at 25 ºC

Hemoprotein	λ_{max} (nm)		
	oxy	deoxy	carbonyl
HbBv	414, 541, 577	430, 555	420, 538, 569
HbBv–HSA_3	414, 541, 577	430, 556	420, 538, 569

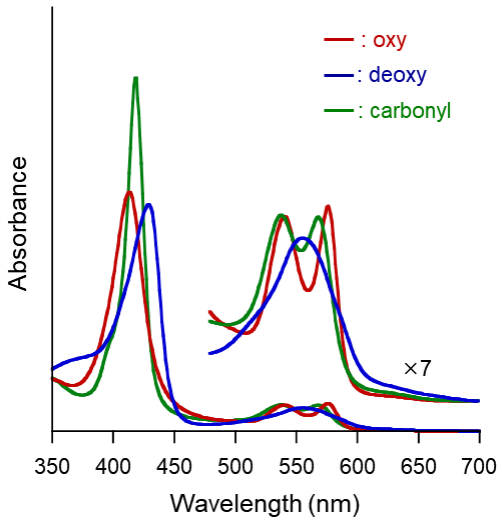

Figure 2-9. Visible absorption spectral changes of the HbBv–HSA_3 cluster in PBS solution (pH 7.4) at 25 ºC.

The P_{50} and n value of the HbBv–HSA$_3$ cluster were 9 Torr and 1.4, respectively (Figure 2-10, Table 2-3). These values show moderately high O_2 affinity compared with naked HbBv (P_{50} = 23 Torr, n = 2.6). Individual cluster components showed the same P_{50} and n values. No clear dependence on the HSA binding number was observed in the O_2-binding parameters. We inferred two structural reasons for high O_2 affinity of the HbBv–HSA$_3$ cluster. The first involved the masking of a sulfhydryl group of Cys-β93 in HbBv by the maleimide terminus of SMP. Blocking of Cys-β93 is known to attenuate the quaternary structure motion of Hb and enhance O_2 affinity.[71–73] This result is consistent with the findings reported by Rosa *et al*. and Acharya *et al*. that chemical modification of Cys-β93 of HbA reduces P_{50} and n values.[71,72] The second reason is the modification of surface Lys residues of Hb by the succinimide terminal of SMP. Palmer *et al*. and Winslow *et al*. demonstrated that HBOCs in which the surface Lys residues were chemically modified possess markedly higher O_2 affinity than that of naked Hb.[39,74] The MA-HbBv showed the same O_2 affinity (P_{50} = 9 Torr, n = 1.4) as the HbBv–HSA$_3$ cluster. We inferred that chemical modification of SMP interfered with the transformation of the relaxed (R)-state conformation (oxy and carbonyl forms) of the Hb core to the tense (T)-state conformation (deoxy form) with low O_2 affinity.

Table 2-3. O_2-binding parameters of HbBv–HSA$_3$ cluster and its components in PBS solution (pH 7.4) at 37 ºC

Hemoprotein	P_{50} (Torr)	n (–)
HbBv	23	2.6
HbBv–HSA$_3$	9	1.4
HbBv–HSA$_1$	9	1.5
HbBv–HSA$_2$	9	1.4
HbBv–HSA$_3$	9	1.4
HbBv–HSA$_4$	9	1.4

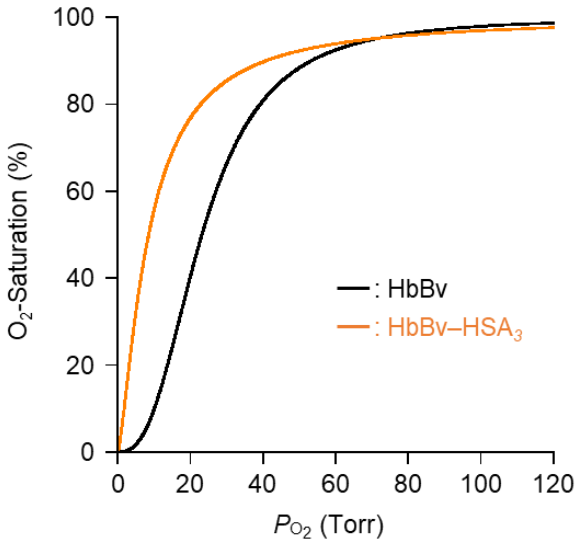

Figure 2-10. O_2-dissociation curves of HbBv and HbBv–HSA$_3$ clusters in PBS solution (pH 7.4) at 37 ºC.

2.5.2 Experimental Section

The visible absorption spectra of HbBv and HbBv–HSA$_3$ clusters ([HbBv unit] = 3 μM) were measured in carbonyl, oxy, and deoxy forms. To prepare the oxy form, carbonyl Hb in a PBS solution (pH 7.4) was irradiated using a 50 W LED lamp while O_2 gas flowed through. The oxy Hb in a PBS solution was deoxygenated in an N_2 atmosphere by adding 20 μM sodium dithionite. HbBv–HSA$_3$ clusters were prepared with the identical procedure.

The O_2 affinity (P_{50}: O_2 partial pressure, where the Hb is 50% saturated) and the Hill coefficient (n) were determined using an automatic recording system for the O_2-dissociation curve (Hemox Analyzer; TCS Scientific Corp.) in PBS (pH 7.4) at 37 ºC ([HbBv unit] = 10 μM).

2.6 Chromogenic LAL Assay of LPS in Hemoglobin–Albumin Cluster

2.6.1 Chromogenic LAL Assay of LPS in Hemoglobin–Albumin Cluster

Bacterial endotoxin lipopolysaccharide (LPS) derived from the exterior cell membrane of Gram-negative bacteria is universally contaminated by trace amounts in distilled water and all

aqueous solutions in the laboratory.[75] LPS causes pyrogenic and shock reactions in host organisms. Therefore, the amounts of LPS in physiological solutions intended for intravenous injection are strictly specified.[76] For HBOC formulations, the LPS content must be measured using a chromogenic Limulus Amoebocyte lysate (LAL) assay, although the charged protein and Hb absorption often hinder quantitative analysis. The high protein concentration inhibits enzyme cascade reactions, leading to a false-negative result. High Hb concentrations, meanwhile, can elevate the visible absorption and lead to false-positive results. The protein concentration of the HbBv–HSA_3 cluster formulation is high (20 g/dL), and the sample must be diluted for measurements.

In general, no standard method is available to remove LPS from a protein solution that is naturally contaminated with LPS.[77,78] SEC and ultrafiltration are unsuitable to exclude LPS with widely various molecular weights (4×10^5 to 1×10^6 Da). Selective adsorption to the cationic polymer resin is applied for protein solutions, but both negatively charged LPS and proteins are adsorbed strongly by the matrix. Given these constraints, various adsorbents of aminated cellulose beads have been developed.[79,80] They provide high removal efficiency of LPS and high recovery yields of the protein.

In this study, the author prepared a sample solution of HbBv–HSA_3 cluster, which was passed through a chromatography column with poly(ε-lysine)-immobilized cellulose beads (Cellufine ET-clean L; JNC Corp.). We measured the LPS content in the effluent by chromogenic LAL assay.[81] Results demonstrated that (i) the eluent must be diluted by a factor of 1000 to avoid inhibition by the protein itself and HbBv absorption, (ii) one-shot passing of the 20 mg/mL cluster through the column chromatography can remove LPS efficiently, (iii) the LPS content decreased in proportion to the flow rate (Figure 2-11), and (iv) the LPS content fell below the detection limit of the apparatus (0.0001 endotoxin unit EU/mL) at a flow rate of 0.05 mL/min (recovery yield of the cluster = 94%). However, the dilution ratio of

the measured sample from the original formulation ([protein] = 200 mg/mL) was 10^{-4}. We concluded that the measurement limit of LPS in the HbBv–HSA_3 cluster formulation by chromogenic LAL assay was restricted to 1.0 EU/mL.

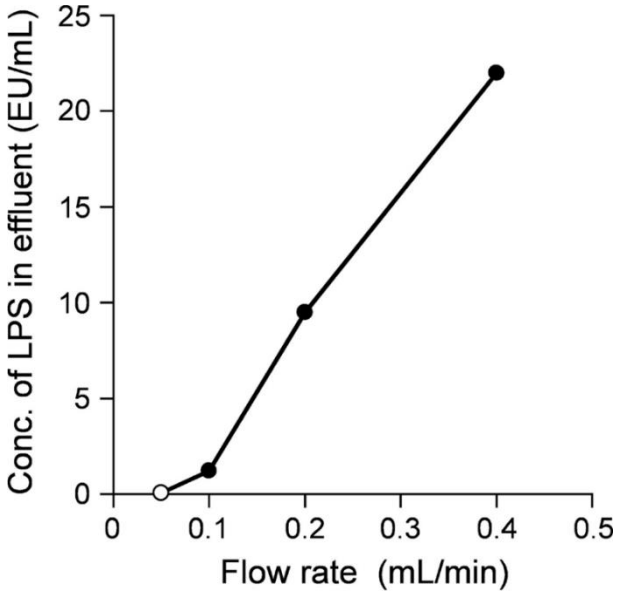

Figure 2-11. Relationship between LPS concentration in the effluent and the flow rate in ET-clean L-column chromatography. The loaded sample ([HbBv–HSA_3] = 20 mg/mL, 20 mL in PBS (pH 7.4), ionic strength μ = 0.16). The sample solution was passed through the column (0.75 cm internal diameter, 2.5 cm length) at 0.4−0.05 mL/min. The white point indicates [LPS] < 0.1 EU/mL.

2.5.2 Experimental Section

A poly(ε-lysine)-immobilized cellulose bead column (Cellufine ET-clean L, approximately 1 mL, 0.75 cm internal diameter, 2.5 cm length; JNC Corp.) was washed with at least a 10-column volume of 0.2 M NaOH and LPS free water. It was then equilibrated with PBS (pH 7.4, ionic strength (μ) of 0.16). The sample solution of HbBv–HSA_3 ([protein] = 20 mg/mL, 20 mL), which was contaminated naturally with LPS, was subjected to the column at flow rates of 0.4−0.05 mL/min. The LPS concentration of the effluent was measured by chromogenic LAL assay[81] using an endotoxin-specific limulus reagent (Endospecy ES-24S

Kit, LAL, < 0.001 EU/mL; Seikagaku Biobusiness Corp.) and observed using a toxinometer (EG Reader SV-12; Seikagaku Corp.).

2.7 Lyophilization of Hemoglobin–Albumin Cluster for Long-Term Storage

2.7.1 Preparation of Lyophilized HbBv–HSA$_3$ Cluster Powder

Lyophilization is one of the most effective procedures to store proteins for extended periods.[82] However, freezing and drying cause denaturation, aggregation, and inactivation. To maintain the protein structure, sugars such as sucrose and trehalose (non-reducing disaccharides) are widely used as lyoprotectants.[82–86] Nevertheless, the dioxygenated HbBv core in the cluster gradually oxidizes to ferric metHb, even at 4 °C, and eventually loses its O_2-transporting ability. If the HbBv–HSA$_3$ cluster solution was lyophilized without protein denaturation and metHb formation, the obtained powder and regenerated solution can be expected to be used in medical applications. The long-term-storable HbBv–HSA$_3$ powder allows us to provide an RBC substitute by adding only water at any time.

To prevent unfavorable oxidation, we added sucrose and trehalose, which are extensively used as lyoprotectants (5 g/dL; [sugar]/[protein] = 0.25 g/g or 15 g/dL; [sugar]/[protein] = 0.75 g/g), to the HbBv–HSA$_3$ cluster solution and lyophilized the resultant mixture, yielding a homogeneous pink powder (Figure 2-12). The powder could be redissolved in water, conferring a clear red solution. Native-PAGE and SEC patterns of the redispersed HbBv–HSA$_3$ cluster were identical to those before freeze-drying. The results imply that the cluster did not aggregate and degrade after redissolving in water.

Figure 2-12. Lyophilized HbBv–HSA$_3$ cluster + sucrose 0.75 g/g.

2.7.2 OxyHb rate and O_2-Binding Property of Lyophilized HbBv–HSA$_3$ Clusters

Long-term storage of HbBv–HSA$_3$ cluster requires suppression of autoxidation of the core Hb. Unfortunately, 20% of HbBv–HSA$_3$ clusters (without any additive) were oxidized by lyophilization (Figure 2-13). The oxyHb rate decreased steadily and reached 50% after 2 months, even at 4 °C. The value continued to decrease more slowly. However, the metHb rate was retarded depending on the amount of sugars. In particular, addition of sucrose 0.75 g/g showed the highest deterrence of metHb formation. The oxyHb rate remained at 94%, even after 2 years. The O_2-binding parameters (P_{50}, n) of HbBv–HSA$_3$ cluster + sucrose 0.75 g/g or trehalose 0.75 g/g (P_{50} = 9 Torr, n = 1.4) were also identical to the value of original solution (Table 2-4).[19,87]

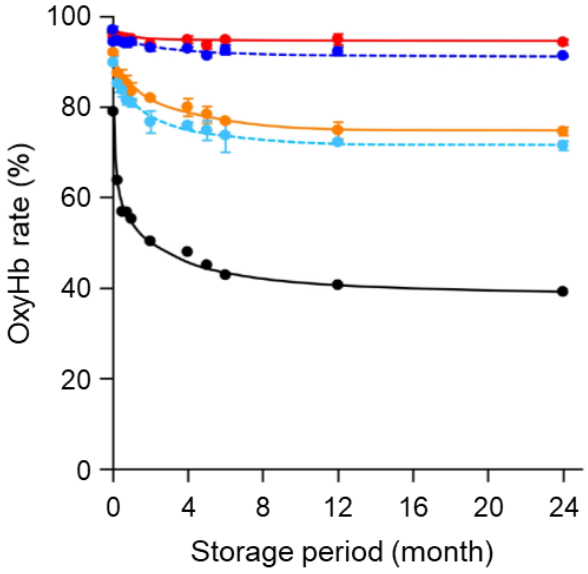

Figure 2-13. OxyHb rate of the lyophilized HbBv–HSA$_3$ cluster containing sugar at 4 °C for 2 years. The HbBv–HSA$_3$ cluster + sucrose 0.75 g/g: red, cluster + sucrose 0.25 g/g: orange, cluster + trehalose 0.75 g/g: blue, cluster + trehalose 0.25 g/g: light blue, cluster without sugar: black.

Table 2-4. O_2-binding parameters of regenerated solution HbBv–HSA$_3$ cluster powder containing sucrose 15 wt% or trehalose 15 wt% after 2 years storage at 37 ºC

Hemoprotein	P_{50} (Torr)	n (–)
HbBv	23	2.6
HbBv–HSA$_3$ before lyophilization	9	1.4
HbBv–HSA$_3$ + Sucrose 0.75 g/g	9	1.4
HbBv–HSA$_3$ + Trehalose 0.75 g/g	9	1.4

2.7.3 Characterization of Lyophilized HbBv–HSA$_3$ Clusters with CD Spectroscopy and FTIR Spectroscopy

CD spectral patterns and intensities of the HbBv–HSA$_3$ cluster + sucrose 0.75 g/g and HbBv–HSA$_3$ cluster + trehalose 0.75 g/g were unaltered before and after lyophilization (Figure 2-14). Furthermore, they coincided closely with the sum spectra of an HbBv and 3-fold enlarged HSA. We concluded that the secondary structure of HbBv–HSA$_3$ cluster was maintained in the presence of sucrose 0.75 g/g or trehalose 0.75 g/g.

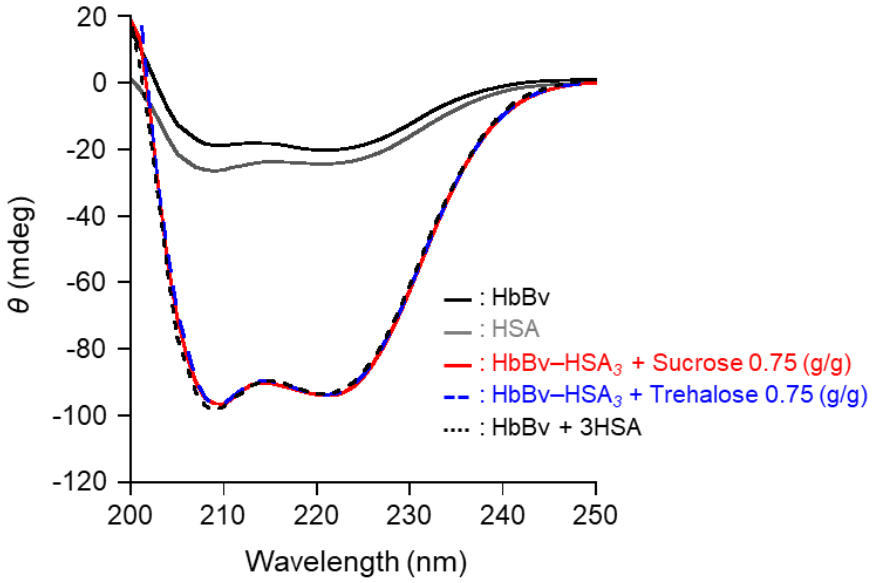

Figure 2-14. CD spectra of HbBv solution, HSA solution, and regenerated aqueous solution of lyophilized HbBv–HSA_3 cluster containing sucrose 0.75 g/g or trehalose 0.75 g/g after 2 years of refrigerator storage. These samples were measured at 25 °C.

Generally, lyophilization of protein without a stabilizer denatures the 3-D structure of the protein by disrupting hydrogen bonds and causing denaturation and aggregation.[83,84] The O_2 coordinated with the heme in Hb is also stabilized by the hydrogen bond, with a distal His in the heme pocket.[88] Distortion of the heme pocket by dehydration induces oxidation of the heme.[84] The coexistence of sucrose or trehalose preserves the protein structure in a natural conformation by creating hydrogen bonds instead of hydrate water molecules (water replacement theory).[82,83,89] These protein-sugar interactions were confirmed by observation of hydrogen bonds between carboxylate groups of amino acids (Asp, Glu) and hydroxyl groups of sugar using infrared (IR) spectroscopy. Carpenter *et al.* reported that the antisymmetric COO^- stretching band, $\nu_{as}(COO^-)$, of the protein carboxylate formed a hydrogen bond with sugar and appeared at 1600–1580 cm^{-1}.[90,91] We measured IR spectra of the lyophilized powder of HbBv–HSA_3 + sucrose 0.75 g/g and HbBv–HSA_3 + trehalose 0.75 g/g (Figure 2-15). In the D_2O solution of HbBv–HSA_3 cluster, the $\nu_{as}(COO^-)$ bands were observed at

1580 cm^{-1}. The freeze-drying HbBv–HSA_3 cluster in the presence of sucrose 0.75 g/g or trehalose 0.75 g/g resulted in retention of the carboxylate band (1579 cm^{-1}). In contrast, the corresponding band was not detectable in lyophilized HbBv–HSA_3 powder without an additive. The wavenumbers of $\nu_{as}(COO^-)$ observed in HbBv–HSA_3 (+ sucrose or trehalose) powder were relatively lower than those of lysozymes and α-lactalbumin (1584–1582 cm^{-1}).[90,91] We reasoned that this could be attributed to the difference in Asp and Glu contents.[92,93] HSA possesses more Glu than Asp (Glu/Asp = 1.7), whereas lysozymes and α-lactalbumin have more Asp than Glu (Asp/Glu = 2–4) (Table 2-5). Consequently, the peak position of $\nu_{as}(COO^-)$ was governed by Glu (1567 cm^{-1}) in the HbBv–HSA_3 cluster and the values of others are governed by Asp (1584 cm^{-1}). Our results revealed that the addition of sucrose 0.75 g/g or trehalose 0.75 g/g allowed us to prepare homogeneous powder of lyophilized HbBv–HSA_3 clusters with original structural conformation and O_2-binidng properties.

Table 2-5. Number of aspartate (Asp) and glutamate (Glu) in proteins

Protein	Asp	Glu
Lysozyme C (chicken)	7	2
α-lactalbumin (bovine)	13	6
Hemoglobin (bovine)	34	26
Human serum albumin	36	62
HbBv–HSA_3	142	212

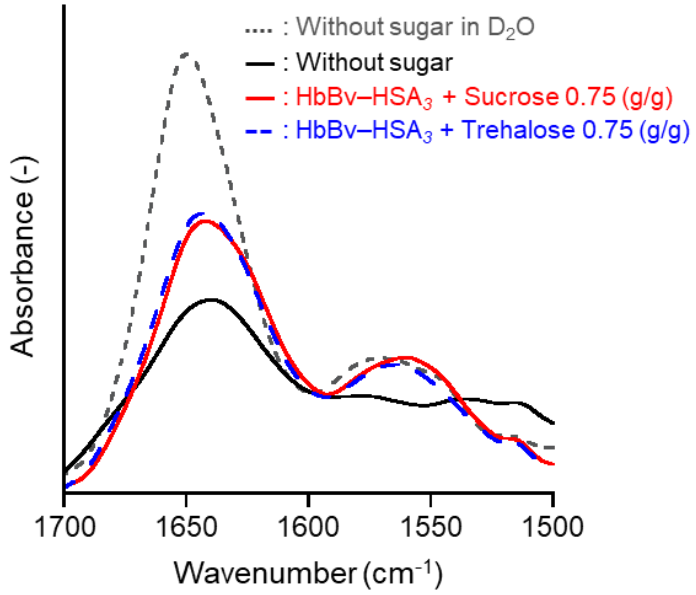

Figure 2-15. IR spectra of an HbBv–HSA_3 cluster solution in D_2O (gray dotted line) and lyophilized powder of an HbBv–HSA_3 cluster; without sugar (black solid line), + sucrose 0.75 g/g (red solid line), + trehalose 0.75 g/g (blue dashed line).

Cleland *et al*. and Gieseler *et al*. investigated the relationship between an additive amount of sugar and the preservation stability of monoclonal antibodies and HSA.[94,95] They concluded that 360 mol/mol (or more) of sugar is necessary to lyophilize the proteins without denaturation. In our case of 0.75 g/g, the molar ratios of sucrose and trehalose to HbBv–HSA_3 clusters were 565 and 517 mol/mol, respectively. These values were sufficient to maintain the 3-D structure of the protein. By contrast, 0.25 g/g, which corresponds to the molar ratio of 188 and 170 mol/mol, respectively, for sucrose and trehalose, was unable to protect the HbBv–HSA_3 cluster, and the core Hb was partially oxidized.

We supposed that trehalose shows superior protective ability compared with sucrose, because the glass transition temperature (T_g) of trehalose (117 °C) is higher than that of sucrose (65 °C).[96] Unexpectedly, the addition of sucrose was effective for both 0.25 g/g and 0.75 g/g. Lerbert *et al*., using a molecular dynamics simulation, reported that the number of hydrogen bonds between lysozyme and sucrose was larger than the value in trehalose.[97] The

T_g of sucrose also reportedly rises to 90–115 °C in the presence of phosphate.[98] We inferred that these reasons enhanced the protection effect of sucrose on HbBv–HSA*3* clusters.

2.7.4 Experimental Section

Preparation of Lyophilized HbBv–HSA*3* Cluster Powder

A carbonyl HbBv–HSA*3* cluster in PBS solution (pH 7.4) ([HbBv unit] = 5 g/dL) was prepared according to our previously reported procedure.[19] The solvent was replaced to 10 mM PB (pH 7.4) using centrifugal filters (Amicon Ultra-15, 10 kDa MWCO). The phosphate concentration was almost adjusted to the value in PBS to maintain the pH at 7.4. The carbonyl HbBv–HSA*3* cluster in PB was oxygenated by light irradiation and O_2 gas aeration. To the oxy HbBv–HSA*3* cluster solution ([HbBv unit] = 5 g/dL), sucrose or trehalose (5 g/dL; [sugar]/[protein] = 0.25 g/g, 15 g/dL; [sugar]/[protein] = 0.75 g/g) was added and the mixture was gently shaken to dissolve the sugar. The resultant solutions were frozen at −20 °C for 1 h and in liquid N_2 bath for 5 min. Subsequently they were freeze-dried under reduced pressure for 14 h using a freeze dryer (FDU-1200; Tokyo Rikakikai Co., LTD.), yielding a lyophilized pink powder of oxy HbBv–HSA*3* cluster.

O_2-Binding Property of Lyophilized HbBv–HSA*3* Clusters

The lyophilized powder of the HbBv–HSA*3* cluster (+ sucrose or trehalose) stored in refrigerator (4 °C) was dissolved in water to regenerate an aqueous sample solution ([HbBv unit] = 10 μM). The oxyHb rate of HbBv–HSA*3* cluster was calculated from absorption intensity at 630 nm based on ferric metHb.[19] After the absorption spectral measurement of the sample, 40 mM $K_3Fe(CN)_6$ (6 μL) was added ([$K_3Fe(CN)_6$]/[HbBv unit] = 16 mol/mol) to prepare 100% ferric met HbBv–HSA*3*. The O_2-binding parameters (P_{50}, n) were determined from the O_2-dissociation curve using an automatic recording system for the O_2-equilibrium

curve (Hemox Analyzer; TCS Scientific Corp.) at 37 °C.

Characterization of Lyophilized HbBv–HSA$_3$ Clusters with CD and FTIR Spectroscopy

The lyophilized powder of an HbBv–HSA$_3$ cluster (+ sucrose or trehalose) was dissolved in water to regenerate an aqueous sample solution ([HbBv unit] = 0.2 μM) for CD spectral measurements. CD spectra were recorded using a CD spectrometer (J-820; Jasco Corp.) at 25 ºC.

The lyophilized powder of an HbBv–HSA$_3$ cluster (+ sucrose or trehalose) was dissolved in D_2O and incubated for 24 h to exchange hydrogen and deuterium (H/D exchange). IR spectrum of the sample solution was measured by a Fourier-transform infrared (FTIR) spectrometer (FT/IR-4000; Jasco Corp.) using a CaF_2 cell (0.025 mm path length; Jasco Corp.). After the H/D exchange, the solution was freeze-dried as described above. The measurements of the solid samples were conducted using an FTIR spectrometer (Cary 630 FTIR; Agilent Technologies Inc.) equipped with attenuated total reflection apparatus in an argon atmosphere in a glovebox. The wavenumber of $\nu_{as}(COO^-)$ was determined from the second derivative of the original spectrum.

2.8 Conclusions

Using a cross-linker SMP, we performed the coupling reaction of HbBv and HSA at high protein concentrations to synthesize HbBv–HSA$_3$ clusters. Purification using AEC can effectively separate HbBv–HSA$_3$ clusters (pI 5.0) and unreacted HSA (pI 4.9). These improvements allowed us to prepare 74 ± 6 mL of HbBv–HSA$_3$ cluster formulations at one time. These techniques are expected to become the basis of production procedures at a scale of several tens of liters at a pilot plant. The HbBv–HSA$_3$ cluster and its components showed identical O_2 affinity, implying that the O_2-binding property of the cluster is unaffected by the

HSA binding number. The measurement limit of LPS in the HbBv–HSA_3 cluster formulation by chromogenic LAL assay was found to be 1.0 EU/mL. The addition of sucrose 0.75 g/g (15 wt%) and trehalose 0.75 g/g (15 wt%) to the HbBv–HSA_3 cluster solution allowed us to prepare lyophilized powder in which oxyHb rate was retained for 2 years in a refrigerator at 4 °C. The long-term-storable HbBv–HSA_3 cluster powder is anticipated to become a useful artificial O_2-carrier that can be regenerated to a desired concentration by adding water and transported anywhere at low cost.

Chapter 3

Expression of Recombinant Human Hemoglobin A (Wild-Type) and Synthesis of Recombinant Hemoglobin–Albumin Clusters

3.1 Introduction

Nagai *et al*. first reported recombinant HbA (rHbA) expressed in an *Escherichia coli* host cell in the 1980s.[99,100] It is now recognized that transgenic bacteria systems have some shortcomings: misfolding, remaining N-terminus methionine, and risk of endotoxin (LPS) contamination.[101–103] Hoffman (Somatogen Inc.) and Ho *et al*. reported an α- and β-globin co-expression system with methionine aminopeptidase (Met-AP) co-expression using *E. coli*.[104,105] Several others have reported rHbA expression systems using insect cells of *Spodoptera frugiperda* (Sf-10)[106] and the yeast *Saccharomyces cerevisiae*.[107,108] However, there has been no report on a *Pichia pastoris* system. In this study, the author aimed to establish an rHbA expression system using *P. pastoris* and prepare synthetic HBOC in the form of an rHbA–rHSA$_3$ cluster, independent of donated blood.

3.2 Expression of Recombinant Human Hemoglobin A (Wild-Type) by *Pichia* Yeast

3.2.1 Construction of Recombinant Human Hemoglobin A (Wild-Type) Expression Plasmid Vector

The author described the efficient preparation of an HbBv–HSA$_3$ cluster in Chapter 2. The same approach can be applied to the synthesis of a cluster using HbA, an HbA–HSA$_3$ cluster. However, using HbA–HSA$_3$ requires regularly securing a certain amount of raw HbA from outdated human RBC. If the raw materials of the cluster were replaced with recombinant proteins, an entirely synthetic O_2-carrier could be produced without donated blood. Komatsu *et al*. described human, dog (canine), and cat (feline) expression systems of for serum albumins using methylotrophic (methanol assimilation) *P. pastoris*.[58,109,110]

The aim of the second study was to establish an expression system using *Pichia* for rHbA(wt) with amino acid sequences and a 3-D structure identical to those of native HbA.

Although *Pichia* yeast can be constructed as a secretory system, we prepared an intracellular expression system of rHbA to avoid of the risk of heme oxidation (Figure 3-1).

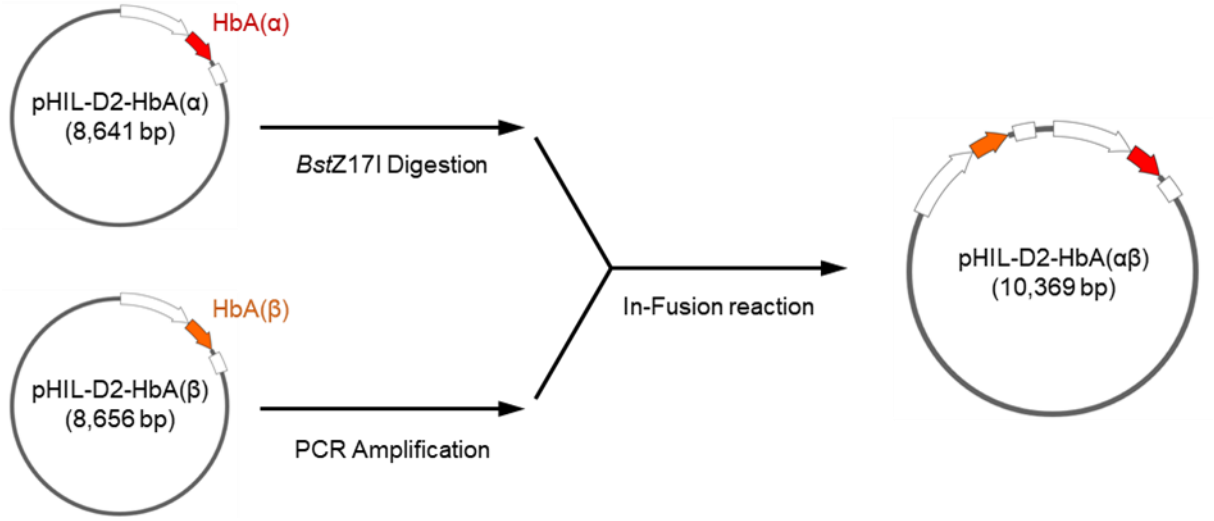

Figure 3-1. Schematic illustration of construction of pHIL-D2-HbA(αβ) expression vector.

An rHbA(wt) expression vector, pHIL-D2-HbA(αβ), was prepared using general procedures with complementary DNA (cDNA) of HbA α- and β-globins. Construction of each vector was checked by agarose-gel electrophoresis. The agarose-gel electrophoresis of the *Hind*III-digested pHIL-D2-HbA(α) and pHIL-D2-HbA(β) showed two bands based on pHIL-D2 fragments and each HbA cDNA region (Figure 3-2). Similarly, agarose-gel electrophoresis of pHIL-D2-HbA(αβ) after an In-Fusion reaction indicated insertion of a 5'AOX1-HbA(β)-3'AOX1(TT) fragment into pHIL-D2-HbA(α) (Figure 3-3). Insertion of the entire HbA α- and β-globins coding region was confirmed using DNA sequencing analysis. Finally, the *P. pastoris* was transformed with linearized pHIL-D2-HbA(αβ) by *Sal*I digestion.

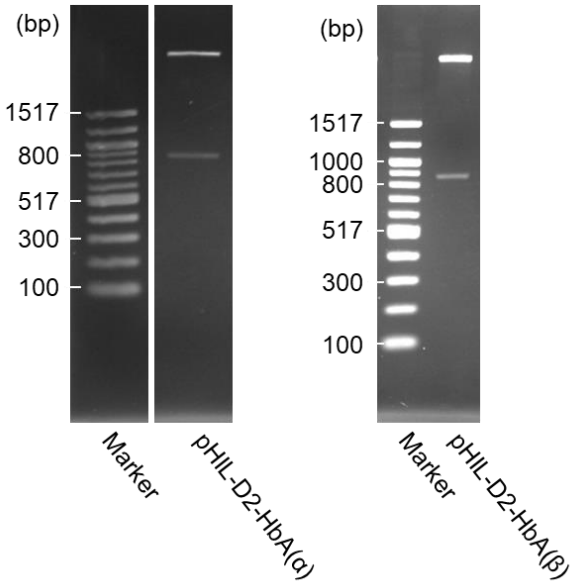

Figure 3-2. Insert check of HbA(α) and HbA(β) regions by 2% agarose-gel electrophoresis of pHIL-D2-HbA(α) and pHIL-D2-HbA(β) by *Hind*III treatment.

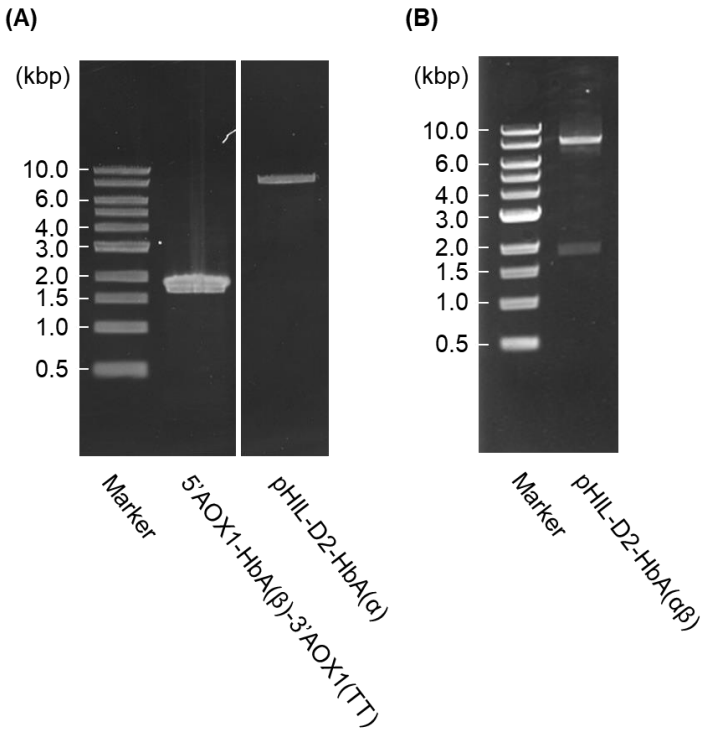

Figure 3-3. The 0.8% agarose-gel electrophoresis of (A) 5'AOX1-HbA(β)-3'AOX1(TT) fragment and linearized pHIL-D2-HbA(α) by *Bst*Z17I treatment, and (B) pHIL-D2-HbA(αβ) fragments digested by *Sac*I.

3.2.2 Expression and Purification of Recombinant Human Hemoglobin A (Wild-Type)

Expression was performed according to a standard protocol using methanol induction with some modification. Specifically, we added hemin to the methanol induction medium. Although the *Pichia* yeast involves a heme biosynthesis pathway, Spadiut *et al*. reported that the addition of hemin to the cultivation medium increased the yield of the target hemoprotein.[111] The rHbA(wt) showed unexpected fluorescence (550–700 nm), which resembles that of Zn(II)-substituted HbA. We inferred that a small amount of apo-protein without heme captures Zn(II)-protoporphyrin IX to generate Zn(II)–rHbA(wt). The addition of hemin (0.3 mM) to the medium rendered the fluorescence intensity negligible, implying that hemin is necessary to produce high yields of rHbA(wt). SDS-PAGE and native-PAGE analysis of rHbA(wt) depicted only two or one band, respectively, in the same positions as those of the α- and β-globins of native HbA (Figure 3-4). The purity of rHbA(wt) calculated by SDS-PAGE was more than 99%.

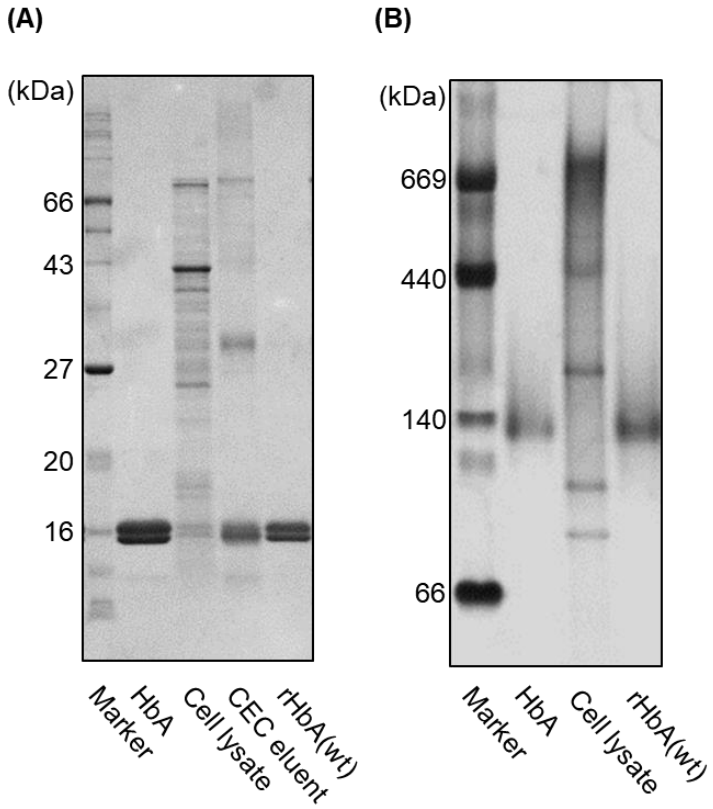

Figure 3-4. (A) SDS-PAGE and (B) native-PAGE patterns of native HbA, cell lysate, and rHbA(wt).

3.2.3 Experimental Section

Construction of a Recombinant Human Hemoglobin A (Wild-Type) Expression Plasmid Vector

The plasmid vectors were constructed by polymerase chain reaction (PCR) using a PrimeSTAR Max DNA polymerase and In-Fusion HD cloning kit (Takara Bio Inc.). The plasmid containing human α-globin [HbA(α)] cDNA, pEx-A2J1-HbA(α) (2,760 bp), and the plasmid containing HbA(β) cDNA, pEx-A2J1-HbA(β) (2,775 base pairs [bp]), were provided by Prof. Satoru Unzai, Hosei University. The full-length of cDNA of HbA(α) and HbA(β) were amplified by PCR using the following oligonucleotide primer set: α-globin forward [5'-TCGAAACGAGGAATTATGGTTCTGTCACCAGCG-3'], α-globin reverse [5'-TGTCTAAGGCGAATTAGCGATATTTGCTGGTCAG-3'], β-globin forward [5'-TCGAAACGAGGAATTATGGTGCATCTGACGCCG-3'], and β-globin reverse [5'-TGTCTAAGGCGAATTAATGGTATTTGTGAGCAAGC-3']. The PCR products were checked by 3% agarose-gel electrophoresis along with a standard marker (100 bp DNA ladder). The amplified fragment was cloned into the *Eco*RI site of the pHIL-D2 plasmid using In-Fusion cloning, yielding pHIL-D2-HbA(α) (8,641 bp) and pHIL-D2-HbA(β) (8,656 bp). Insertion of the entire HbA α- and β-globins coding region was confirmed using DNA sequencing analysis. Next, the expression cassette of the *5'alcohol oxidase 1 (AOX1)-HbA(β)-3'AOX1(TT)* was amplified by PCR using following oligonucleotide primer set: β2-forward [5'-ATAGTTAAGCCAGTAGATCTAACATCCAAAGACGA-3'] and β2-reverse [5'-CGATAGCGGAGTGTAAGCTTGCACAAACGAACTTC-3']. The amplified fragment was subsequently cloned into the *Bst*Z17I site of the pHIL-D2-HbA(α) plasmid using In-Fusion cloning, yielding pHIL-D2-HbA(αβ) (10,369 bp). This plasmid vector was linearized by *Sal*I digestion and introduced into the GS115 strain of *P. pastoris* (Thermo Fisher Scientific K.K.) by electroporation using an Electroporator (MicroPulser; Bio-Rad

Laboratories, Inc.).

Expression and Purification of Recombinant Human Hemoglobin A (Wild-Type)

Expression of rHbA(wt) was conducted by standard protocols provided by Thermo Fisher Scientific K.K. with some modifications. Transformed clone cells were grown in a buffered mineral glycerol-complexes medium (total 4 L) in a shaking incubator (Bio-Shaker G·BR-200; Taitec Corp.) (30 °C, 200 rpm). Subsequently, the growth cell was resuspended in a buffered mineral methanol-complexes medium containing 0.3 mM hemin (Fujifilm Wako Pure Chemical Corp.). To induce expression, the suspension was shaken in an incubator (30 °C, 200 rpm) for 7 days. During the cultivation, methanol (1.5% volume of medium) was added every 24 h. The induced medium was centrifuged and washed with a 20 mM sodium PB (pH 6.0) containing 1 mM phenylmethylsulfonyl fluoride. The cells were then disrupted using a homogenizer (BeadBeater; BioSpec Products Inc.) with 0.5 mm glass beads. After centrifugation (12,000 *g* for 1 h), the obtained supernatant was flowed through CO gas to avoid rHbA(wt) oxidation. The lysate was subjected to CEC with an SP Sepharose Fast Flow (GE Healthcare UK Ltd.) using 20 mM PB (pH 6.0) as the running buffer. After flushing the same buffer to exclude unnecessary proteins and contaminated nucleic acids, the rHbA(wt) was eluted with 50 mM Tris-HCl (pH 8.0) and loaded onto AEC with a Q Sepharose Fast Flow (GE Healthcare UK Ltd.) using 50 mM Tris-HCl (pH 8.0). The rHbA(wt) was eluted by PBS (pH 7.4). The rHbA(wt) was dialyzed against the PBS solution using centrifugal filters (Amicon Ultra 15, 10 kDa MWCO; Merck Millipore Ltd.) and transferred into a 50 mL glass flask sealed with a rubber septum. After the CO gas flowed into the flask to prepare carbonyl rHbA(wt), the solution was heated at 70 ºC for 2 h with gentle stirring in the dark. Finally, the resulting solution was centrifuged (3000 *g* at 4 ºC) for 20 min to remove the precipitate.

3.3 Structure and O_2-Binding Property of Recombinant Human Hemoglobin A (Wild-Type)

3.3.1 Structure of Recombinant Human Hemoglobin A (Wild-Type)

The CD spectrum of rHbA(wt) coincided with that of native HbA (Figure 3-5), suggesting that their secondary structures are equivalent.

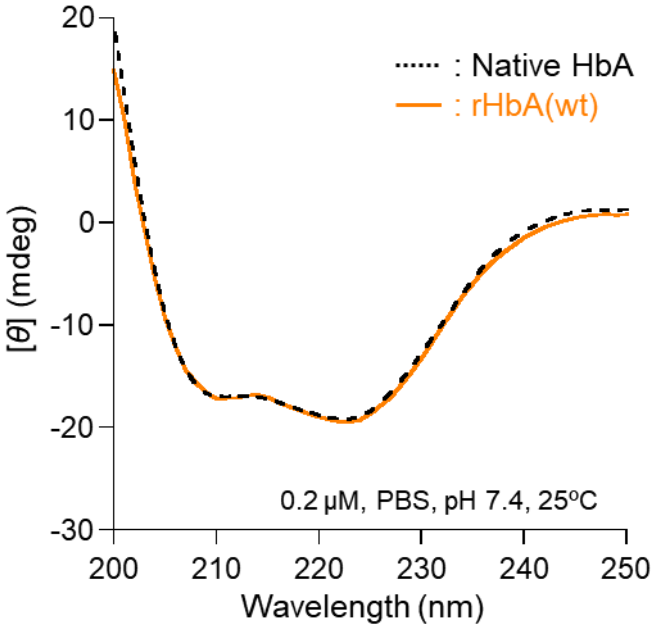

Figure 3-5. The CD spectra of native HbA (black dotted line) and rHbA(wt) (orange solid line) in a PBS solution (pH 7.4) at 25 °C.

When expressed in *E. coli*, rHbA(wt) contains an abnormal isomer in which the asymmetric prosthetic heme group is rotated 180° to the α-δ axis of porphyrin (Figure 3-6A).[112,113] This reversed heme form of rHbA(wt) exhibits high O_2 affinity and low O_2-binding cooperativity. Nagai *et al*. determined the percentage of heme orientation in the rHbA by ^{1}H nuclear magnetic resonance spectroscopy. The CD spectral pattern of carbonyl rHbA and the negative CD band at 413 nm indicated the presence of reversed heme (Figure 3-6B).[113] The visible CD spectrum of our rHbA(wt) after AEC showed a small negative band at 413 nm. The reversed heme ratio in this sample was estimated at 30%. However, in the CD

spectrum of the heat-treated rHbA(wt) sample, the negative CD band disappeared. The whole spectrum was identical to that of native HbA. This suggests that the two heme orientations were aligned in their natural form, which is thermodynamically favored.

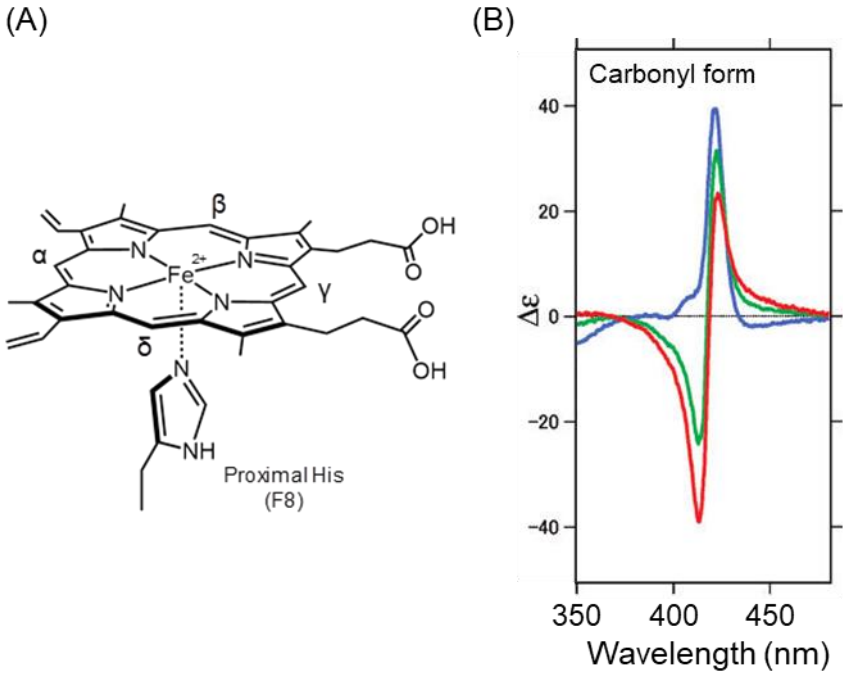

Figure 3-6. (A) The chemical structure of normally heme orientation and proximal His in HbA, (B) CD spectra of each fraction in SP column (percentage of normally orientation; blue: 88%, green: 49%, red: 14%, respectively).[113]

Matrix-assisted laser desorption/ionization time-of-flight (MALDI-TOF) mass spectrum of the rHbA(wt) showed molecular ion peaks at 15,128 and 15,869 Da, which were almost identical to those of theoretical masses of the α- and β-globins, respectively (± 0.02%) (Table 3-1). These results indicate that the extra N-terminal methionine was cleaved completely.

Table 3-1. MALDI-TOF mass spectral data of rHbA(wt) (mean ± SD, *n* = 3)

Sample	Observed (Da)	Calculated (Da)
α-globin	15,128.1 ± 0.6	15,126
β-globin	15,869.3 ± 1.3	15,867

By crystallizing carbonyl rHbA(wt) under a microgravity environment in the Japanese Experimental Module "Kibo" of the International Space Station (ISS), the 3-D structure of carbonyl rHbA(wt) was revealed by X-ray diffraction measurement at 2.3 Å resolution. Crystals of carbonyl rHbA(wt) belong to the monoclinic space group $P\ 1\ 2_1\ 1$ (Table 3-2). As expected, the superimposed images of rHbA(wt) (PDB ID: 6KYE) and carbonyl native HbA (PBD ID: 2DN3)[114] illustrate the near-identical configurations of the 4 subunits (Figure 3-7A). Root mean square deviation value of the polypeptide C_α atoms of these proteins was within 0.51 Å. We confirmed that the N-terminates of α- and β-globins are both valines, and the heme orientations are aligned in the normal form. Typical salt bridges in the triads of carbonyl HbA (Asp-$\alpha_1$94, Trp-$\beta_2$37, and Asn-$\beta_2$102), which stabilize the R-state conformation,[114] were also definitively identified in carbonyl rHbA(wt) (Figure 3-7B).

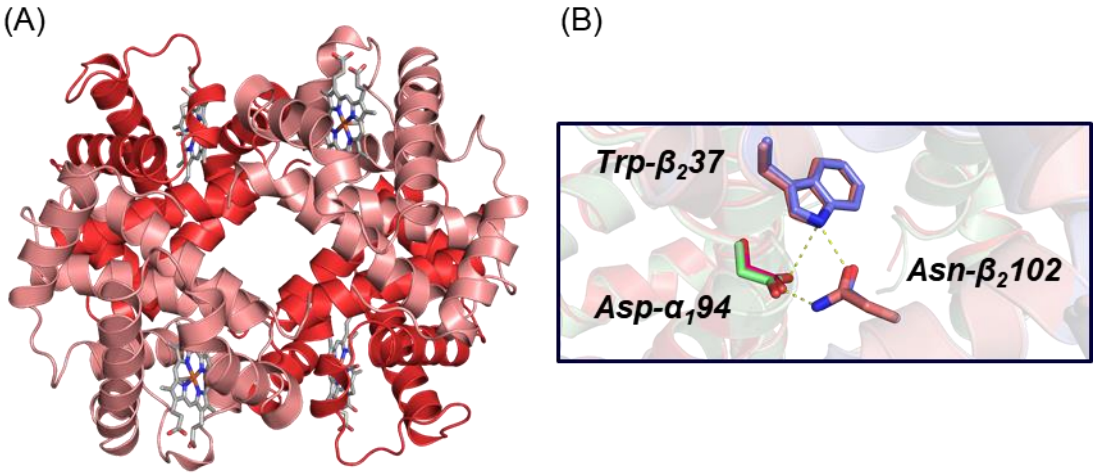

Figure 3-7. (A) X-ray crystallography of carbonyl rHbA(wt) (PDB ID: 6KYE; α-globin: red, β-globin: pink), and (B) superimposed structure of carbonyl native HbA (PDB ID: 2DN3) and carbonyl rHbA(wt), which are characteristic salt bridges stabilizing the R-state.

Table 3-2. X-ray crystallography data collection and refinement statistics of rHbA(wt)

Wavelength (Å)	1.0000
Resolution range (Å)	48.42–2.28 (2.33–2.28)
Space group	$P\ 1\ 2_1\ 1$
Cell dimensions	a = 123.031 Å, b = 55.947 Å, c = 133.156 Å α = 90.00°, β = 98.27°, γ = 90.00°
Total reflections	233,642
Unique reflections	80,208 (12,565)
Multiplicity	2.9 (2.9)
Completeness (%)	97.6 (93.6)
Mean I/sigma (I)	5.4 (0.7)
R_{meas}	0.17 (1.984)
R_{pim}	0.095 (1.116)
CC(1/2)	0.993 (0.338)
Refinement	
Resolution range (Å)	48.42–2.28
No. reflections	80,196
R_{work}/R_{free}	0.226/0.268
No. atoms	
Amino acids	13085
Ligands	540
Waters	139
B-factors	
Amino acids	54.41
Ligands	49.46
Waters	43.19
RMS (bonds)	0.0039
RMS (angles)	1.337
Ramachandran favored (%)	95.98
Ramachandran outliers (%)	0.18
Clashscore	6.28

Statistics for the highest-resolution shell are shown in parentheses.

3.3.2 O_2-Binding Parameters of rHbA(wt)

The visible absorption spectral patterns of rHbA(wt) under N_2, O_2, and CO atmospheres (deoxy, oxy, carbonyl forms) were fundamentally equivalent to those of native HbA (Figure 3-8A, Table 3-3). The O_2-dissociation curves of rHbA(wt) and native HbA in a PBS solution (pH 7.4, at 37 °C) also showed close agreement. The P_{50} and the Hill coefficient (n) of rHbA(wt) were 11 Torr and 2.3, respectively (Figure 3-8B). O_2-complex stability of rHbA(wt) in PBS solution (pH 7.4) was evaluated using the autoxidation rate constant (k_{ox}) at 37 °C. The k_{ox} value of rHbA(wt) was determined to be 0.028 h^{-1} (Table 3-4), which is a similar value to that of native HbA (k_{ox} = 0.020 h^{-1}). We concluded that the maximum absorption wavelength (λ_{max}), P_{50}, n, and k_{ox} values of rHbA(wt) were almost identical to those observed for native HbA.

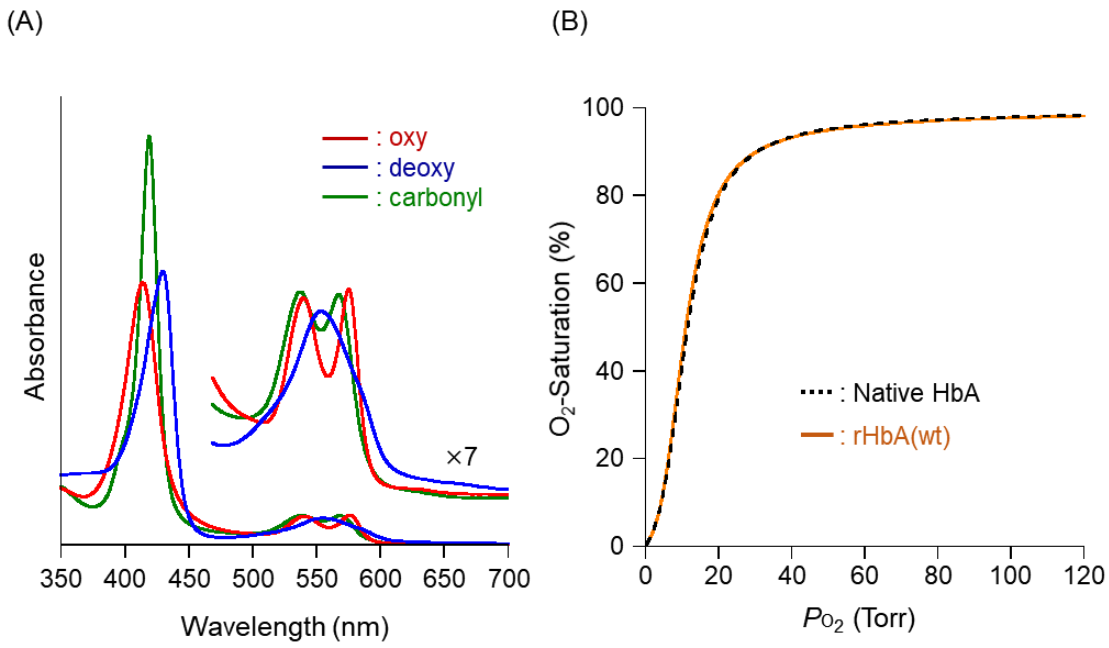

Figure 3-8. The O_2-binding properties of the rHbA(wt). (A) Visible absorption spectra of the rHbA(wt) in oxy (red), deoxy (blue), carbonyl (green) forms in a PBS solution (pH 7.4) at 25 °C, (B) O_2-dissociation curves of native HbA (black dotted line) and rHbA(wt) (orange solid line) in PBS solution (pH 7.4) at 37 °C.

Table 3-3. The UV-visible spectral data of native HbA and rHbA(wt) in PBS solution (pH 7.4) at 25 °C

Sample	λ_{max} (nm)		
	oxy	deoxy	carbonyl
Native HbA	414, 541, 577	430, 555	420, 539, 569
rHbA(wt)	415, 541, 576	430, 555	419, 539, 569

Table 3-4. The O_2-binding parameters of native HbA and rHbA(wt) in PBS solution (pH 7.4) at 37 °C

Hemoprotein	P_{50} (Torr)	n (–)	k_{ox} (h^{-1})
HbA	12	2.4	0.020
rHbA(wt)	11	2.3	0.028

3.3.3 Experimental Section

CD Spectroscopy and Mass Spectroscopy of rHbA(wt)

The secondary structure and heme orientation of rHbA(wt) were confirmed by CD spectroscopy using a CD spectrometer (J-820; Jasco Corp.). The rHbA(wt) concentration of the sample was adjusted to [HbA] = 0.2 μM in PBS solution (pH 7.4) for the far-ultraviolet CD region (200–250 nm) and [HbA] = 3 μM in PBS for the visible CD region (230–500 nm), respectively, at 25 °C. The mass spectra were obtained using a MALDI-TOF mass spectrometer (ultrafleXtreme; Bruker Japan K. K.).

Crystallization, Data Collection, and Structure Determination of Recombinant Human Hemoglobin A (Wild-Type)

The crystallization of rHbA(wt) was conducted in the “Kibo” module of the ISS. The solution samples were launched aboard a Progress MS-11 spacecraft (72P) from the Baikonur Cosmodrome (Kazakhstan). Crystal growth in space was performed in a portable space freezer, FROST2, in Kibo. Red crystals (0.15 × 0.05 × 0.05 mm) grew from a 20 mg/mL protein solution in 26% PEG3350, 0.2 M NaCl, and 0.1 M MES (pH 6.0) at 293 K. After the

grown crystals returned to Earth aboard the Soyuz MS-11 spacecraft (57S), they were flash-frozen in liquid N_2. XRD data were collected using an EIGER X 16M (Dectris USA Inc.) detector with a synchrotron radiation source at the SPring-8 beamline BL41XU (Hyogo, Japan). All data were collected at 100 K and processed with XDS (Table 3.4).[115] The rHbA(wt) structure was ascertained using molecular replacement with PHASER in CCP4.[116,117] The native carbonyl HbA structure (PDB ID: 2DN3) was used as the search model.[118] The sequence assignment of the atomic model was conducted using the amino acid sequence for HbA [UniProt ID: P69905; HbA(α), P68871; HbA(β)]. Further iterative model-building and refinement were performed using refmac and COOT.[119–122] Atomic coordinates of the rHbA(wt) structure reported in this study were deposited in the PDB under accession code 6KYE. All molecular images were produced using PyMOL (Schrödinger LLC).

O_2-Binding Property of rHbA(wt)

The preparation of oxy and deoxy forms was conducted by the same procedure as with HbBv. To prepare oxy rHbA(wt), O_2 gas was flowed to the PBS solution of the carbonyl rHbA(wt) ([HbA] = 3 μM, 3 mL) in a 10 mm optical quartz cuvette sealed with a rubber septum under LED light irradiation (50 W) in an ice-water bath. Then, N_2 gas was flowed continuously and 20 μM sodium dithionite (in a PBS solution) was added to the oxy form solution, yielding deoxy rHbA(wt). The autoxidation rate constant (k_{ox}) of the rHbA(wt) was determined from absorption intensity at 630 nm with time under aerobic conditions at 37 °C.[123] The O_2-binding parameters (P_{50}, n) were ascertained from the O_2-dissociation curve, which was observed by an automatic recording system for the O_2-equilibrium curve (Hemox Analyzer) in PBS (pH 7.4) at 37 °C ([HbA] = 10 μM).

3.4 Synthesis of Recombinant Hemoglobin–Albumin Cluster

3.4.1 Synthesis of rHbA(wt)–rHSA$_3$ Cluster

The rHbA(wt)–rHSA$_3$ cluster was prepared according to the procedure described in Chapter 2. The yield of rHbA(wt)–rHSA$_3$ clusters was 58% based on rHbA(wt) (Figure 3-9A). The average binding number of rHSA on the rHbA(wt) core was 3.0 as measured by protein and Hb assays. The CD spectrum of rHbA(wt)–rHSA$_3$ clusters coincided well with the sum of the rHbA(wt) spectrum and rHSA spectrum, which was enlarged by a factor of 3 (Figure 3-9B). The major component of the rHbA(wt)–rHSA$_3$ cluster is a heterotetramer. The 4.5-fold molar excess rHSA was sufficient to synthesize the rHbA(wt)–rHSA$_3$ cluster, because the mercapto rate of Cys-34 in rHSA (as a percentage of free sulfhydryl groups) was higher (by approximately 75%) than that of HSA (40–50%).

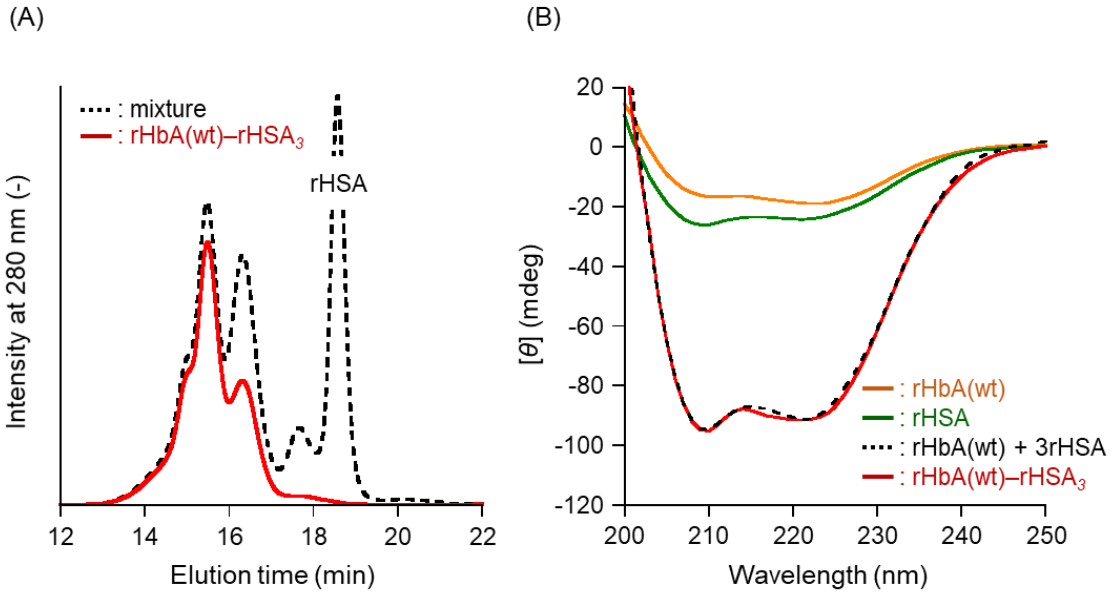

Figure 3-9. (A) SEC profiles of the reaction mixture (black dotted line; MA-rHbA[wt] + rHSA) and rHbA(wt)–rHSA$_3$ cluster (red solid line) and (B) the CD spectra of rHbA(wt) (orange solid line), rHSA (green solid line), rHbA(wt)–rHSA$_3$ cluster (red solid line) in PBS (pH 7.4) at 25 °C.

3.4.2 Experimental Section

A DMSO solution of SMP (150 mM, 0.1 mL) was added dropwise into carbonyl rHbA(wt) (1 mM, 1 mL) in PBS (pH 7.4). After the mixture was stirred for 30 min at 4 ºC, unreacted cross-linkers in the reactant were removed using GFC, and MA-rHbA(wt) was concentrated to 3 mL ([HbA] = 0.33 mM). A PBS solution of rHSA (2.25 mM, 2 mL) was then added to 3 mL of the MA-rHbA(wt) with stirring for 70 h at 4 ºC. Next, 2 mL of the resulting reaction mixture was subjected to AEC with HiTrap Q Sepharose Fast Flow (GE Healthcare UK Ltd.) using PBS as the running buffer. After flushing of PBS containing 30 mM NaCl (pH 7.4) to remove excess rHSA, the rHbA(wt)–rHSA$_3$ cluster was eluted with PBS containing 160 mM NaCl. Finally, the eluent was dialyzed against PBS (pH 7.4) using centrifugal filters (Amicon ultra 15, 10 kDa MWCO). A thiol assay of rHSA was performed by reacting it with 4,4'-dithiopyridine, which binds the sulfhydryl group of the protein to generate 4-thiopyridinone (4-TP, $\varepsilon_{324} = 1.98 \times 10^4$ M^{-1} cm^{-1}).[124]

3.5 O_2-Binding Property of Recombinant Hemoglobin–Albumin Cluster

3.5.1 O_2-Binding Property of Recombinant Hemoglobin–Albumin Cluster

The visible absorption spectral patterns of rHbA(wt)–rHSA$_3$ clusters of deoxy, oxy, and carbonyl forms were identical to those of rHbA(wt) (Table 3-5). By contrast, the P_{50} and the Hill coefficient (n) of rHbA(wt)–rHSA$_3$ clusters (8 Torr, 1.4) showed moderately lower values compared with naked rHbA(wt). (Figure 3-10, Table 3-6). Moreover, the autoxidation rate constant (k_{ox}) value of rHbA(wt)–rHSA$_3$ clusters in PBS (pH 7.4) was 0.038 h^{-1} (Table 3.5), which showed a slightly higher value of rHbA(wt) (k_{ox} = 0.028 h^{-1}), was identical to that of the HbA–HSA$_3$ clusters. The coupling of a cross-linker such as SMP on rHbA(wt) generally increases O_2 affinity and decreases cooperatively. This can be attributed either to chemical modification of the surface Lys group on core Hb or the covalent connection of SMP to the

Cys-β93 in core Hb. Details are described in Chapter 2.

Table 3-5. The UV-visible spectral data of rHbA(wt) and its cluster in PBS solution (pH 7.4) at 25 °C

Sample	λ_{max} (nm) oxy	deoxy	carbonyl
rHbA(wt)	415, 541, 576	430, 555	419, 539, 569
rHbA(wt)–rHSA$_3$	414, 541, 576	430, 555	419, 539, 569

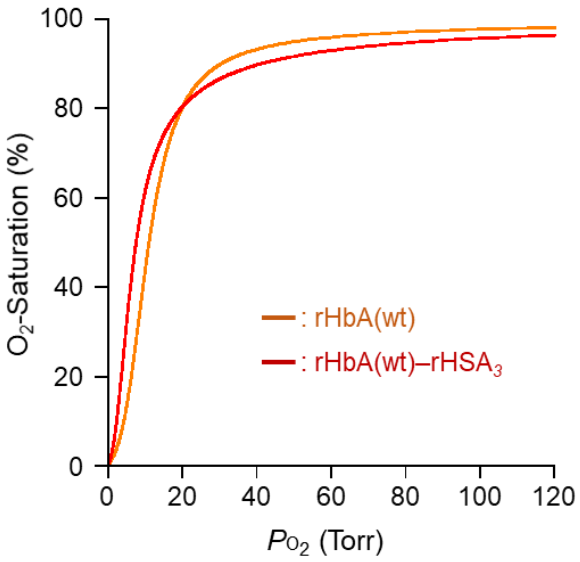

Figure 3-10. The O_2-dissociation curves of rHbA(wt) (orange) and its cluster (red) in PBS solution (pH 7.4) at 37 °C.

Table 3-6. The O_2-binding parameters of native HbA, rHbA(wt), and its clusters in PBS solution (pH 7.4) at 37 °C

Hemoprotein	P_{50} (Torr)	n (–)	k_{ox} (h^{-1})
HbA	12	2.4	0.020
HbA–HSA$_3$	8	1.4	0.038
rHbA(wt)	11	2.3	0.028
rHbA(wt)–rHSA$_3$	8	1.4	0.038

3.5.2 Experimental Section

To prepare oxy rHbA(wt), O_2 gas was flowed to the PBS solution of the carbonyl rHbA(wt)–rHSA$_3$ cluster ([HbA unit] = 10 μM, 3 mL) in a 10 mm optical quartz cuvette sealed with a

rubber septum under a 50 W LED lamp in an ice-water bath. Then, N_2 gas was flowed continuously and 20 μM sodium dithionite (6 μL) was added to the oxy form solution, yielding deoxy an rHbA(wt)–rHSA$_3$ cluster. The autoxidation rate constant (k_{ox}) of the rHbA(wt)–rHSA$_3$ cluster was determined from the absorption intensity at 630 nm with time under aerobic conditions at 37 °C. O_2-binding parameters (P_{50}, n) were determined using a Hemox Analyzer at 37 °C.

3.6 Conclusion

We established an rHbA(wt) expression system using *P. pastoris* and a purification procedure. The heme orientation disorder was aligned to the norm by heating at 70 °C. The structure of rHbA(wt) coincided perfectly with that of native HbA, as confirmed by MALDI-TOF spectroscopy, CD spectroscopy, and X-ray crystal structural analysis. The ultraviolet (UV)-visible absorption pattern and O_2-binding property of rHbA(wt) were also identical to those of native HbA. We synthesized an rHbA(wt)–rHSA$_3$ cluster, and revealed that its structure and O_2-binding parameters were identical to those reported for an HbA–HSA$_3$ cluster. The genetically engineered rHbA(wt)–rHSA$_3$ cluster is independent of donated blood, and is expected to serve as an entirely synthetic RBC substitute and O_2-therapeutic reagent.

Chapter 4

Synthesis of Recombinant Hemoglobin–Albumin Clusters with a Genetically Engineered Heme Pocket

4.1 Introduction

The O_2 affinity of rHbA(wt)–rHSA$_3$ clusters (P_{50} = 8 Torr) is somewhat higher than that of human RBC (P_{50} = 25 Torr). We believe that regulation of O_2 affinity is useful not only for blood transfusion but other O_2-based therapeutic applications as well. There are two approaches to reducing the O_2 affinity of rHbA. First, disruption of the R-state–stabilizing salt bridges by mutagenesis moves the quaternary structure of Hb transition to the T state, which has low O_2 affinity. For example, Hb Kansas (βN102T) and Hb Titusville (αD94N) are T-state–stabilizing abnormal forms of Hb, in which the R-state–stabilizing salt bridge between Asp-α94 and Asn-β102 is disrupted.[125–127] Second, introduction of the mutation in the heme pocket decreases O_2 affinity. Hydrogen bonds between distal His (E7 position: α58, β63) and the coordinated O_2 molecule,[128–130] and Leu at B10 position (α29, β28) affect steric hindrance to O_2 binding.[131–133] In the Hb–HSA$_3$ cluster, control of O_2 affinity by the T-R transition was difficult, because the core Hb was fixed in a near R-state.[87] Therefore, we used the second approach and prepared 4 rHbA variants, replacing Leu-β28 and/or His-β63 with Phe (rHbA[βL28F]), Trp (rHbA[βL28W]), Gln (rHbA[βH63Q]), Tyr/Gln (rHbA[βL28Y/βH63Q]), respectively (Figure 4-1). Furthermore, their clusters have been synthesized.

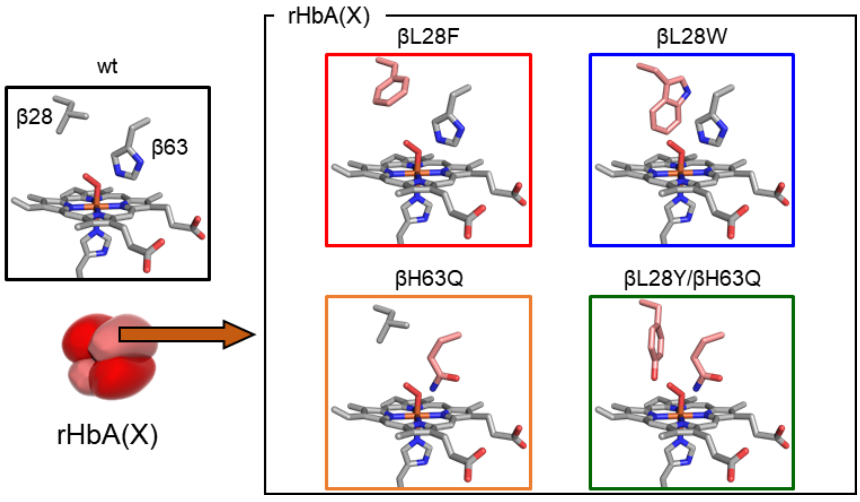

Figure 4-1. Structure of the mutated position of the heme pocket in β-globin.

4.2 Expression of Recombinant Hemoglobin with a Mutated Heme Pocket

4.2.1 Mutagenesis and Expression of rHbA Variants

The construction of 4 rHbA(X) (X = βL28F, βL28W, βH63Q, and βL28Y/βH63Q) variant expression plasmids was performed by site-specific mutation using a QuikChange II XL site-directed mutagenesis kit (Agilent Technologies Inc.). A sequence analysis revealed that all the plasmids included the target codon sequence. The rHbA(X) variant expression plasmids were linearized by *Sal*I and transformed *P. pastoris* (GS115 strain), by electroporation, as with rHbA(wt).

Expression and purification of all rHbA(X) variants were carried out following a procedure similar to that used for rHbA(wt). However, purification of rHbA(βL28W) was conducted without heat treatment because its denaturation temperature (T_m) in carbonyl form was 65 °C, which is 13 °C lower than that of native HbA (T_m = 78 °C) (Table 4-1). The T_m values were determined from CD spectral changes to be 25 °C to 90 °C at 222 nm of α-helices. It is described in detail in the experimental section.

Table 4-1. Denaturation temperature and set temperature for heat treatment of each rHbA(X) variants

Hemoglobin	Denaturation temp. (°C)	Heating temp. (°C)
Native HbA[a]	78	–
rHbA(βL28F)	73	70
rHbA(βL28W)	65	–
rHbA(βH63Q)	71	68
rHbA(βL28Y/βH63Q)	68	61

[a] Ref. 134.

SDS-PAGE of each rHbA(X) variant depicted only two bands, which were in positions identical to those of native HbA (Figure 4-2). The CD spectral patterns of 3 rHbA(X) variants (X = βL28F, βL28W, and βH63Q) were identical to that of native HbA (Figure 4-3). Only rHbA(βL28Y/βH63Q) showed a CD spectral pattern that was slightly different from that of

native HbA. In general, the CD spectrum of α-helical structure has two characteristic negative peaks at 208 nm (π-π* parallel transition) and 222 nm (*n*-π* transition).[135] Doig and Hirst reported that Tyr conformation affects the intensity of CD at 220 nm within ± 5000 deg·cm^2 dmol^{-1}.[136,137] We inferred that rHbA(βL28Y/βH63Q) exhibited different CD spectral pattern from other rHbA(X)s.

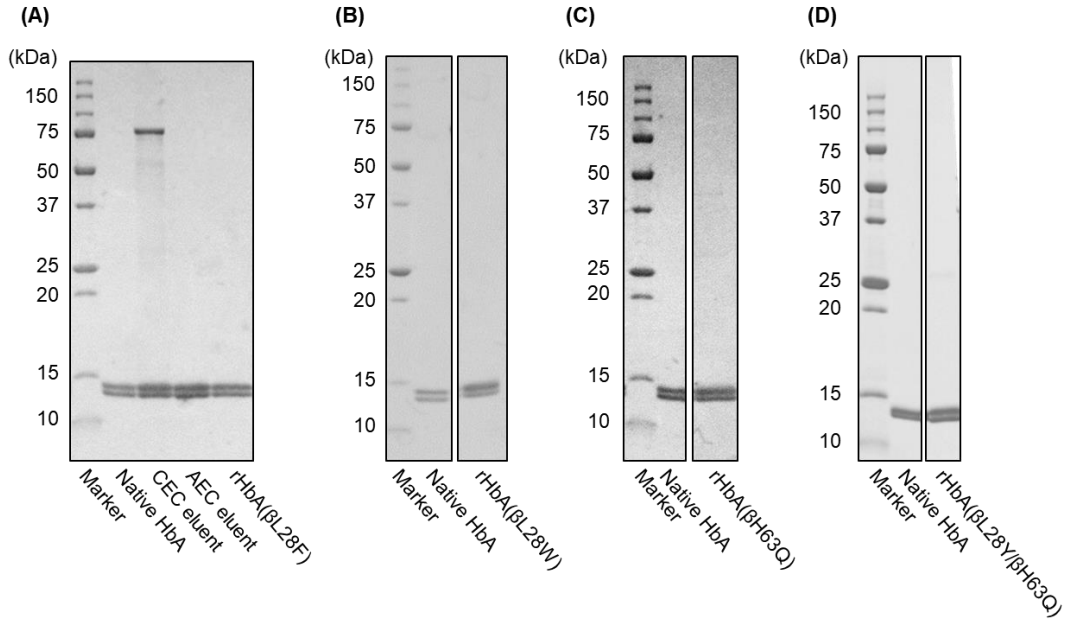

Figure 4-2. SDS-PAGE analysis of native HbA and rHbA(X) variants: (A) rHbA(βL28F), (B) HbA(βL28W), (C) rHbA(βH63Q), and (D) rHbA(βL28Y/βH63Q).

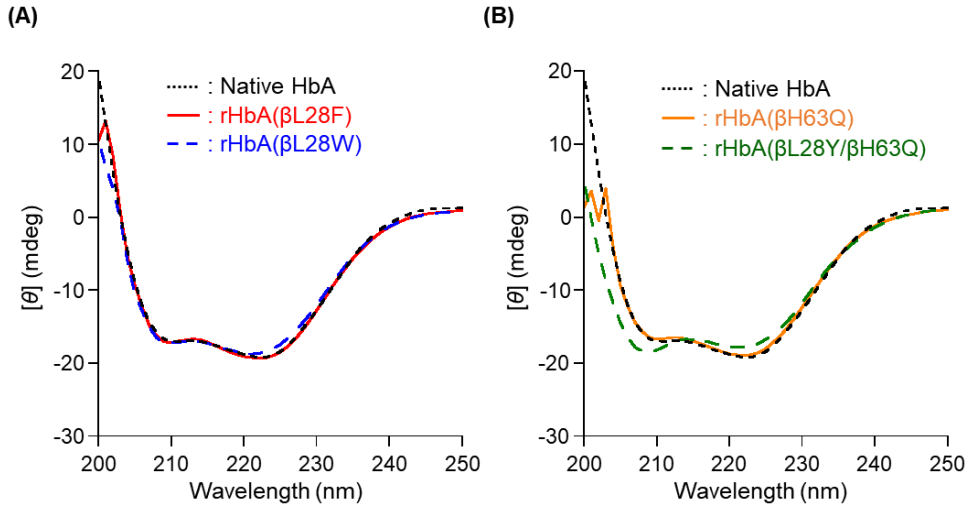

Figure 4-3. CD spectra of native HbA and rHbA(X) variants in PBS (pH 7.4) at 25 °C. (A) Native HbA: black dotted line; rHbA(βL28F): red solid line; rHbA(βL28W): blue dashed line. (B) Native HbA: black dotted line; rHbA(βH63Q): orange solid line; rHbA(βL28Y/ βH63Q): green dashed line.

In addition, the MALDI-TOF mass spectra of the 4 rHbA(X) variants (X = βL28F, βL28W, βH63Q, and βL28Y/βH63Q) exhibited almost the same values as those of the theoretical mass of each β-globin mutant (Table 4-2).

Table 4-2. MALDI-TOF mass spectral data of rHbA(X) variants (mean ± SD, *n* = 3)

Hemoglobin	α-globin (Da)		β-globin (Da)	
	Observed	Calculated	Observed	Calculated
rHbA(βL28F)	15,128.1 ± 1.8	15,126.2	15,903.5 ± 1.9	15,901.0
rHbA(βL28W)	15,129.3 ± 0.8	15,126.2	15,942.6 ± 1.1	15,940.1
rHbA(βH63Q)	15,134.6 ± 0.7	15,126.2	15,863.5 ± 3.2	15858.0
rHbA(βL28Y/βH63Q)	15,126.9 ± 0.0	15,126.2	15,909.2 ± 0.1	15,908.0

4.2.2 O_2-Binding Properties of rHbA Variants

Each maximum absorption wavelength (λ_{max}) in oxy, deoxy, and carbonyl forms of four rHbA(X) variants (X = βL28F, βL28W, βH63Q, and βL28Y/βH63Q) exhibited values almost equal to those of native HbA (Table 4-3). The P_{50} values were 32 Torr for rHbA(βL28F), 60 Torr for rHbA(βL28W), 11 Torr for rHbA(βH63Q), and 43 Torr for rHbA(βL28Y/βH63Q) (Table 4-4).

Table 4-3. Visible absorption spectral data of native HbA and rHbA mutants in PBS solution (pH 7.4) at 25 °C

Hemoglobin	λ_{max} (nm)		
	oxy	deoxy	carbonyl
Native HbA	414, 541, 577	430, 555	420, 539, 569
rHbA(βL28F)	415, 541, 577	430, 555	419, 539, 569
rHbA(βL28W)	415, 541, 577	430, 556	419, 538, 569
rHbA(βH63Q)	415, 541, 577	430, 555	419, 540, 569
rHbA(βL28Y/βH63Q)	414, 540, 576	430, 555	420, 539, 569

Table 4-4. O_2-binding parameters of native HbA and rHbA mutants in PBS (pH 7.4) at 37 °C

Hemoglobin	P_{50} (Torr)	n (–)	k_{ox} (h^{-1})
Native HbA	12	2.4	0.020
rHbA(βL28F)	32	1.8	0.122
rHbA(βL28W)	60	1.5	0.075
rHbA(βH63Q)	11	2.0	0.026
rHbA(βL28Y/βH63Q)	43	1.5	0.047

The O_2 affinities (P_{50} values) of the rHbA(X) variants with mutated Leu-β28 were similar to those of the previous reports.[133,138] Olson *et al*. reported O_2-association-rate constants (k_{on}^{O2}) of the rHbA(βL28F) and rHbA(βL28W) mutants in the R-state by laser flash photolysis.[139] The high P_{50} value (low O_2 affinity) of the rHbA(βL28W) mutant can be attributed to the bulky Trp side group (indole ring) at the β28 position, which reduced the room for the distal heme pocket cavity, causing an approximately 4,800-fold reduction in the k_{on}^{O2} value. In contrast, the k_{on}^{O2} value of the α-globin was unchanged. Brunori *et al*. reported that the k_{on}^{O2} value of β-globin in rHbA(βL28Y/βH63Q) was 3.6 times higher than that of native HbA.[140] The Tyr at the β28 position generates a hydrogen bond with Gln at the β63 position, which introduces steric hindrance of O_2-binding to the heme iron.

In the case of the rHbA(βH63Q) mutant, we expected low O_2 affinity similar to opossum Hb [Hb(αH58Q)].[130,141,142] However, our results showed the same O_2 affinity as native HbA.

4.2.3 Experimental Section

Mutagenesis and Expression of rHbA Variants

Site-directed mutagenesis of the rHbA(wt) expression plasmid pHIL-D2-HbA(αβ) employed the standard protocol of the QuikChange II XL kit (Agilent Technologies). All mutagenic primers containing desired mutation were purchased from Fasmac Co., Ltd. (Table 4-5). The

transformation of *Pichia* yeast using the rHbA(X) expression plasmid followed the same procedure used for rHbA(wt).

Table 4-5. Primers used for construction of rHbA(X) variants (X = βL28F, βL28W, βH63Q, and βL28Y/βH63Q)

Primer name	Sequence
βL28F forward	5'-GATGAAGTGGGTGGTGAAGCA**TTT**GGTCGTCTGCTGGTAGTG-3'
βL28F reverse	5'-CACTACCAGCAGACGACC**AAA**TGCTTCACCACCCACTTCATC-3'
βL28W forward	5'-GATGAAGTGGGTGGTGAAGCA**TGG**GGTCGTCTGCTGGTAGTG-3'
βL28W reverse	5'-CACTACCAGCAGACGACC**CCA**TGCTTCACCACCCACTTCATC-3'
βH63Q forward	5'-CCCAAGGTCAAAGCA**CAA**GGGAAGAAAGTCCTGGGCGCG-3'
βH63Q reverse	5'-CGCGCCCAGGACTTTCTTCCC**TTG**TGCTTTGACCTTGGG-3'
βL28Y forward	5'-GATGAAGTGGGTGGTGAAGCA**TAC**GGTCGTCTGCTGGTAGTG-3'
βL28Y reverse	5'-CACTACCAGCAGACGACC**GTA**TGCTTCACCACCCACTTCATC-3'

Expression and column purification of all rHbA(X) variants were conducted by the procedure uses for rHbA(wt). The temperatures during heat treatment process of rHbA(βL28F), rHbA(βH63Q), and rHbA(βL28Y/βH63Q) were set at 70 °C, 68 °C, and 61 °C, respectively, which were 3 °C or lower than their corresponding thermal denaturation temperatures. In the case of rHbA(βL28W) mutants, no heat treatment was conducted because of significant loss by denaturation.

The T_m value is the thermal denaturation temperature at which 50% of the protein secondary structure unfolds.[143] This value was determined from CD spectral changes at 222 nm α-helices. We prepared carbonyl rHbA(X) ([HbA] = 0.5 μM) in PBS (pH 7.4) in a 10 mm optical quartz cuvette sealed with a rubber septum, and CO gas was the flowed in. CD spectral data (25–90 °C) at 222 nm was collected by a CD spectrometer (J-820, Jasco Corp.). The rate of heating was 1 °C/min and the T_m value was the temperature when α fell below 0.5 was calculated by:

$$\alpha = (\theta_t - \theta_U)/(\theta_F - \theta_U),$$

where α is the content ratio of the unfolded form, θ_t is the observed ellipticity at any temperature, θ_F is the ellipticity of the fully folded form (at 25 °C), and θ_U is the ellipticity of the unfolded form at 90 °C.[143]

O_2-Binding Properties of rHbA Variants

Preparation of the oxy and deoxy forms used the procedure for rHbA(wt). To prepare the oxy rHbA(X) variant, O_2 gas was flowed to the PBS solution of the carbonyl rHbA(X) ([HbA] = 3 μM) in a 10 mm optical quartz cuvette sealed with a rubber septum under a 50 W LED lamp in an ice-water bath. N_2 gas was then flowed continuously and 20 μM sodium dithionite (in PBS) was added to the oxy form solution to yield deoxy rHbA(X).The O_2-binding properties (P_{50}, n) were measured by an automatic recording system for the O_2-equilibrium curves (Hemox Analyzer) in PBS (pH 7.4) at 37 °C ([HbA] = 10 μM).

4.3 Synthesis of Recombinant Hemoglobin–Albumin Clusters with a Mutated Heme Pocket

4.3.1 Synthesis of rHbA(X)–rHSA$_3$ Cluster Variants

Preparation of each rHbA(X)–rHSA$_3$ cluster variant was carried out with a method similar to that used for rHbA(wt)–rHSA$_3$ clusters (Figure 4-4). SEC profiles of the reaction mixture of rHbA(βL28W) or rHbA(βL28Y/βH63Q) suggested that reactivity of surface Lys on the rHbA(X) was lower than that of rHbA(wt) (Figure 4-4C). Therefore, we increased the molar ratio of rHSA added to rHbA(X) from 4.5-fold to 10-fold for rHbA(βL28W) and 6-fold for rHbA(βL28Y/βH63Q), respectively. It is described in detail in the experimental section.

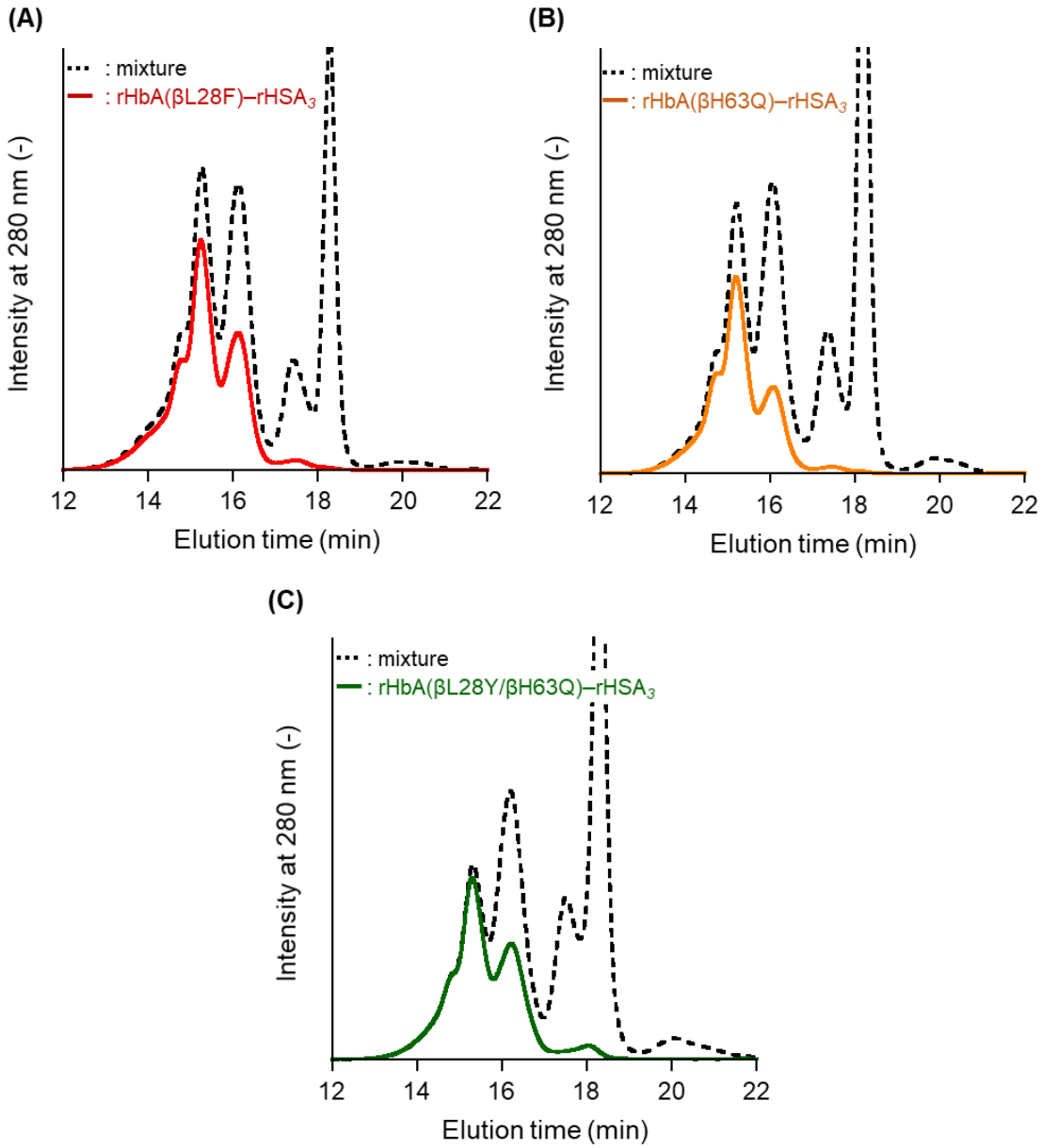

Figure 4-4. SEC profiles of the reaction mixture and rHbA(X)–rHSA$_3$ clusters: (A) rHbA(βL28F)–rHSA$_3$ (red), (B) rHbA(βH63Q)–rHSA$_3$ (orange), and (C) rHbA(βL28Y/βH63Q)–rHSA$_3$ (green).

4.3.2 Experimental Section

Preparation conditions for the two rHbA(X)–rHSA$_3$ clusters (X = βL28F, βH63Q) were identical to that used for rHbA(wt)–rHSA$_3$. However, reactivity of core rHbA(X) (X = βL28W and βL28Y/βH63Q) was reduced compared with rHbA(wt), and the molar ratio of rHSA was therefore increased. For rHbA(βL28Y/βH63Q)–rHSA$_3$ and rHbA(βL28W)–rHSA$_3$,

the additional molar ratio of rHSA to rHbA(X) was increased to 6-fold and 10-fold, respectively.

Synthesis of rHbA(βL28Y/βH63Q)–rHSA$_3$ Clusters

A DMSO solution of SMP (150 mM, 50 μL) was added dropwise to carbonyl rHbA(βL28Y/βH63Q) (1 mM, 0.5 mL) in PBS (pH 7.4). After the mixture was stirred for 1 h at 4 ºC, unreacted cross-linkers in the reactant were removed using GFC and the MA-rHbA(βL28Y/βH63Q) was concentrated to 1.45 mL ([HbA] = 0.35 mM). A PBS solution of rHSA (2.85 mM, 1.05 mL) was the added to MA-rHbA(βL28Y/βH63Q) with stirring for 72 h at 4 ºC ([rHSA]/[rHbA] = 6 mol/mol).

Synthesis of rHbA(βL28W)–rHSA$_3$ Cluster

A DMSO solution of SMP (150 mM, 50 μL) was added dropwise to carbonyl rHbA(βL28W) (1 mM, 0.5 mL) in PBS (pH 7.4). After the mixture was stirred for 1 h at 4 ºC, unreacted cross-linkers in the reactant were removed using a centrifugal filter (Amicon Ultra 15, 10 kDa MWCO; Merck Millipore Ltd.). The MA-rHbA(βL28W) was adjusted to 1.246 mL ([HbA] = 0.4 mM). A PBS solution of rHSA (2.85 mM, 1.754 mL) was the added to MA-rHbA(βL28W) with stirring for 72 h at 4 ºC ([rHSA]/[rHbA] = 10 [mol/mol]).

4.4 O_2-Binding Property of Recombinant Hemoglobin–Albumin Clusters with a Mutated Heme Pocket

4.4.1 O_2-Binding Property of Recombinant Hemoglobin–Albumin Cluster with a Mutated Heme Pocket

The maximum absorption wavelengths in oxy, deoxy, and carbonyl forms of rHbA(X)–rHSA$_3$ cluster variants exhibited values almost equal to those of naked rHbA(X) (Table 4-6).

Table 4-6. Visible absorption spectral data of rHbA(X)–rHSA$_3$ cluster variants in PBS solution (pH 7.4) at 25 °C

Hemoprotein	λ_{max} (nm)		
	oxy	deoxy	carbonyl
rHbA(βL28F)–rHSA$_3$	415, 541, 577	430, 556	420, 539, 569
rHbA(βL28W)–rHSA$_3$	414, 541, 576	430, 556	419, 538, 569
rHbA(βH63Q)–rHSA$_3$	415, 541, 576	430, 556	420, 539, 569
rHbA(βL28Y/βH63Q)–rHSA$_3$	413, 540, 576	430, 556	420, 539, 569

The O_2-binding parameters (P_{50}, n) of rHbA(X)–rHSA$_3$ cluster variants indicated a reducing tendency similar to that of wild-type clusters. The P_{50} and n values of rHbA(βH63Q)–rHSA$_3$ were found to be 8 Torr and 1.4, respectively, which were identical to wild-type cluster values (Table 4-7). The P_{50} values of rHbA(X)–rHSA$_3$ clusters (X = βL28F, βL28W, and βL28Y/βH63Q), were 14 Torr, 24 Torr, and 15 Torr, respectively.

Table 4-7. The O_2-binding parameters of rHbA(X)–rHSA$_3$ cluster variants in PBS solution (pH 7.4) at 37 °C

Hemoglobin	P_{50} (Torr)	n (–)	k_{ox} (h^{-1})
rHbA(βL28F)–rHSA$_3$	14	1.2	0.130
rHbA(βL28W)–rHSA$_3$	24	1.0	0.082
rHbA(βH63Q)–rHSA$_3$	8	1.4	0.040
rHbA(βL28Y/βH63Q)–rHSA$_3$	15	1.1	0.115

The rHbA(X)–rHSA$_3$ cluster variants showed a lower P_{50} and Hill coefficient (n) compared with naked rHbA(X). The reductions can be attributed to the chemical modifications of the carbonyl rHbA(X) by cross-linkers, as in the case of HbBv–HSA$_3$ clusters. First, the chemical modification of surface Lys on carbonyl rHbA(X) fixed the quaternary structure in the R-state (high O_2 affinity). Second, the masking of Cys-β93 in rHbA by the maleimide group of SMP inhibited quaternary structural conversion between the R and T state. However, the O_2 affinity of rHbA(X)–rHSA$_3$ clusters was lower than that of the wild-type cluster. This suggests that replacing the Leu-β28 reduced the O_2 affinity of the

rHbA(X) β-globin in the R-state.

The P_{50} values of the rHbA(X)s (X = βL28F, βL28W, and βL28Y/βH63Q) and their clusters showed a liner dependence on the increment of the side group volume at the β28 position (Figure 4-5).[144] Suppression of T-R structural alterations in core rHbA induced by SMP modification reduced the slope of the clusters relative to that of naked rHbA(X)s.

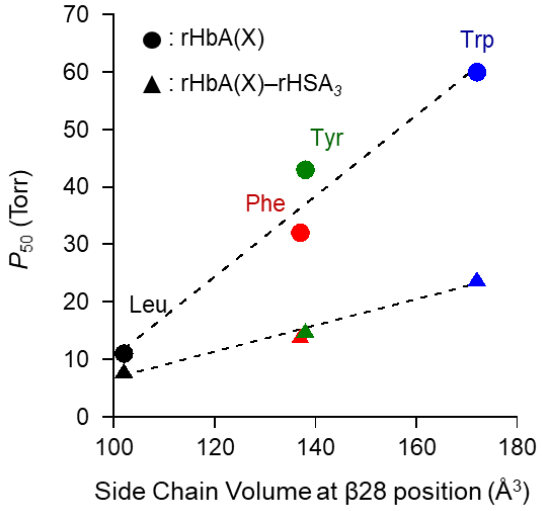

Figure 4-5. Dependence of P_{50} values on the β28 position side-chain volume.[144] The circle symbol denotes rHbA(X), the triangle symbol respresents the rHbA(X)–rHSA$_3$ cluster. rHbA(wt): black; rHbA(βL28F): red; rHbA(βL28W): blue; and rHbA(βL28Y/βH63Q): green.

4.4.2 Experimental section

To prepare oxy forms, O_2 gas was flowed to the PBS solution of the carbonyl rHbA(X)–rHSA$_3$ cluster ([HbA unit] = 10 μM, 3 mL) in a 10 mm optical quartz cuvette sealed with a rubber septum under an LED lamp in an ice-water bath. N_2 gas was then flowed continuously and 20 μM sodium dithionite was added to the oxy form solution to yield deoxy an rHbA(X)–rHSA$_3$ cluster. The autoxidation rate constant (k_{ox}) of the rHbA(X)–rHSA$_3$ cluster was determined from absorption intensity at 630 nm with time in aerobic conditions a 37 °C, which was based on metHb formation. O_2-binding parameters (P_{50}, n) were determined by a Hemox Analyzer in PBS (pH 7.4) at 37 °C.

4.5 Conclusion

We prepared 4 rHbA(X) variants in which the β-globin heme pocket was mutated by site-directed mutagenesis. The O_2 affinity of rHbA(X)–rHSA$_3$ clusters (X = βL28F, βL28W, and βL28Y/βH63Q) was moderately higher (as measured by P_{50} value) than that of rHbA(wt)–rHSA$_3$ clusters. By replacing the Leu-β28 position of core Hb with bulky amino acid residues, we tuned the O_2 affinity of the cluster. The P_{50} values of these clusters exhibited linear dependence on the side-chain volume at the β28 position. In particular, the P_{50} value of rHbA(βL28W)–rHSA$_3$ clusters was 24 Torr, which was almost identical to the RBC value. The estimated O_2-transporting efficiency of rHbA(βL28W)–rHSA$_3$ cluster between lungs (100 Torr) and muscles (40 Torr) was also the same as that of RBC (18%). We expect that various rHbA(X)–rHSA$_3$ clusters with different O_2 affinities could be used for diverse clinical applications.

Chapter 5

Evaluations of Hemoglobin–Albumin Cluster by Animal Experiments

5.1 Introduction

By establishing large-scale preparation of HbBv–HSA_3 clusters, it was possible to evaluate safety and efficacy by exchange transfusion[145] and brain neuroprotection from ischemia/reperfusion injury.[146,147] This chapter describes the physiological responses after 20% exchange transfusion in anesthetized rats and blood-circulation persistence in dogs with an HbBv–HSA_3 cluster. In the case of 20% exchange transfusion in rats, 4 mL of an HbBv–HSA_3 cluster formulation ([HbBv unit] = 5 g/dL) is required at one time. In the experiments using dogs, the required volume of HbBv–HSA_3 cluster formulation is 1.8 mL for measurement of blood-circulation time, and 18 mL for anti-HSA antibody measurements in blood plasma.

5.2 Safety Evaluation of Hemoglobin–Albumin Cluster by 20% Exchange Transfusion

5.2.1 Blood Compatibility of HbBv–HSA_3 Clusters with Human Blood *in vitro*

Human blood was mixed with HbBv–HSA_3 cluster formulation ([HbBv unit] = 5 g/dL), and the blood, including RBC, white blood cell (WBC), and platelet (PLT) components, in a homogeneous suspension were quantified. The basal values (BVs) of the blood components were 457 ± 12 × 10^4 cells/μL in RBCs, 43 ± 4 × 10^2 cells/μL in WBCs, and 24 ± 1 × 10^4 cells/μL in PLTs, respectively. The RBC, WBC, and PLT quantities decreased depending on the HbBv–HSA_3 cluster volume ratio: ca. 90, 80, and 60% of the baseline value, respectively, in 10, 20, and 40 vol% HbBv–HSA_3 cluster samples (Figure 5-1A). These results were the same as those observed in the HSA groups (Figure 5-1B).

The influence of HbBv–HSA_3 clusters on blood coagulation was evaluated by prothrombin time (PT) assays, which estimated the extrinsic and common pathways of coagulation cascades.[148,149] After centrifugation of the blood/HbBv–HSA_3 mixture, the plasma

phase turned pale red in the presence of HbBv–HSA_3 clusters. The dilution of blood generally caused a decrease in the amount of thrombin, prolonging coagulation time. The PT values increased slightly depending on the HbBv–HSA_3 cluster volume ratio (10, 20, and 40 vol%) (Figure 5-1C). The results were identical to those observed in the PBS and HSA groups.

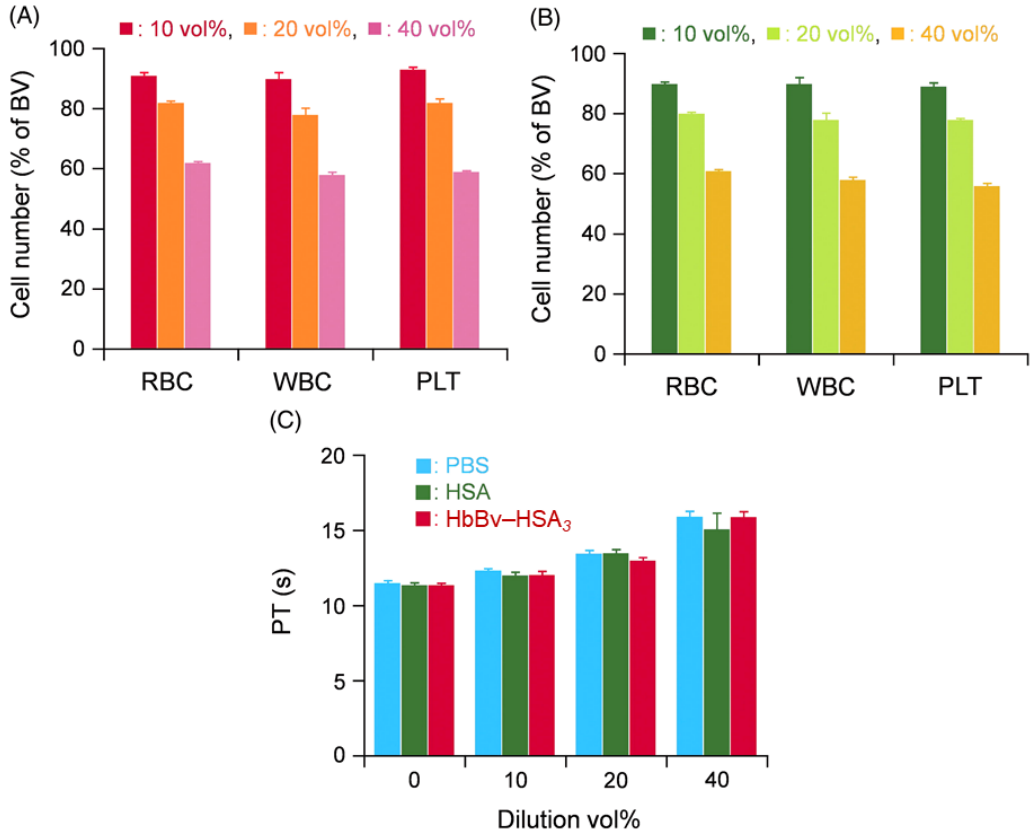

Figure 5-1. Blood compatibility of HbBv–HSA_3 clusters with human blood. (A) Blood cell component (RBC, WBC, and PLT) numbers in a human blood/HbBv–HSA_3 mixture suspension ([HbBv–HSA_3] = 10, 20, and 40 vol%) (n = 3). BVs were 457 ± 12 × 10^4 cells/μL in the RBC group, 43 ± 4 × 10^2 cells/μL in the WBC group, and 24 ± 1 × 10^4 cells/μL in the PLT group. (B) Blood cell numbers in the human blood/HSA mixture suspension (n = 3). BVs were 458 ± 11 × 10^4 cells/μL in the RBC group, 43 ± 4 × 10^2 cells/μL in the WBC group, and 24 ± 1 × 10^4 cells/μL in the PLT group. (C) PT values of human blood samples after mixing with HbBv–HSA_3 clusters, HSA, and PBS solution (10, 20, and 40 vol%) (n = 3).

5.2.2 Circulation and Blood-Gas Parameters in Rats

Results of the 20% exchange transfusion test in rats showed that all animals in the HbBv–

HSA_3 cluster group were alive during the experimental period (6 h) (Figure 5-2) and no remarkable changes in appearance were noted. The hematocrit (Hct) value decreased rapidly by blood replacement from 36.9% to 28.7%, and the values were then constant for 6 h (Figure 5-2A). A similar change was observed in the HSA group. The Hct of the sham (without replacement) group remained constant through the end of measurements. The time courses of mean arterial pressure (MAP) in the HbBv–HSA_3 cluster group showed only a small deviations of 98–112 mmHg (Figure 5-2B). No hypertensive action was observed after hemodilution with the HbBv–HSA_3 cluster group. In the sham and HSA groups, the changes in MAP were almost identical to those of the HbBv–HSA_3 cluster group. The heart rate (HR) and respiration rates (RESP) of animals in each group did not change during monitoring (Figure 5-2C, D). The body temperatures of the sham, HSA, and HbBv–HSA_3 animals remained stable between 36.7 and 37.1 °C during the experiment (6 h) (Figure 5-2E).

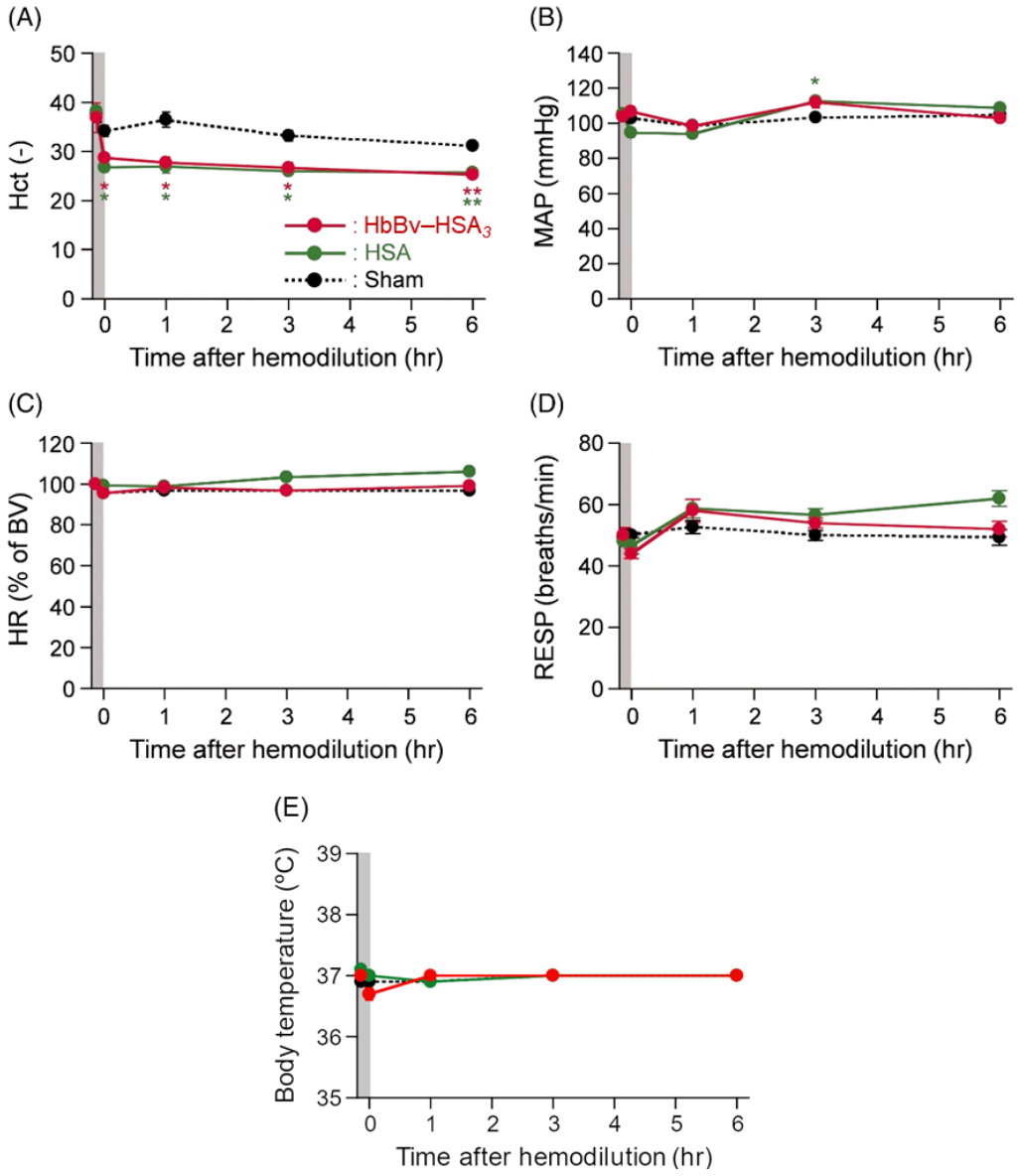

Figure 5-2. Changes in the circulation parameter. Time causes of circulation parameters of anesthetized rats after 20% exchange transfusion with HbBv–HSA$_3$ cluster HSA solution: (A) Hct, (B) MAP, (C) HR, (D) RESP, and (E) body temperature. Each datum represents mean ± standard error (n = 3). *p < 0.05 vs. sham group, **p < 0.01 vs. sham group.

The O_2 partial pressures in arterial blood (PaO_2) of the sham, HSA, and HbBv–HSA$_3$ cluster groups were constant in a range of 112–145 mmHg by the end of the experimental period (6 h) (Figure 5-3A). The O_2 partial pressures in venous blood (PvO_2) of each group also exhibited small changes within 41–59 mmHg (Figure 5-3B). No significant difference in

the $PaCO_2$, pH, and HCO_3^- was found in the sham, HSA or HbBv–HSA_3 cluster group during the observation term (Figure 5-3C, D, E).

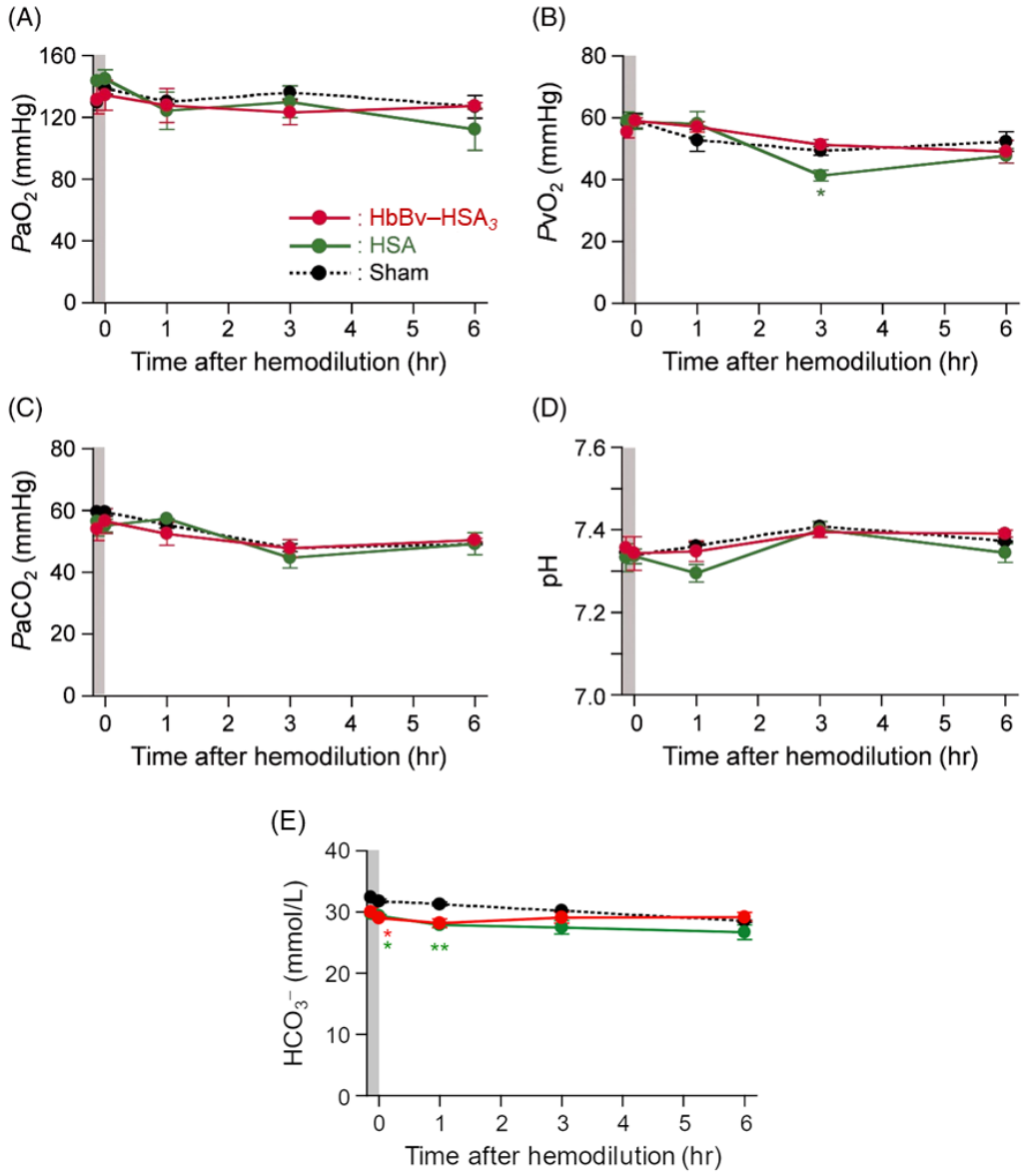

Figure 5-3. Changes of blood-gas parameters. Time causes of blood-gas parameters of anesthetized rats after 20% exchange transfusion with HbBv–HSA_3 cluster HSA solution: (A) PaO_2, (B) PvO_2, (C) $PaCO_2$, (D) pH, and (E) HCO_3^-. Each datum represents mean ± standard error (n = 3). *$p < 0.05$ vs. sham group, **$p < 0.01$ vs. sham group.

5.2.3 Measurement of Blood-Circulation Lifetime of HbBv–HSA_3 Cluster in Dogs

First, we confirmed the compatibility of HbBv–HSA_3 clusters with canine blood. The blood cell components after mixing with HbBv–HSA_3 clusters were then counted. The quantities of

RBCs, WBCs, and PLTs decreased in relation to the HbBv–HSA_3 cluster volume ratio (Figure 5-4A). These results were also recorded in the HSA groups (Figure 5-4B). The influence of HbBv–HSA_3 clusters on blood coagulation was also evaluated by determination of PT. The PT values increased slightly depending on HbBv–HSA_3 cluster volume ratio, at 10, 20, and 40 vol% (Figure 5-4C), because the amount of thrombin fell with blood dilution.

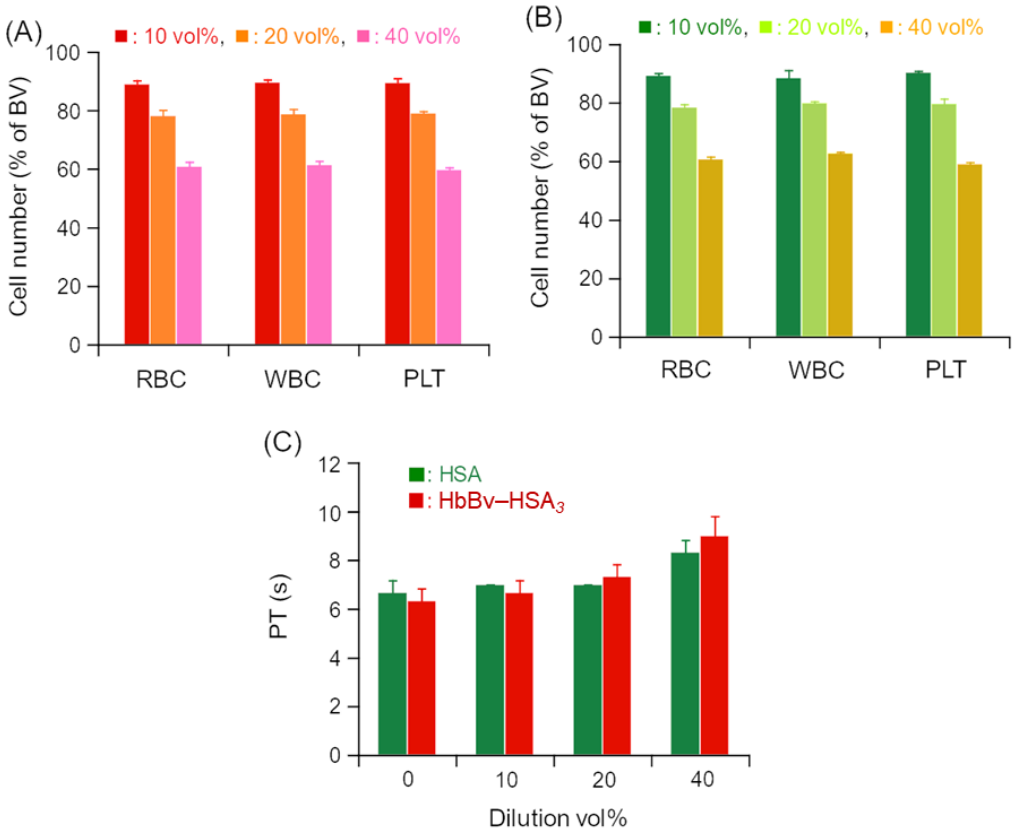

Figure 5-4. Blood compatibility with canine blood. (A) Blood cell (RBC, WBC, and PLT) numbers in canine blood/HbBv–HSA_3 mixture suspension ([HbBv–HSA_3] = 10, 20, 40 vol%). BVs were 801 ± 14 × 10^4 cells/μL in the RBC group, 94 ± 5 × 10^2 cells/μL in the WBC group, and 39 ±1 × 10^4 cells/μL in the PLT group. Each datum represents mean ± SEM (n = 3). (B) Blood cell numbers in canine blood/HSA mixture suspension ([HSA] = 10, 20, 40 vol%). BVs were 810 ± 17 × 10^4 cells/μL in the RBC group, 99 ± 5 × 10^2 cells/μL in the WBC group, and 40 ± 1 × 10^4 cells/μL in the PLT group. Each datum represents mean ± SEM (n = 3). (C) PT values of canine blood samples after mixing with HbBv–HSA_3 clusters and HSA solution (10, 20, 40 vol%). Each datum represents mean ± SEM (n = 3).

Next, we measured the retention time of HbBv–HSA$_3$ clusters in dog blood-circulation using a fluorescence reagent, a Cyanine 5.5–bound derivative (HbBv–HSA$_3$[Cy5.5]). The binding number of Cy5.5 on HbBv–HSA$_3$ clusters was 3.2. The fluorescence intensity of HbBv–HSA$_3$(Cy5.5) clusters in human plasma was stable over 48 h at 37 °C *in vitro*, whereas gradual breeching was observed in PBS (Figure 5-5). Cy5.5 labeling did not alter the charge and size of HbBv–HSA$_3$ clusters (pI: 5.0, diameter: 15 nm).[19,150]

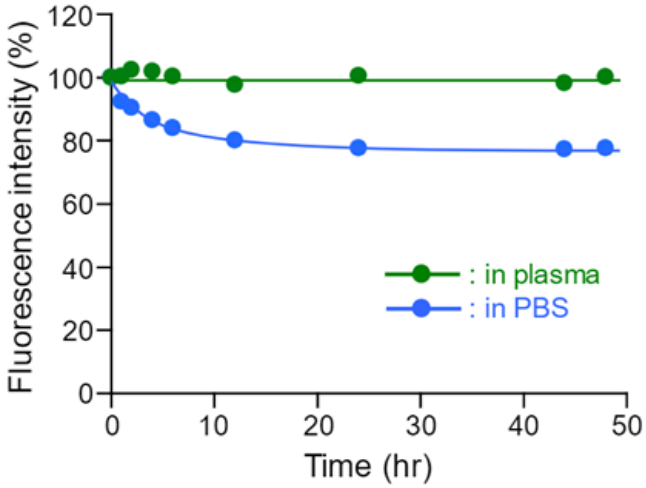

Figure 5-5. Fluorescence stability of HbBv–HSA$_3$(Cy5.5). Time courses of fluorescence intensities of HbBv–HSA$_3$(Cy5.5) (λ_{em} = 707 nm) in human plasma and PBS at 37 °C.

We inferred that the HbBv–HSA$_3$(Cy5.5) cluster was useful as a fluorescence probe to investigate the pharmacokinetics, distribution, and metabolism of HbBv–HSA$_3$ cluster. A test sample (HbBv–HSA$_3$/HbBv–HSA$_3$[Cy5.5] = 9/1 vol/vol) was injected intravenously to dogs via a jugular vein. For pharmacokinetic experiments of artificial O_2-carriers, a dose of more than 10 % of the total blood volume is generally desirable. However, pure dynamics of HbBv–HSA$_3$ cluster cannot be assessed under such conditions, because the metabolism and excretion system of HbBv–HSA$_3$ clusters may be saturated. Instead, we injected 1% of the total blood volume, which does not saturate the metabolism and excretion system. The time course of the relative plasma concentration of HbBv–HSA$_3$(Cy5.5) showed slow kinetics in a

biphasic manner. The blood-circulation half-time (τ_{50}) of the HbBv–HSA$_3$ cluster was 46.9 ± 1.9 h (Figure 5-6). The negative net surface charge and large molecular size of HbBv–HSA$_3$ clusters prevented not only extravasation through the vascular endothelium, but also filtration by the renal glomerulus.

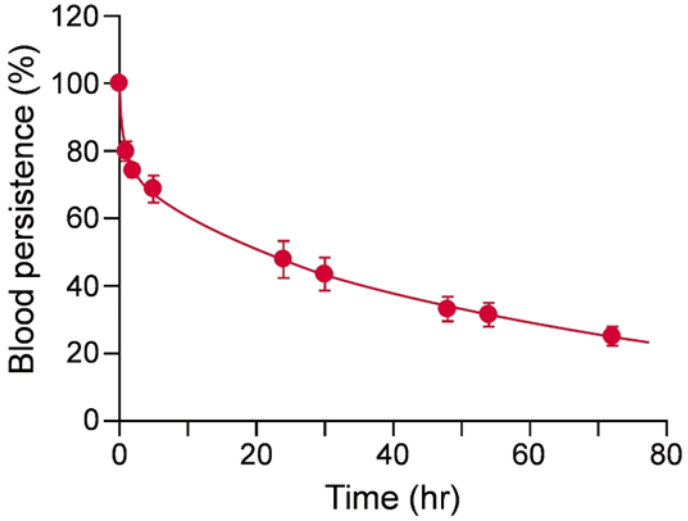

Figure 5-6. Circular lifetime. Relative plasma concentration of HbBv–HSA$_3$(Cy5.5) in dogs after intravenous administration. Each datum represents mean ± SEM (n = 5).

5.2.4 Test of Anti-HSA Antibody Generation in Blood Plasma

To observe the immunological response, the HbBv–HSA$_3$ cluster was injected into a beagle dog at a dose of 10% of total blood volume. The number of antibodies against HSA in canine plasma increased 14 days after the injection and remained constant during monitoring (35 days) (Figure 5-7). Administration of HSA generated significant numbers of anti-HSA antibodies: 2.3 to 2.9 times that of the HbBv–HSA$_3$ cluster.

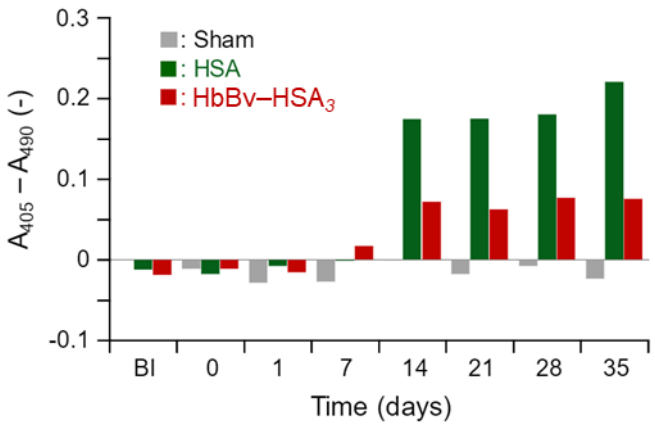

Figure 5-7. Generation of anti-HSA antibodies in canine plasma. Time courses of differential absorption (A_{405}−A_{490}) of the specimen, which are proportional to concentration of anti-HSA antibody in blood plasma after intravenous administration of HbBv–HSA_3 cluster and HSA solution in dogs. The dose rate was 10% of total blood volume. BI: just before infusion, 0: immediately after infusion.

5.2.6 Experimental Section

Materials and Apparatus

HSA was purchased from the Japan Blood Products Organization (Tokyo, Japan) and purified using GFC to remove stabilizing reagents such as *N*-acetyl-tryptophan and octanoate (caprylate). For exchange transfusion, a PBS (pH 7.4) solution of HSA was used. The concentration of HbBv units in HbBv–HSA_3 cluster formulation was 5 g/dL in PBS. A fluorescence-labeling reagent, Cyanine5.5 (Cy5.5) *N*-hydroxysuccinimide ester, was purchased from Lumiprobe Corp. (Maryland, USA). All other chemical reagents were purchased from commercial sources as special grades and were used without further purification. UV-visible absorption spectra were measured using a UV-visible spectrometer (8543; Agilent technologies Inc.) with an attached Peltier temperature controller (89090A; Agilent Technologies Inc.) Fluorescence emission spectra were recorded using a spectrofluorometer (FP-6500; Jasco Corp.). The molecular size was determined by DLS measurements using a particle-size analyzer (ELSZ-200; Otsuka Electronics Co., Ltd.).

Preparation of Cy5.5-Labeled HbBv–HSA$_3$ Clusters

A DMSO solution of Cy5.5 *N*-hydroxysuccinimide ester (12 mM, 80.4 μL) was added to a 0.1 M $NaHCO_3$ solution (pH 8.4) of HbBv–HSA$_3$ clusters ([HbBv unit] = 150 μM, 724 μL) ([Cy5.5]/[HSA] = 8 mol/mol), and stirred in the dark for 24 h at 25 °C. The obtained reaction mixture was subjected to GFC (Sephadex G-25 superfine; GE Healthcare UK Ltd.) to remove unreacted Cy5.5 with PBS as a running buffer. The eluent was concentrated to 156 μL ([HbBv unit] = 5 g/dL, 775 μM) using a centrifugal filter (Amicon Ultra 15, 30 kDa MWCO; Merck Millipore Ltd.). After CO gas was flowed into HbBv–HSA$_3$(Cy5.5) to prevent core Hb oxidation, the UV-visible absorption spectrum was used to measure the Cy5.5/HbBv–HSA$_3$ molar ratio. From the absorbance of HbBv–HSA$_3$(Cy5.5) at 420 nm (based on carbonyl core Hb) and at 684 nm (based on Cy5.5), HbBv units and Cy5.5 were assayed using their molar extinction coefficients (carbonyl Hb: $\varepsilon_{420} = 7.64 \times 10^5$ M^{-1} cm^{-1}, Cy5.5: $\varepsilon_{684} = 2.09 \times 10^5$ M^{-1} cm^{-1}). The Cy5.5/HbBv–HSA$_3$ ratio was 3.2.

Blood Compatibility of HbBv–HSA$_3$ Clusters with Human Blood *in vitro*

Human blood was withdrawn from the authors and stored in a blood collection tube (Venoject II, EDTA-2Na; Terumo Corp.). HbBv–HSA$_3$ cluster formulation was then added to the blood ([HbBv–HSA$_3$] = 0, 10, 20, and 40%, total volume = 1.0 mL each) in a plastic microtube, and individual samples were mixed by inverting. The blood cell number of each sample was measured using an automated hematology analyzer (pocH-100iV Diff; Sysmex Corp.). The results are represented as percent ratios against the blood cell numbers of samples without dilution (0 vol% HbBv–HSA$_3$). As control groups, blood suspensions mixed with HSA (15 g/dL) ([HSA] = 10, 20, and 40 vol%) were also measured. Data are shown as mean ± standard error of the mean (SEM) (n = 3). Human blood was withdrawn from the authors into a vacuum blood collection tube (Neotube, 3.2% sodium citrate; Nipro Corp.). After HbBv–

HSA_3 cluster formulation was added to the blood ([HbBv–HSA_3] = 0, 10, 20, and 40 vol%, total volume = 1.2 mL each) in a plastic microtube, the individual samples were mixed by inverting. These samples were centrifuged (2800 *g*) for 15 min at 4 °C. The supernatant (0.6 mL) was immediately transferred to a separation tube (S-1; BML Inc.) and frozen at −80 °C. The determination of PT was conducted by BML Inc. (Tokyo, Japan). As control groups, blood suspensions diluted with HSA (15 g/dL) or PBS (10, 20, and 40%) were also measured. Data are shown as mean ± SEM (n = 3).

Circulation Parameters and Blood-Gas Parameters in Rats

Nine male Wister rats (277 ± 10 g) were placed on a heating pad under an inhalation anesthesia with sevoflurane (3.0–4.0% concentration). After an incision was made in the digastric muscle, a heparinized catheter (SP-31; Natsume Seisakusho Co. Ltd.) was introduced into the right common carotid artery for blood withdrawal and continuous MAP monitoring (A-line). SP-31 catheters were inserted approximately 2 cm into the left jugular vein for sample injection (V-line). After stabilization of the animal condition, the 20% exchange transfusion (total blood volume of rat estimated as 56 mL/kg weight) was conducted by 1 mL blood withdrawal via the A-line and 1 mL HbBv–HSA_3 infusion via the V-line (each 1 mL/min) with 3 repeating cycles (HbBv–HSA_3 group, n = 3). Blood samples were taken from the A-line (0.3 mL) and V-line (0.2 mL) at the following 5 time-points: before exchange transfusion and 0 (immediately after), 1, 3, and 6 h after exchange transfusion. Simultaneously, MAP and HR were recorded using an invasive blood pressure measurement system (BPM100-PC; Star Medical Inc.). The blood sample was dropped rapidly on a test cartridge (i-STAT test cartridge CG4+; Abbot Point of Care Inc.) to measure O_2 partial pressure (PaO_2), CO_2 partial pressure ($PaCO_2$), pH, and HCO_3^- for the arterial blood, and O_2 partial pressure for the venous blood (PvO_2). Furthermore, the Hct value was

measured using a heparinized Hct capillary (C-H075H; Terumo Corp.). After 6 h, 4 mL of the arterial blood was withdrawn from the A-line using a non-treated syringe before sacrifice by hemorrhage. The blood samples were transferred into a vacuum blood collection tube (Venoject II) and centrifuged at 4000 *g* and 4 °C for 15 min. The plasma phase was transferred to a separation tube (S-1; BML Inc.) and frozen at −80 °C for serum biochemical tests. Other rats without infusion (operation only) were set as a sham group (n = 3).

Measurement of Blood-Circulation Lifetime of HbBv–HSA$_3$ Clusters in Dogs

First of all, we evaluated the chemical stability of HbBv–HSA$_3$(Cy5.5) *in vitro*. The HbBv–HSA$_3$(Cy5.5) solution (1 mM) in human plasma, which was derived from the blood of the author, or in PBS solution was incubated at 37 °C, subsequently fluorescence spectrum was measured for 48 h. Next, animal experiments were conducted with 5 male beagle dogs (~2 kg, n = 5). The gender difference of the dogs was small compared with the rats, but we used male dogs to be safe. The test sample (non-labeled HbBv–HSA$_3$/ HbBv–HSA$_3$[Cy5.5] = 9/1 [vol/vol], 1.8 mL), which corresponded to 1% of the total blood volume of the dog (90 mL/kg weight), was injected intravenously via the jugular vein without anesthesia. Blood samples were then taken from the jugular vein (2.0 mL) using a non-treated syringe at the following 9 time-points: 0 (immediately after injection) and 1, 2, 5, 24, 30, 48, 54, and 72 h after injection. The Hct value was measured using a heparinized Hct capillary. After Hct measurements, the remaining blood was transferred into a blood collection tube (NP-SP0715; Nipro Corp.) and centrifuged (2800 *g*) for 15 min at 4 °C to remove blood cell components. The supernatant (0.5 mL) was moved into a plastic microtube and stored at 4 °C in the dark. The fluorescence spectrum of each sample was then measured (λ_{ex} = 684 nm, λ_{em} = 707 nm). The relative plasma concentration of HbBv–HSA$_3$(Cy5.5) (C) was found using the equation

$$C = (F / F_0) \times 100\ (\%),$$

where F is fluorescence intensity of the supernatant at each time-point and F_0 signifies the fluorescence intensity of the supernatant immediately after the infusion. The blood-circulation half-time (τ_{50}) was ascertained using Moment analysis.

Test of Anti-HSA Antibody Generation in Blood Plasma

Experiments were performed with 3 male beagle dogs (~2 kg). The HbBv–HSA$_3$ cluster solution (18 mL), which corresponded to 10% of the total blood volume of the dog, was injected intravenously via the femoral vein under a sedation with medetomidine hydrochloride. Then blood samples were taken from the jugular vein (2.0 mL) using a non-treated syringe at 8 time-points: before infusion and 0 (immediately after infusion), 1, 7, 14, 21, 27, and 35 days after infusion. The blood sample was transferred into a blood collection tube and centrifuged (2800 *g*) for 15 min at 4 °C to remove the blood cell components. The supernatant was then moved into the separation tube and was frozen at −80 °C. An anti-HSA antibody assay was performed by an enzyme-linked immunosorbent assay method using an alkaline phosphatase-labeled rabbit anti-dog immunoglobin G antibody. Alkaline phosphatase activity was determined colorimetrically by adding *p*-nitrophenyl phosphate disodium salt (Merk KGaA) as a substrate. The absorbance of the resulting product was measured at 405 nm (product) and 490 nm (background). As a control, the HSA solution (15 g/dL) was administrated to a beagle dog. Another beagle without infusion (operation only) was used as a sham. At 35 days from the infusion, the beagles were sacrificed by exsanguination.

5.3 Conclusion

Dilution of human blood with 10–40 vol% HbBv–HSA$_3$ clusters showed appropriate decreases in RBC, WBC, and PLT numbers. The coagulation function of the blood was

maintained in the presence of HbBv–HSA$_3$ clusters. No physicochemical interaction was observed between HbBv–HSA$_3$ clusters and the human blood cell components. Replacing 20% of blood with the HbBv–HSA$_3$ cluster solution produced no acute toxicity or negative side effects in the rats. The physiological responses in blood-circulation and gas equilibria in the HbBv–HSA$_3$ cluster group were almost identical to those of the sham and HSA groups. Moreover, MAP and HR remained constant for 6 h, implying that HbBv–HSA$_3$ clusters do not engender vasoconstrictive effects. The fluorescent HbBv–HSA$_3$(Cy5.5) allowed us to measure the blood-circulation time in dogs using a fluorescence spectrometer. The nonvasopressor response and superior blood retention property of HbBv–HSA$_3$ can be attributed to the negative net surface charge and larger molecular size of the clusters. All results from this study indicate the preclinical safety of the HbBv–HSA$_3$ solution, which allows us to conduct further advanced preclinical testing of this protein cluster as a new class of RBC substitutes.

Chapter 6

Conclusions and Future Prospects

Conclusions

The final goal of the study was the practical application of the Hb–HSA_3 cluster as an RBC substitute. As a first step, enlargement of the synthetic scale of Hb–HSA_3 cluster is required. In this thesis, the author demonstrated efficient preparation procedures that can be expanded to a scale of several tens of liters. First, the cross-linker was changed to a water soluble derivative, SMP. We can synthesize HbBv–HSA_3 without side reactions even at a high Hb concentration (1 mM, 65 g/L). This improvement shortened the reaction time and increased reaction efficiency. Second, the author established a purification procedure using AEC. Reproducibility and separation efficiency of HbBv–HSA_3 clusters increased significantly compared with conventional GFC. These two improvements allowed us to prepare 74 mL of an HbBv–HSA_3 cluster formulation ([HbBv unit] = 5 g/dL) at one time, which is approximately 20-fold greater than is possible using the conventional method. Chromogenic LAL assay of LPS in the HbBv–HSA_3 cluster formulation was also conducted. We found that adding disaccharide, sucrose, and trehalose to the HbBv–HSA_3 cluster formulation allowed for lyophilization without protein denaturing. The lyophilized HbBv–HSA_3 cluster powder could be stored for 2 years.

As a second step, we expressed and purified recombinant HbA [rHbA(wt)], which can be used as raw material for the cluster. An rHbA(wt) expression strain was constructed by transforming a methylotrophic yeast, *P. pastoris*. The structure and O_2-binding property of rHbA(wt) were identical to those of native HbA, as revealed by MALDI-TOF mass spectroscopy, X-ray crystal analysis, and O_2-dissociation curve measurements. This is the first example of rHbA expressed in *P. pastoris* as a host cell. Moreover, rHbA(wt)–$rHSA_3$ clusters showed the same O_2-binding property as that of HbA–HSA_3 cluster. The rHbA(wt)–$rHSA_3$ cluster is an entirely synthetic artificial O_2-carrier that requires no donated blood as raw materials.

Subsequently, the author revealed that the O_2 affinity of rHbA(X)–rHSA$_3$ clusters can be modulated through mutations of distal amino acid residues in the core Hb. We prepared 3 rHbA(X) variants in which Leu-β28 was replaced with a bulky amino acid (Phe, Tyr, or Trp). All rHbA(X)–rHSA$_3$ cluster variants showed lower O_2 affinity compared with rHbA(wt)–rHSA$_3$ clusters. In particular, the P_{50} value of rHbA(βL28W)–rHSA$_3$ cluster was 24 Torr, which was almost identical to that of human RBCs. This suggests that genetically engineered rHbA(X)–rHSA$_3$ clusters can become not only a promising RBC substitute but also an O_2 therapeutic reagent.

Finally, the author evaluated the safety and efficacy of the HbBv–HSA$_3$ cluster formulation as an RBC substitute by animal experiments.

All these results demonstrated that HbBv–HSA$_3$ and rHbA(X)–rHSA$_3$ clusters can be of great medical importance, not only as RBC substitutes, but also as O_2 therapeutic reagents in various clinical situations.

Future Prospects

The author believes that Hb–HSA$_3$ cluster formulation is a promising RBC substitute for current HBOCs because the cluster can not only transport O_2 but also provide cytoprotective effects by HSA. The adverse effects of organ injury caused by free heme remain problematic for PEGylated Hb formulation. The combination of Hb and HSA is important, because HSA can capture free heme and may suppress adverse effects. Moreover, it is difficult to administrate the cluster formulation at Hb concentrations over 5 g/dL, because of the viscosity limits. Furthermore, the low cooperatively (n) of Hb–HSA$_3$ clusters leads to low O_2-transporting efficiency compared with that of human RBCs. In this thesis, the author synthesized rHbA(βL28W)–rHSA$_3$ clusters with the same O_2-transporting efficiency as human RBCs.

If HbA and HSA are produced as a genetically connected fusion protein, rHbA–HSA_x, a novel artificial O_2-carrier with high cooperativity can be synthesized. Some examples of fusion protein with HSA are known, such as insulin (Blondel *et al*., **2005**)[151] and interferon (Zhou *et al*., **2007**)[152], for expanding the blood-circulation lifetime. According to a report on HSA subdomain I conjugation (Patterson and Rader *et al*., **2016**)[153], molecular weight per transported O_2 molecule will improve.

Finally, HSA has a secretory signal sequence at the N-terminus. If rHbA–HSA_x, in which HSA is located at the N-terminus of Hb, can be constructed as a secretory system, the yield will reach to several g/dL, making it a promising, and profitable, artificial O_2-carrier.

Publication List

Original papers

1. Iwasaki, H.; Yokomaku, K.; Kureishi, M.; Igarashi, K.; Hashimoto, R.; Kohno, M.; Iwazaki, M.; Haruki, R.; Akiyama, M.; Asai, K.; Nakamura, Y.; Funaki, R.; Morita, Y.; Komatsu, T.

   Hemoglobin-Albumin Cluster: Physiological Responses after Exchange Transfusion into Rats and Blood Circulation Persistence in Dogs. *Artif. Cells, Nanomed., Biothecnol.* **2018**, *46*, S621-S629.

2. Funaki, R.; Kashima, T.; Okamoto, W.; Sakata, S.; Morita, Y.; Sakata, M.; Komatsu, T.

   Hemoglobin–Albumin Clusters Prepared Using *N*-Succinimidyl 3-maleimidopropionate as an Appropriate Cross-Linker. *ACS Omega* **2019**, *4*, 3228-3233.

3. Funaki, R.; Okamoto, W.; Endo, C.; Morita, Y.; Kihira, K.; Komatsu, T.

   Genetically Engineered Haemoglobin Wrapped Covalently with Human Serum Albumins as an Artificial O_2 Carrier. *J. Mater. Chem. B* **2020**, *8*, 1139-1145.

4. Funaki, R.; Iwasaki, H.; Kashima, T. Komatsu, T.

   Lyophilized Hemoglobin–Albumin Cluster: Long-Term Storable Powder of Artificial O_2 Carrier. *Polym. Adv. Technol.* **2020**, *31*, in press.

Related Papers

1. Gekka, M.; Abumiya, T.; Komatsu, T.; Funaki, R.; Kurisu, K.; Shimbo, D.; Kawabori, M.; Osanai, T.; Nakayama, N.; Kazumata, K.; Houkin, K.

   A Novel Hemoglobin-Based Oxygen Carrier Bound with Albumin Shows Neuroprotection with Possible Antioxidant Effects. *Stroke* **2018**, *49*, 1960-1968.

2. Morita, Y.; Igarashi, K.; Funaki, R.; Komatsu, T.

   Hemoglobin(βC93A)–Albumin Cluster: Mutation of Cysteine-β93 to Alanine Allows Moderate Reduction of O_2 Affinity by Inositol Hexaphosphate. *ChemBioChem* **2019**, *20*, 1684-1687.

3. Ito, Y.; Abumiya, T.; Komatsu, T. Funaki, R.; Gekka, M.; Kurisu, K.; Sugiyama, T.; Kawabori, M.; Osanai, T.; Nakayama, N, Kazumata, K.; Houkin, K.

   Neuroprotective Effects of Combination Therapy of Regional Cold Perfusion and Hemoglobin-based Oxygen Carrier Administration on Rat Transient Cerebral Ischemia. (submitted).

References

1. Antonini, E. *Physiol. Rev.* **1965**, *45*, 123-170.
2. Mozzarelli, A.; Bruno, S.; Ronda, L. Biochemistry of hemoglobin. In *Hemoglobin-based oxygen carriers as red blood cell substitutes and oxygen therapeutics*; Kim, H. W., Greenburg, A. G., Eds.; Springer-Verlag: Berlin, 2013; pp 55-73.
3. Bhagavan, N. V.; Ha, C.-E. *Essentials of medical biochemistry, second edition*; Elsevier Inc.: San Diego, 2015; pp 489-509.
4. Bellelli, A.; Brunori, M.; Miele, A. E.; Panetta, G. Vallone, B. *Curr. Protein Pept. Sci.* **2006**, *7*, 17-45.
5. Perutz, M. F.; Rossmann, M. G.; Cullis, A. F.; Murhead, H.; Will, G.; North, A. T. C. *Nature* **1960**, *185*, 416-422.
6. Perutz, M. F. *Science* **1963**, *140*, 863-869.
7. Arnone, A. *Nature* **1972**, *237*, 146-149.
8. Richard, V.; Dodson, G. G.; Mauguen, Y. *J. Mol. Biol.* **1993**, *233*, 270-274.
9. Sun, K.; D'Alessandro, A.; Ahmed, M. H.; Zhang, Y.; Song, A.; Ko, T.-P.; Nemkov, T.; Reisz, J. A.; Wu, H.; Adebiyi, M.; Peng, Z.; Gong, J.; Liu, H.; Huang, A.; Wen, Y. E.; Wen, A. Q.; Berka, V.; Bogdanov, M. V.; Absulmalik, O,; Han, L.; Tsai, A.-L.; Isowu, M.; Juneja, H. S.; Kellems, R. E.; Dowhan, W.; Hansen, K. C.; Safo, M. K.; Xia, Y. *Sci. Rep.* **2017**, *7*, 15281: 1-16.
10. Adair, G. S. *J. Biol. Chem.* **1925**, *63*, 529-545.
11. Monod, J.; Wyman, J.; Changeuz, J.-P. *J. Mol. Biol.* **1965**, *12*, 88-118.
12. Imai, K. *Biochemistry* **1973**, *12*, 798-808.
13. Weber, R. E.; Jensen, F. B.; Cox, R. P. *J. Comp. Physiol. B* **1987**, *157*, 145-152.
14. Perutz, M. F.; Fermi, G.; Poyart, C.; Pagnier, J.; Kister, J. *J. Mol. Biol.* **1993**, *233*,

536-545.

15. Perutz, M. F.; Imai, K. *J. Mol. Biol.* **1980**, *136*, 183-191.

16. Nagababu, E.; Ramasamy, S.; Rifkind, J. M; Jia, Y.; Alayash, A. I. *Biochemistry* **2002**, *41*, 7407-7415.

17. Li, D.; Hu, T.; Manjula, B. N.; Acharya, S. A. *Bioconjugate Chem.* **2009**, *20*, 2062-2070.

18. Kimura, T.; Shinohara, R.; Böttcher, C.; Komatsu, T. *J. Mater. Chem. B* **2015**, *3*, 6157-6164.

19. Funaki, R.; Kashima, T.; Okamoto, W.; Sakata, S.; Morita, Y.; Sakata, M.; Komatsu, T. *ACS Omega* **2019**, *4*, 3228-3233.

20. Jia, Y.; Ramasamy, S.; Wood, F.; Alayash, A. I.; Rifkind, J. M. *Biochem. J.* **2004**, *384*,367-375.

21. Joung, C.-H.; Shin, J.-Y.; Koo, J.-K.; Lim, J. J.; Wang, J.-S.; Lee, S.-J.; Tan, H,-K.; Kim, S.-L.; Lim, S.-M. *Protein Expression Purif.* **2009**, *68*, 137-145.

22. Bruno, S.; Ronda, L.; Faggiano, S.; Bettati, S. Mozzarelli, A. Oxygen delivery via allosteric effectors and blood substitutes, In *Burger's Medical Chemistry, Drug Discovery, and Development, Seventh Edition*; Abraham, D. J., Rotella, D. P. Eds., VHC: N. Y., 2010. pp 1-50.

23. Blood Service 2019. http://www.jrc.or.jp/english/pdf/BloodServices2019_WEB.pdf (accessed December 12, 2019), Japanese Red Cross Society.

24. Riess, J. G. *Chem. Rev.* **2001**, *101*, 2797-2919.

25. Lowe, K. C. Fluorocarbon emulsions as blood substitutes. In *Blood substitutes, present and future perspectives*; Tsuchida, E. Eds.; Elsevier Inc. 1998; pp 327-338.

26. Lowe, K. C. Fluosol®: The first commercial injectable perfluorocarbon oxygen carrier, In *Blood substitutes*;Winslow, R. M. Eds., Elsevier Inc.:San Diego, 2006. pp 276-287.

27. Keipert, P. E. Oxygent™,a a perfluorochemical-based oxygen therapertic for surgical patients, In *Blood substitutes*;Winslow, R. M. Eds.; Elsevier Inc.:San Diego, 2006, pp 312-323.

28. Hunt, C. A.; Burnette, R. R.; MacGregor, R. D.; Strubbe, A. E.; Lau, A. E.; Taylor, N.; Kiwada, H. *Science* **1985**, *230*, 1165-1168.

29. Abe, H.; Fujihara, M.; Azuma, H. Ikeda, H.; Ikebuchi, K.; Takeoka, S.; Tsuchida, E.; Harashima, H. *Artif. cells, Blood Substitutes, Biotechnol.* **2006**, *34*, 1-10.

30. Sakai, H.; Sou, K.; Horinouchi, H.; Kobayashi, K.; Tsuchida, E. *Artif. Organs* **2009**, *33*, 139-145.

31. Chatterjee, R.; Welty, E. V.; Walder, R. Y.; Pruitt, S. L.; Rogers, P. H.; Arnone, A.; Walder, J. A. *J. Biol. Chem.* **1986**, *261*, 9929-9937.

32. Looker, D.; Abbott-Brown, D.; Cozart, P.; Durfee, S.; Hoffman, S.; Mathews, A. J.; Miller-Roehrich, J.; Shoemaker, S.; Trimble, S.; Fermi, G.; Komiyama, N. H.; Nagai, K.; Stetler, G. L. *Nature* **1992**, *356*, 258-260.

33. Bucci, E.; Razynska, A.; Kwansa, H.; Matheson-Urbaitis, B.; O'hearne, M.; Ulatowski, J. A.; Koehler, R. C. *J. Lab. Clin. Med.* **1996**, *128*, 146-153.

34. D'Agnillo, F.; Alayash, A. I. *Adv. Drug Delivery Rev.* **2000**, *40*, 199-212.

35. Scannon, P. J. *Crit. Care Med.* **1982**, *10*, 261-265.

36. DeVenuto, F.; Zegna, A. *J. Surg. Res.* **1983**, *34*, 205-212.

37. Matheson, B.; Kwansa, H. E.; Bucci, E.; Rebel, A. Koehler, R. C. *J. Appl. Physiol.* **2002**, *93*, 1479-1486.

38. Jahr, J. S.; Moallempour, M.; Lim, J. C. *Expert Opin. Biol. Ther.* **2008**, *8*, 1425-1433.

39. Vandegriff, K. M.; Malavalli, A.; Wooldridge, J.; Lohman, J.; Winslow, R. M. *Transfusion* **2003**, *43*, 509-516.

40. Manjula, B. N.; Tsai, A.; Upadhya, R.; perumalsamy, K.; Smith, P. K.; Malavalli, A.;

Vandergiff, K.; Winslow, R. M.; Intaglietta, M. Prabhakaran, M.; Friedman, J. M.; Achaya, A. S. *Bioconjugate Chem.* **2003**, *14*, 464-472.

41. Lui, F. E.; Yu, B.; Baron, D. M.; Lei, C.; Zapol, W. M.; Kluger, R. *Transfusion* **2012**, *52*, 974-982.

42. Tam, S.-C.; Blumenstein, J.; Wong, J. T.-F. *Proc. Natl. Acad. USA* **1976**, *73*, 2128-2131.

43. Baldwin, J. E.; Gill, B.; Whitten, J. P.; Taegtmeyer, H. *Tetrahedron* **1981**, *37*, 1723-1726.

44. Iwasaki, K.; Ajisaka, K.; Iwashita, Y. *Biochem. Biophys. Res. Commun.* **1983**, *113*, 513-518.

45. Hsia, J.-C. Pasteurizable, freeze-driable hemoglobin-based blood substitute. U. S. Patent 4,857,636, Aug. 15, 1989.

46. D'Anillo, F.; Chang, T. M. S. *Biomater., Artif. Cells, Immobilization Biotechnol.* **1993**, *21*, 609-621.

47. Hu, T.; Su, Z. *Biotechnol. Lett*.**2002**, *24*, 275-278.

48. Tomita, D.; Kimura, T.; Hosaka, H.; Daijima, Y.; Haruki, R.; Ludwig, K.; Böttcher, C.; Komatsu, T. *Biomacromolecules* **2013**, *14*, 1816-1825.

49. Singh, S.; Kluger, R. *Biochemistry* **2016**, *55*, 2875-2882.

50. Alayash, A. I. *Nat. Rev. Drug Discovery* **2004**, *3*, 152-159.

51. Meng, F.; Kassa, T.; Jana, S.; Wood, F.; Zhang, X.; Jia, Y.; D'Agnillo, F.; Alayash, A. I. *Bioconjugate Chem.* **2018**, *29*, 1560-1575.

52. Sloan, E. P.; Koenigsberg, M.; Gens, D.; Cipolle, M.; Runge, J.; Mallory, M. N.; Rodman, G. *JAMA* **1999**, *282*, 1857-1864.

53. Rice, J.; Philbin, N.; Light, R.; Arnaud, F.; Steinbach, T.; McGwin, G.; Collier, S.; Malkevich, N.; Moon-Massatt, P.; Rentko, V.; Pearce, L. B.; Ahlers, S.; McCarron, R.;

Handrigan, M.; Freillch, D. *J. Trauma* **2008**, *64*, 1240-1257.

54. Moore, E. E.; Moore, F. A.; Fabian, T. C.; Bernard, A. C.; Fulda, G. J.; Hoyt, D. B.; Duane, T. M.; Weireter, G. H., Jr.; Gomez, G. A.; Cipolle, M. D.; Rodman, G. H., Jr.; Malangoni, M. A.; Hides, G. A.; Omert, L. A.; Gould, S. A. *J. Am. Coll. Surg.* **2009**, *208*, 1-13.

55. Young, M. A.; Malavalli, A.; Winslow, N.; Vendegriff. K. D.; Winslow. R. M. *Trans. Res.* **2007**, *149*, 333-342.

56. Olofsson, C. I.; Górecki, A. Z.; Dirksen, R.; Kofranek, I.; Majewski, J. A.; Mazurkiewicz, T.; Jahoda, D.; Fagrell, B.; Keipert, P. E.; Hardiman, Y. J.; Levy, H. *Anesthesiology* **2011**, *114*, 1048-1063.

57. Haruki, R.; Kimura, T.; Iwasaki, H.; Yamada, K.; Kamiyama, I.; Kohno, M.; Taguchi, K.; Nagao, S.; Maruyama, T.; Otagiri, M.; Komatsu, T. *Sci. Rep.* **2015**, *5*, 12778: 1-9.

58. Yamada, K.; Yokomaku, K.; Haruki, R.; Taguchi, K.; Nagao, S.; Maruyama, T.; Otagiri, M.; Komatsu, T. *PLoS One* **2016**, *11*, e149526: 1-15.

59. Jungbauer, A. *J. Chromatogr. A* **2005**, *1065*, 3-12.

60. Peters, T., Jr. The albumin molecule: its structure and chemical properties. In *All about albumin: biochemistry, genetics, and medical applications.* Academic Press: San Diego, CA, 1995, pp 9-75.

61. Lawn, R. M.; Adelma, J.; Bock, S. C.; Franke, A. E.; Houck, C. M.; Najarian, R.; Seeburg, P. H.; Wion, K. L. *Nucleic Acids Res.* **1981**, *9*, 6103-6114.

62. Chen, Z.; He, Y.; Shi, B.; Yang, D. *Biochim. Biophys. Acta* **2013**, *1830*, 5515-5525.

63. Sleep, D.; Belfield, G. P.; Goodey, A. R. *Bio/Technology* **1990**, *8*, 42-46.

64. Kobayashi, K.; Kuwae, S.; Ohya, T.; Ohsa, T.; Ohyama, M.; Ohi, H.; Tomomitsu, K.; Ohmura, T. *J. Biosci. Bioeng.* **2000**, *89*, 55-61.

65. Dosio, F.; Arpicco, S.; Brusa, P.; Stella, B.; Cattel, L. *J. Controlled Release* **2001**, *76*,

107-117.

66. Chuang, V. T. G.; Kragh-Hansen, U.; Otagiri, M. *Pharm. Res.* **2002**, *19*, 569-577.

67. Duttaroy, A.; Kanakaraj, P.; Osborn, B. L.; Schneider, H.; Pickeral, O. K.; Chen, C.; Zhang, G.; Kaithamana, S.; Singh, M.; Schulingkamp, R.;Crossan, D.; Bock, J.; Kaufman, T. E.; Reavey, P.; Carey-Barber, M.; Krishnan, S. R.; Garcia, A.; Murphy, K.; Siskind, J. K.; McLean, M. A.; Ruben, S.; Birse, C. E.; Blondel, O. *Diabetes* **2005**, *54*, 251-258.

68. Huang, Y.-S.; Chen, Z.; Yang, Z.-Y.; Wang, T.-Y.; Zhou, L.; Wu, J.-B.;Zhou, L.-F. *Eur. J. Pharm. Biopharm*. **2007**, *67*, 301-308.

69. Lowe, K. C. *J. Mater. Chem.* **2006**, *16*, 4189-4196.

70. Matsuoka, T. *Biol. Pharm. Bull.* **1997**, *20*, 1208-1211.

71. Garel, M. C.; Beuzard, Y.; Thillet, J.; Domenget, C.; Martin, J.; Galacteros, F.; Rosa, J. *Eur. J. Biochem*. **1982**, *123*, 513−519.

72. Li, D.; Hu, T.; Manjula, B. N.; Acharya, S. A. *Bioconjugate Chem.* **2009**, *20*, 2062-2070.

73. Cheng, Y.; Shen, T.-J.; Simplaceanu, V.; Ho, C. *Biochemistry* **2002**, *41*, 11901−11913.

74. Eike, J. H.; Palmer, A. F. *Biotechnol. Prog.* **2004**, *20*, 946−952.

75. Raetz, C. R. H.; Whitfield, C. *Annu. Rev. Biochem.* **2002**, *71*, 635-700.

76. The Japanese Pharmacopoeia Seventeenth Edition. https://www.mhlw.go.jp/file/06-Seisakujouhou-11120000-Iyakushokuhinkyoku/JP17_REV.pdf (accessed December 1, 2018), The Ministry of Health, Labour and Welfare.

77. Petsch, D.; Anspach, F. B. *J. Biotechnol.* **2000**, *76*, 97-119.

78. Magalhães, P. O.; Lopes, A. M.; Mazzola, P. G.; Rangel-Yagui, C.; Penna, T. C. V.; Pessoa, A., Jr. *J. Pharm. Pharmaceut. Sci.* **2007**, *10*, 388-404.

79. Todokoro, M.; Sakata, M.; Matama, S.; Kunitake, M.; Ohkuma, K.; Hirayama, C. *J.*

Liq. Chromatogr. Relat. Technol. **2002**, *25*, 601-614.

80. Sakata, M.; Fukuma, Y.; Todokoro, M.; Kunitake, M. *Anal. Biochem.* **2009**, *385*, 368-370.

81. Obayashi, T.; Tamura, H.; Tanaka, S.; Ohki, M.; Takahashi, S.; Arai, M.; Masuda, M.; Kawai, T. *Clin. Chim. Acta*, **1985**, *149*, 55-65.

82. Mensink, M. A.; Frijink, H. W.; van der Voort Maarschalk, K.; Hinrichs, W. L. J. *Eur. J. Pharm. Biopharm.* **2017**, *114*, 288-295.

83. Carpenter, J. F.; Crowe, J. H. *Biochemistry* **1989**, *28*, 3916-3922.

84. Johnston, D. S.; Castelli, F. *Thermochim. Acta* **1989**, *144*, 195-208.

85. Yoshioka, S.; Miyazaki, T.; Aso, Y.; Kawanishi, T. *Pharm. Res.* **2007**, *24*, 1660–1667.

86. Lewis, L. M.; Johnson, R. E.; Oldroyd, M. E.; Ahmed, S. S.; Joseph, L.; Saracovan, I.; Sinha, S. *AAPS PharmSciTech.* **2010**, *11*, 1580–1590.

87. Morita, Y.; Yamada, T.; Kureishi, M.; Kihira, K.; Komatsu, T. *J. Phys. Chem. B* **2018**, *122*, 12031-12039.

88. Birkou, I.; Schweers, R. L.; Olson, J. S. *J. Biol. Chem.* **2010**, *285*, 8840-8854.

89. Fedorov, M. V.; Goodman, J. M.; Nerukh, D.; Schumm, S. *Phys. Chem. Chme. Phys.* **2011**, *13*, 2294-2299.

90. Prestrelski, S. J.; Tedeschi, N.; Arakawa, T.; Carpenter, J. F. *Biophys. J.* **1992**, *65*, 661-671.

91. Remmele, R. L., Jr.; Stushnoff, C.; Carpenter, J. F. *Pharm. Res.* **1997**, *14*, 1548-1555.

92. Rahmelow, K; Hübner, W., Ackermann, Th. *Anal. Biochem.* **1997**, *257*, 1-11.

93. Barth, A. *Biochim. Biophys. Acta* **2007**, *1767*, 1073-1101.

94. Cleland, J. L.; Lam, X.; Kendrick, B.; Yang, J.; Yang, T.-H.;Overcashier, D.; Brooks, D.; Hsu, C.; Carpernter, J. F. *J. Pharm. Sci.* **2001**, *90*, 310-321.

95. Meister, E.; Gieseler, H. *J. Pharm. Sci.* **2009**, *98*, 3072-3087.

96. Jain, N. K.; Roy, I. *Protein. Sci*. **2008**, *18*, 24–36.

97. Lerbert, A.; Bordat, P.; Affouard, F.; Hédoux, A.; Guinet, Y.; Descamps, M. *J Phys Chem. B* **2007**, *111*, 9410–9420.

98. Ohtake, S.; Schebor, C.; Pelecek, S. P.; de Pablo, J. J. *Pharm. Res.* **2004**, *21*, 1615–1621.

99. Nagai, K.; Thøgersen, H. C. *Nature* **1984**, *309*, 810-812.

100. Nagai, K.; Perutz, M. F.; Poyart, C. *Proc. Natl. Acad. Sci. USA* **1985**, *82*, 7252-7255.

101. Varnado, C. L.; Mollan, T. L.; Birukou, I.; Smith, B. J. Z.; Henderson, D. P.; Olson, J. S. *Antioxd. Redox Signaling* **2013**, *18*, 2314-2328.

102. Ahmed, I.; Nawaz, N.; Darwesh, N. M.; Rahman, Su.; Mustafa, M. Z.; Khan, S. B.; Patching, S. G. *Protein Expression Purif.* **2018**, *144*, 12-18.

103. Kaur, J.; Kumar, A. Kaur, J. *Int. J. Biol. Macromol.* **2018**, *106*, 803-822.

104. Hoffman, S. J.; Looker, D. L.; Roehrich, J. M.; Cozart, P. E.; Durfee, S. L.; Tedesco, J. L.; Stetler, G. L. *Proc. Natl. Acad. Sci. USA* **1990**, *87*, 8521-8525.

105. Shen, T.-J.; Ho, N. T.; Simplaceanu, V.; Zou, M.; Green, B. N.; Tam, M. F.; Ho, C. P *Proc. Natl. Acad. Sci. USA* **1993**, *90*, 8108-8112.

106. Groebe, D. R.; Busch, M. R.; Tsao, T. Y. M.; Luh, F. Y.; Tam. M. F.; Chung, A. E.; Gaskell, M.; Liebhaber, S. A.; Ho, C. *Protein Expression Purif.* **1992**, *3*, 134-141.

107. Wagenbach, M.; O'Rourke, K.; Vitez, L.; Wieczorek, A.; Hoffman, S.; Durfee, S.; Tedesco, J.; Stetler, G. *Bio/Technology* **1991**, *9*, 57-61.

108. Ogden, J. E.; Harris, R.; Wilson, M. T. Production of recombinant human hemoglobin A in *Saccharomyces cerevisiae*. In *Methods in Enzymology, Hemoglobins, Part B: Biochemical and Analytical Methods*; Abelson, J. N., Simon, M. I., Everese, J., Vandegriff, K. D., Winslow, R. M., Eds.; Academic Press: San Diego, 1994; Vol. 231, pp 374-390.

109. Kato, R.; Kobayashi, Y.; Akiyama, M.; Komatsu, T. *Dalton Trans.* **2013**, *42*, 15889-15892.

110. Yokomaku, K.; Akiyama, M.; Morita, Y.; Kihira, K.; Komatsu, T. *J. Mater. Chem. B* **2018**, *6*, 2417-2425.

111. Shen, T.-J.; Ho, N. T.; Zou, M.;Sun, D. P.; Cottam, P. F.; Simplaceanu, V.; Tam, M. F.; Bell, D.A., Jr.; Ho, C. *Protein Eng.* **1997**, *10*, 1085-1097.

112. Nagai, M; Nagai, Y; Aki, Y.; Imai, K.; Wada, Y.; Nagatomo, S.; Yamamoto, Y. *Biochemistry* **2008**, *47*, 517-525.

113. Park, S.-Y.; Yokoyama, T.; Shibayama, N.; Shiro, Y.; Tame, J. R. H. *J. Mol. Biol.* **2006**, *360*, 690-701.

114. Krainer, F. W.; Capone, S.; Jäger, M.; Vogl, T.; Gerstmann, M.; Glieder, A.; Herwig, C. Spadiut, O. *Microb. Cell Fact.* **2015**, *14*, 2-9.

115. Kabsch, W. XDS. *Acta Crystallogr. D Struct. Biol.* **2010**, *66*, 125-132.

116. McCoy, A. J.; Grosse-Kunstleve, R. W.; Adams, P. D.; Winn, M. D.; Storoni, L. C.; Read, R. J. *J. Appl. Crystallogr.* **2007**, *40*, 658-674.

117. Winn, M. D.; Ballard, C. C.; Cowtan, K. D.; Dodson, E. J.; Emsley, P.; Evans, P. R.; Keegan, R. M.;Krissinel, E. B.; Leslie, A. G.W.; McCoy, A.; McNicholas, S. J.; Murshudov, G. N.; Pannu, N. S.; Potterton, E. A.; Powell, H. R.; Read, R. J.; Vagin, A.; Wilson, K. S. *Acta Crystallogr.,Sect. D: Struct. Biol.* **2011**, *67*, 235-242.

118. *Desmond Molecular Dynamics System*; D. E. Shaw Research: New York, NY, 2016; Maestro-Desmond Interoparability Tools, Schrödinger, New York, NY, 2016.

119. Nichols, R. A.; Tykac, M.; Kovalevskiy, O.; Murshudov, G. N. *Acta Crystallogr., Sect. D: Struct. Biol.* **2018**, *74*, 492-505.

120. Murshudov, G. N.; Skubák, P.; Lebedev, A. A.; Pannu, N. S.; Steiner, R. A.; Nicholls, R. A.; Winn, M. D.; Long, F.; Vagin, A. A. *Acta Crystallogr., Sect. D: Biol. Crystallogr.*

2011, *67*, 355-367.

121. Murshudov, G. N.;Vagin, A. A.; Dodson, E. J. *Acta Crystallogr., Sect. D: Biol. Crystallogr.* **1997**, *53*, 240-255.

122. Emsley, P.; Lohkamp, B.; Scott, W. G.; Cowtan, K. *Acta Crystallogr., Sect. D: Biol. Crystallogr.* **2010**, *66*, 486-501.

123. Hosaka, H.; Haruki, R.; Yamada, K.; Bottcher, C.; Komatsu, T. *PLoS One* **2014**, *9*, e110541: 1-9.

124. Grassetti, D. R.; Murray, J. F., Jr. *Arch. Biochim. Biophys.* **1967**, *119*, 41-49.

125. Bonaventura, J.; Riggs, A. *J. Biol. Chem.* **1968**, *243*, 980-991.

126. Schneider, R. G.; Atkins, R. J.; Hosty, T. S.; Tomlin, G.; Casey, R.; Lehmann, H.; Lorkin, P. A.; Nagai, K. *Biochim. Biophys. Acta* **1975**, *400*, 365-373.

127. Kwiatkowski, L. D.; Hui, H. L.; Karasik, E.; Colby, J. E.; Noble, R. W. *Biochemistry* **2007**, *46*, 2037-2049.

128. Springer, B. A.; Egeberg, K. D.; Sligar, S. G.; Rohlfs, R. J.; Mathews, A. J.; Olson, J. S. *J. Biol. Chem.* **1989**, *264*, 3057-3060.

129. Mathews, A. J.; Rohlfs, R. J.; Olson, J. S.; Tame, J.; Renaud, J.-P.;Nagai, K. *J. Biol. Chem.* **1989**, *264*, 16573-16583.

130. Brunori, M. Savino, C. C.; Travaglini-Allocatelli, C.; Vallone, B.; Gibson, Q. H. *Biophys. J.* **1999**, *76*, 1259-1269.

131. Allocatelli, C. T.; Cutruzzolá, F.; Brancaccio, A.; Vallone, B.; Brunori, M. *FEBS Lett.* **1994**, *352*, 63-66.

132. Dou, Y.; Maillett, D. H.; Eich, R. F.; Olson, J. S. *Biophys. Chem.* **2002**, *98*, 127-148.

133. Wiltrout, M. E.; Giovannelli, J. L.; Simplaceanu, V.; Lukin, J. A.; Ho, N. T.; Ho, C. *Biochemistry* **2005**, *44*, 7207-7217.

134. Sakai, H.; Masada, Y.; Takeoka, S.; Tsuchida, E. *J. Biochem.* **2002**, *131*, 611-617.

135. Bulheller, B. M.; Hirst, J. D. *Ab initio* calculations for circular dichroism and synchrotron radiation circular dichroism spectroscopy of proteins. In *Modern techniques for circular dichroism spectroscopy*; Wallace, B. A., Janes, R. W., Eds.; IOS Press: Amsterdam, 2009; pp 202-215.

136. Andrew, C. D.; Bhattacharjee, S.; Kokkoni, N.; Hirst, J. D.; Jones, G. R, Doig, A. J. *J. Am. Chem. Soc.* **2002**, *124*, 12706-12714.

137. Hirst, J. D. *J. Phys. Chem. B* **2003**, *107*, 8682-8688.

138. Miele, A. E. Santanché, S.; Travaglini-Allocatelli, C.; Vallone, B.; Brunori, M.; Bellelli, A. *J. mol. Biol.* **1999**, *290*, 515-524.

139. Birukou, I.; Maillett, D. H.; Birukova, A.; Olson, J. S. *Biochemistry* **2011**, *50*, 7361-7374.

140. Miele, A. E.; Draghi, F.; Arcovito, A.; Bellelli, A.; Brunori, M.; Travaglini-Allocatelli, C.; Vallone, B. *Biochemistry* **2001**, *40*, 14449-14458.

141. Waterman, M. R.; Stenzel, P. *Biochim. Biophys. Acta* **1974**, *359*, 401-410.

142. Alayash, A. I.; Ryan, B. A. R.; Fratantoni, J. C. *Comp. Biochem. Physiol.* **1993**, *106B*, 427-432.

143. Greenfield, N. J. *Nat. Protoc.* **2006**, *1*, 2527-2535.

144. Chothia, C. *Nature*, **1975**, *254*, 304-308.

145. Iwasaki, H.; Yokomaku, K.; Kureishi, M.; Igarashi, K.; Hashimoto, R.; Kohno, M.; Iwazaki, M.; Haruki, R.; Akiyama, M.; Asai, K.; Nakamura, Y.; Funaki, R.; Morita, Y.; Komatsu, T. *Artif. Cells, Nanomed., Biotechnol.* **2018**, *46*, S621-S629.

146. Gekka, M.; Abumiya, T.; Komatsu, T.; Funaki, R.; Kurisu, K.; Shimbo, D.; Kawabori, M.; Osanai, T.; Nakayama, N.; Kazumata, K.; Houkin, K. *Stroke* **2018**, *49*, 1960-1968.

147. Ito, Y.; Abumiya, T.; Komatsu, T. Funaki, R.; Gekka, M.; Kurisu, K.; Sugiyama, T.; Kawabori, M.; Osanai, T.; Nakayama, N, Kazumata, K.; Houkin, K. To be submitted.

148. Kirkwood, T. B. L. *Thromb. Haemostasis* **1983**, *49*, 238-244.

149. Rao, L. V.; Okorodudu, A. O.; Petersen, J. R.; Elghetany, M. T. *Clin. Chim. Acta* **2000**, *300*, 13-21.

150. Shinohara, R.; Yamada, T.; Schade, B.; Böttcher, C.; Sato, T.; Sugiura, N.; Shibue, T.; Komatsu, T. *J. Phys. Chem. Lett.* **2017**, *8*, 819-824.

151. Duttaroy, A.; Kanakaraj, P.; Osborn, B. L.; Schneider, H.; Pickeral, O. K.; Chen, C.; Zhang, G.; Kaithamana, S.; Singh, M.; Schulingkamp, R.; Crossan, D.; Bock, J.; Kaufman, T. E.; Reavey, P.; Carey-Barber, M.; Krishnan, S. R.; Garcia, A.; Murphy, K.; Siskind, J. K.; McLean, M. A.; Cheng, S.; Ruben, S.; Birse, C. E.; Blonedel, O. *Diabetes* **2005**, *54*, 251-258.

152. Huang, Y.-S.; Chen, Z.; Yang, Z.-Y.; Wang, T.-Y.; Zhou, L.; Wu, J.-B.; Zhou, L.-F. *Eur. J. Pharm. Biopharm.* **2007**, *67*, 301-308.

153. Petterson, J. T.; Wilson, H. D.; Asano, S.; Nilchan, N.; Fuller, R. P.; Roush, W. R.; Rader, C.; Barbas, C. F. III *Bioconjugate Chem.* **2016**, *27*, 2271-2275.

Acknowledgment

The study in this thesis has been carried out under the supervisor of Prof. Teruyuki Komatsu, Department of Applied Chemistry in Chuo University during 2014–2020. I would like to express the deepest gratitude to Prof. Teruyuki Komatsu for his valuable advice, incisive comments, extensive discussion, and constant encouragement. I would also like to express deep gratitude to Assistant Prof. Motofusa Akiyama for his invaluable help, advice, and contributions while starting this project, and to Assistant Prof. Yoshitsugu Morita for practical advice, feedback, and discussion.

I would like to extend my grateful gratitude to Dr. Kiyohito Kihira, Japan Aerospace Exploration Agency for MALDI-TOF mass spectroscopy measurements and X-ray crystal structure analysis. I would like to acknowledge the help of Associate Prof. Satoru Unzai, Department of Frontier Bioscience in Hosei University, in providing cDNA of HbA. I would like to also thanks Associate Prof. Masayo Sakata, Graduate School of Science and Technology in Kumamoto University; Associate Prof. Mitsutomo Kohno, Department of Thoracic Surgery in Tokai University; and Associate Prof. Takeo Abumiya, Department of Neurosurgery in Hokkaido University, for their support.

I am grateful to Hitomi Iwasaki, Takumi Anekawa, Tomonori Kashima, Sho Sakata, Wataru Okamoto, Chihiro Endo, and Tatsuhiko Hamano for their support and contributions. I would like to thank the work of all past and current laboratory members.

Finally, I would like to express my deep gratitude to my family, Masashi Funaki, Motoe Funaki, Akari Funaki, and Yugo Funaki, for their powerful moral support.

March 2020

Ryosuke Funaki